THE UNIVERSITY
of EDINBURGH

THE CONTINUOUS FLOW SYNTHESIS OF CHEMICAL BUILDING BLOCKS FOR BIOLOGICAL APPLICATION

THINGSOON JONG

DOCTOR OF PHILOSOPHY

THE UNIVERSITY *of* EDINBURGH

COLLEGE OF SCIENCE AND ENGINEERING

SCHOOL OF CHEMISTRY

2014

ABSTRACT

THE CONTINUOUS FLOW SYNTHESIS OF CHEMICAL BUILDING BLOCKS FOR BIOLOGICAL APPLICATION

by

ThingSoon Jong

A collection of twenty three selectively mono-protected di- and triamines, masked with the Boc, Fmoc or Dd*iv* protecting groups, were synthesised via continuous flow synthesis in a self-assembled meso-scale PTFE flow reactor. The continuous flow strategy offered direct access to the mono-protected compounds in good yields, especially in the case of the Fmoc carbamates which circumvented the use of another sacrificial protecting group. Two of the mono-Boc-protected carbamates were used as starting materials to generate *N*-alkylglycine monomers; synthesised via tandem mono-alkylation and Fmoc carbamation, linked by an in-line scavenging protocol using a silica-based trisamine scavenger resin. The final step of the monomer synthesis employed catalytic transfer hydrogenolysis using 20% $Pd(OH)_2$/C and 1,4-cyclohexadiene. The three-step flow procedure gave access to two monomers, with one of them being a novel *N*-alkylglycine unit bearing a triethylene glycol bridge.

The monomers were used as building blocks to assemble new oligo-*N*-alkylglycines (peptoids) via microwave-assisted solid phase synthesis. Three different types of peptoids were synthesised: (i) oligo-*N*-(6-aminohexyl)glycines ("standard" peptoids), (ii) oligo-*N*-{2-[2-(2-aminoethoxy)ethoxy]ethyl}glycines ("triethylene glycol" [TEG] peptoids) and (iii) hetero-oligomers of alternating "standard" and "TEG" monomers ("hybrid" peptoids). The peptoids were evaluated for their cellular permeability and cytotoxicity with HeLa, HEK-293 and CHO cells. All the peptoids were shown to be non-cytotoxic at 10 μM based on cell proliferation assays. In general, it was found that the cellular uptake of the hybrid peptoids outperformed their standard and TEG analogues. Flow cytometry and confocal microscopy results revealed that the hybrid nonamer had the highest cellular uptake efficiency of all the peptoids synthesised. At a concentration of 1 μM, it outperformed the second best molecular transporter (standard nonamer) by a factor of seven.

LAY SUMMARY

Chemical synthesis is broadly defined as the process of designing and constructing molecular structures. The conventional way of performing chemical synthesis relies heavily on traditional glassware set-ups that have remained relatively unchanged since the first lab reaction was performed in the 19th century. While round bottom flasks are cheap and easily replaceable, they are non-ideal in assisting reaction control due to their rigidity and size. An alternative technology in the form of tube-shaped plastic reactors, with shrunken dimensions (big enough to only fit a pinhead), has allowed chemists to manipulate chemical reactions in entirely different ways and this has led to the emergence of *flow chemistry*.

This project has utilised flow chemistry to make peptoid monomers, the fundamental components of peptoids (a type of biologically active compounds), in a more efficient process. The monomers were built by linking a series of individual chemical reactions together in a flow reactor to increase productivity and minimise waste. They were then used as "building blocks", much like the individual pieces in a *Lego*'s play kit, to assemble more complicated molecules (peptoids) for biological evaluation. The peptoids were tested for their efficiency in penetrating the plasma membrane of cancer cells, as well as their inherent potential to cause cell death. A chemical dye was attached to the peptoids to serve as a tracker to observe the movement of these compounds in cells.

Peptoids that can cross the cellular barrier efficiently, without causing any significant cell mortality, can be used as delivery agents. Cargos such as drugs or genes (which would otherwise have problem penetrating the plasma membrane) can be transported into cells, for investigative or therapeutic purposes, by attaching them to peptoids. This research showed that peptoids that were built from two different types of monomers (hybrid peptoids) were much better transporters compared to those made entirely of a single monomer type (standard peptoids). The hybrid system possesses just the right balance of characteristics needed for membrane penetration. As a result, the hybrid peptoids have immense potential to be used as transporters in biochemical research.

DECLARATION OF AUTHORSHIP

The research work presented in this thesis was carried out under the supervision of Professor Mark Bradley at the School of Chemistry, University of Edinburgh from April 2009 to May 2014.

No part of this thesis has been previously submitted at this university, or any other institution of higher learning, for any other degree or a professional qualification.

Signed: *Signature on Printed Copy*

Author: ThingSoon Jong

Date: *20 May 2014*

ACKNOWLEDGEMENTS

My PhD is a product of help and support from many people and I would like to take this opportunity to highlight those who have gone on this journey with me since the very beginning. Firstly, I would like to acknowledge my supervisor, Prof. Bradley, for his support and encouragement throughout my PhD. He has given me the invaluable opportunity to explore and develop my research interests and his supervision is much appreciated.

Next, I would like to express my sincere gratitude to Dr. Ana Maria Lopez-Perez for our research collaboration and all the assistance that she's given me, professionally and personally, in the past couple of years. A special mention goes to Dr. Emma Johannsson for her help in establishing some preliminary biological results of my chemical compounds prior to her departure from the group. I've also been fortunate to have the opportunity to evaluate a couple of loaned instruments during my PhD which contributed tremendously to the overall understanding of my research work. On this note, I would like to acknowledge Dr. Kerry Elgie of Uniqsis and Mr. Robert Hardy of CEM for making the trials possible.

Moving on, I would like to thank a select few postdoctoral fellows (past and present) in the Bradley group for their advice, guidance and mentoring during my time in the lab. They include Drs. Jeffrey and Tashfeen Walton, Dr. Nicos Avlonitis, Dr. Sunay Chankeshwara, Dr. Annamaria Lilienkampf, Dr. Eftychia Koini, Dr. Rong Zhang and Dr. Miren Aiertza Otxotorena. Following closely, my thanks go to Frank B, Mariona, Geraldine, Song, Rahimi and Mei, seniors who have taught me plenty during the early days of my PhD. To Frank T, Anne, Martha, Aurelie, Neil, Martin, Cairnan and Liz, thank you for the wonderful times that we've shared together, in and outside of the lab. It's been a real pleasure knowing each one of you and your friendship will always be dear to my heart.

A massive thank you goes out to my family members and friends back in Malaysia for urging me to persevere when times got tough. It hasn't been easy to say the least but your prayers and well wishes have seen me through. Moreover, I would like to dedicate this thesis to two distinct individuals who have made a real difference in my life. Alex, to whom I'm forever indebted to for seeing me through my thesis

write-up in its entirety; and my mom, who's living her aspirations and dreams through me. Thank you!

Last but not least, my heartfelt appreciation goes to the School of Chemistry's MTEM Studentship and the Edinburgh University's Innovation Initiative Grant for their financial support. Undertaking this PhD wouldn't have been possible without the scholarship and I'm truly grateful to everyone who's made it possible for me to experience such a remarkable journey in Edinburgh (and further afield) in the last few years. Tapadh leibh!

LIST OF ABBREVIATIONS

Abbreviation	Full Name
Ahx	6-Aminohexanoic acid
Boc	*tert*-Butoxycarbonyl
BPR	Back Pressure Regulator
CHO	Chinese Hamster Ovary cells
CPP	Cell Penetrating Peptides
CPPos	Cell Penetrating Peptoids
d	Doublet
DBU	1,8-Diazabicyclo[5.4.0]undec-7-ene
DCM	Dichloromethane
Dde	1-(4,4-Dimethyl-2,6-dioxocyclohexylidine)ethylene
Dd*iv*	1-(4,4-Dimethyl-2,6-dioxocyclohexylidine)isovaleryl
DIC	*N*,*N*'-Diisopropylcarbodiimide
DIPEA	Diisopropylethylamine
DMF	Dimethylformamide
DMSO	Dimethylsulfoxide
DNA	Deoxyribonucleic Acid
DRF	Detector Response Factor
EG	Ethylene Glycol
ELSD	Evaporative Light Scattering Detector
em	Emission
equiv	Equivalent
ESI	Electrospray Ionisation
Et	Ethyl
ex	Excitation
FACS	Fluorescence Activated Cell Sorting
FFKM	Perfluoroelastomer
Fmoc	9-Fluorenylmethyloxycarbonyl
HEK-293	Human Embryonic Kidney cells
HeLa	Human Cervical Carcinoma cells
hep	Heptet

HIV	Human Immunodeficiency Virus
HOBt	Hydroxybenzotriazole
HPLC	High Performance Liquid Chromatography
Hz	Hertz
I.D.	Internal Diameter
J	Coupling constant
LC-MS	Liquid Chromatography-Mass Spectometry
m	Multiplet
M.p.	Melting point
MALDI-TOF	Matrix Assisted Laser Desorption / Ionisation – Time of Flight
Me	Methyl
MFI	Mean Fluorescence Intensity
MHz	Mega Hertz
MTT	3-(4,5-Dimethylthiazol-2-yl)-2,5-diphenyltetrazolium bromide
m/z	Mass-to-charge ratio
NMR	Nuclear Magnetic Resonance
Oxyma	Ethyl 2-cyano-2-(hydroxyimino)acetate
P.G.	Protecting Group
PBS	Phosphate Buffer Saline
PEEK	Poly(ether)etherketone
PEG	Poly(ethylene glycol)
PGF	Protecting Group Free
PI	Propidium Iodide
Ppm	Parts per million
PS	Polystyrene
PSA	Polar Surface Area
PTFE	Polytetrafluoroethylene
Re	Reynolds number
RFI	Relative Fluorescence Intensity
q	Quartet

quin	Quintet
s	Singlet
sex	Sextet
SCX	Strong Cation Exchange Chromatography
SPPS	Solid Phase Peptide Synthesis
t	Triplet
Tat	Transactivator of transcription protein
TEA	Triethylamine
TEG	Triethylene Glycol
TFA	Trifluoroacetic acid
THF	Tetrahydrofuran
TIS	Triisopropylsilane
t_R	Retention time
UV/Vis	Ultra Violet / Visible
δ	Chemical shift
τ	Residence time

TABLE OF CONTENT

CHAPTER 1
INTRODUCTION

1.1 Continuous Flow Synthesis – An Overview

The concept of continuous flow processing has been used extensively in industrial manufacturing and processing activities, long before it was explored and adopted by bench chemists.[1] Industrial scale processes such as the production of fine chemicals and petroleum refining inherently restrict the exclusive use of batch processing due to engineering issues as well as health and safety concerns.[2] The continuous flow approach not only reduces the risks associated with scaled-up chemical processing, but also increases overall production capacity as a result of improved output generated by a "non-stop" feed stream of raw materials and reduces down-time of capital expensive plants.[3,4] The potential of continuous flow processing caught the attention of research chemists working on laboratory scale syntheses and hence, the technology has been gradually developed and transferred to the bench over time.[5-7]

The use of microreactors was heavily favoured when flow chemistry was first introduced, with these chip-based reactors fabricated using a diverse selection of materials (i.e. glass, elastomers, silicon, quartz, fluoropolymers, metals and ceramics).[8-10] A wide range of organic synthetic transformations have been carried out in microreactors and extensive reviews have since been published which summarise the breadth of work performed by academic and industrial groups.[11-13] While chip-based reactors were immensely popular early on, technical issues such as irreversible channel blockage due to material precipitation and joint leakage seriously affected the reliability of microreactors. Over time, attention slowly shifted to other types of flow reactors with larger reaction chambers.[14,15] The increased dimension of flow reactors from micro- to mesoscale not only improved plugging issues but also expanded the usability of the reactors. New generation flow reactors are commonly fitted with auxiliary components such as mixers, back pressure regulators and heat exchangers to enable a full range of chemically useful processing parameters.[16-18] The reactor accessories, for example, promote enhanced solution mixing and enable super heating of solvents above their respective boiling points to allow a whole new level of reaction manipulation.[19,20]

"Shrinking" the reaction vessel's volume provides access to vastly different physical properties, not normally seen at the macro level.[21] As the internal volume of reaction is often kept to within a few millilitres, the reaction time of a chemical transformation is significantly shortened due to the marked improvement in heat transfer, mass transport and diffusional flux per unit volume / unit area.[22] Precise control over the overall reaction time increases reaction selectivity, and the formation of side products is greatly reduced as a result of optimised contact time between substrates and reagents. Due to the small internal volume of flow reactors, rapid screening of chemical reactions can be achieved using only small quantities of reagents and catalysts.[23] Hence, reaction optimisation can be economically accomplished with minimal generation of waste.[24,25] Isothermal conditions are easily achieved due to the highly efficient heat exchange between a flow reactor and its surrounding environment.[26] A narrow thermodynamic profile prevents the formation of hotspots which can lead to the initiation of unwanted side reactions and product decomposition.[27] The continuous flow method thus serves as an excellent alternative to batch synthesis, which suffers from many physical drawbacks such as low reactor surface area to volume ratio and progressively declining rate of reaction as the concentration of reactants drop over time. As a consequence, chemical systems in batch reactors can experience poor heat transfer as well as inefficient mass transport which in turn can lead to poor reaction selectivity and product yields.

1.2 Physical Characteristics of Flow Reactors

Flow synthesis exploits the intrinsic properties of flow reactors which differ significantly from conventional macroscale organic laboratory synthetic apparatus.[28] Hollow channels, with well-defined internal diameter, are used as the physical reaction platform as opposed to ubiquitous round bottom flasks. In essence, a flow reactor is a modular, three dimensional reaction platform which enables spatial and temporal manipulation of mobile fluid streams (Figure 1.1). The inner dimension of a flow reactor typically exists in the range of 0.01 – 1.00 mm offering a very different physical environment in comparison to batch reactors. Starting materials are introduced separately via different inlets and converge at a mixing zone. From this point onwards, the mixture is fed into a common tubular space in which the chemical reaction occurs as the stream moves along the reactor channel.

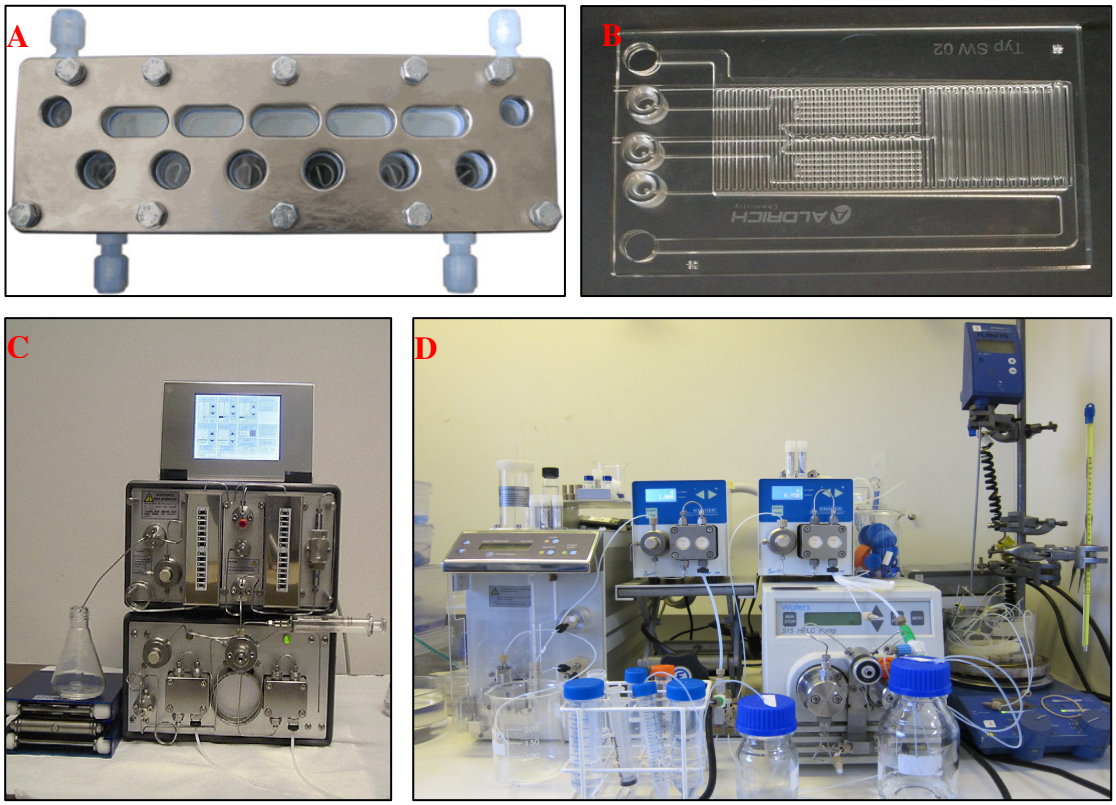

Figure 1.1 An assortment of flow reactors made from different materials: AM Technology's CoFlore disc reactor (A); Sigma-Aldrich's glass microreactor (B); Thales Nano's X-Cube stainless steel reactor (C); **PTFE-based flow reactor (right) and a modified Thales Nano's H-Cube (left) used for experimental work in this thesis** (**D**).

As the phrase 'continuous flow' itself suggests, substrates or reagents are continuously fed into the reactor to derive synthetically useful compounds. This is normally achieved via hydrodynamic pumping using standard high pressure liquid chromatography (HPLC) pumps. The reaction essentially begins at the point of mixing and ends upon exiting the reactor; effectively establishing a space-to-time relationship.[21] In a flow reactor with fixed volume, the duration of the reaction is determined by the total flow rate of the reaction stream. The residence time (τ) of a reaction is defined as the total time spent within the flow reactor; as the reaction stream travels from the point of entry to the point of exit, and immediately quenched thereafter. This is represented by Equation 1:

$$\tau = VQ^{-1} \qquad \textbf{(1)}$$

where τ = Residence time

V = Internal volume of the flow reactor

Q = Total flow rate of the reaction

By keeping the internal volume of the flow reactor constant, the residence time can be controlled by adjusting the total flow rate of reaction.

In addition, a continuous flow platform is often modular in nature and thus, has the flexibility to incorporate additional experimental set-ups to enable the comprehensive management of a chemical reaction. This *build-as-you-go-to* architecture works much like a Lego® play kit, giving users the ability to tailor their hardware according to different synthetic needs. As a result, individual stages of synthesis, reaction sampling, work-up and purification can be combined into a linear sequence to produce a seamless automated process.[29-31] In contrast, conventional batch synthesis tends to be segmented with multiple sampling and intermediate purification steps involving manual processing.

1.3 Challenges and Opportunities in Practical Flow Chemistry

The use of flow chemistry as an alternative method to conventional batch synthesis presents vastly different challenges.[32] In general, the continuous flow method has been lauded to deliver superior reaction selectivity. Better reaction selectivity leads to the minimisation of side product formation and thus, higher product yields. However, achieving significant reaction selectivity via the continuous flow route necessitates the use of specialised flow instruments which are not readily available to most chemists. While there are instrument manufacturers which specialise in the production of ready-to-use continuous flow platforms (e.g. Syrris, Uniqsis and Vapourtec), these commercial systems can be cost prohibitive.

In addition, most commercial flow systems are built for specific purposes and performing different chemical transformations requires switching of instruments. As a consequence, a substantial investment of hardware (i.e. mechanical pumps, reactors and accessories) has become a prerequisite prior to adopting the technology. Furthermore, each chemical reaction is typically assessed in batch mode before performing a continuous flow trial due to the significant risk of material incompatibility. Precipitation of reactants, products or side products during the course of synthesis will inevitably result in channel blockage and could damage the expensive flow reactors. Therefore, transferring a routinely performed synthesis from the round bottom flask to the continuous flow platform requires careful reaction scoping; taking into consideration solvent compatibility and reactant selection.

Despite the aforementioned challenges, flow chemistry does offer two key opportunities that are immensely attractive to research chemists.[33] The promise of product scalability is rooted in the principle of 'scaling out' which replaces the conventional approach of batch 'scale up'. Once an optimal reaction condition is identified, a continuous flow reaction is simply left to run for an extended duration to produce the desired quantity of product.[34] This approach removes the process of re-optimisation carried out in batch synthesis which is not only laborious but also introduces variability in product yield. Another option uses the 'numbering up' approach which promotes the use of parallelisation by splitting common feed streams into multiple flow reactors to achieve higher throughput.[35,36]

Hence, it is possible to produce multi-gram quantities of target compounds using a relatively compact platform without the need to increase the foot print of the synthetic set-up. The same synthetic platform can be used for the initial reaction screening as well as the subsequent product scale out. In flow synthesis, the yield of a reaction can be conveniently transformed into a measurement of productivity.[37] The second defining hallmark of the continuous flow method is the possibility of linking multiple synthetic steps into one linear process.[38-40] With fewer intermediate purification steps, the duration of the overall synthesis could be shortened and product loss can be minimised to give higher product yield. Contrary to popular belief, multi-step continuous flow synthesis does not necessarily entail the use of packed reagents, catalysts or scavengers.[41-43] A target compound can be synthesised by linking several sequential reactions together without undergoing any intermediate purification as long as the chemical components within the reaction system are mutually compatible.[44,45]

1.4 Analysis of Flow Literature

An analysis of the flow literature from 2009 to 2013 revealed a growing trend of synthetic diversification which explores the many possibilities of utilising the continuous flow method to perform new synthetic endeavours. Due to the breadth of published work associated with flow chemistry, the term "*continuous flow synthesis*" was used as the key search phrase in identifying the most relevant publications in the literature pool. Using SciFinder, a topic query on the database of American Chemical Society's Chemical Abstract Services returned a total of 121 publications. From 2009 to 2013, there was an approximately four-fold increase in the number of papers

published, showing a growing influence of the continuous flow approach in different areas of chemistry (Figure 1.2).

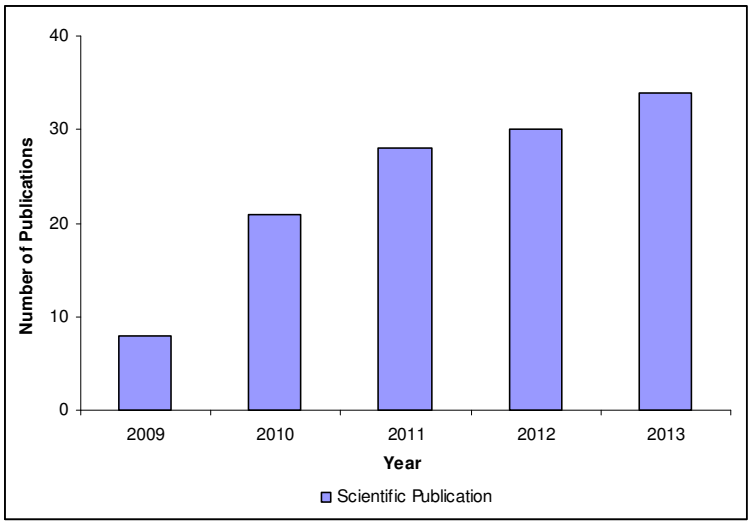

Figure 1.2 The number of scientific publications directly associated with the term "*continuous flow synthesis*" based on the results returned by SciFinder on American Chemical Society's Chemical Abstract Services (data as of March 2014).

A further breakdown of the publication output reveals six main areas which have successfully adopted flow chemistry as shown in Figure 1.3. Using the continuous flow method to synthesise organic compounds is by far the most prevalent undertaking among research chemists in the past five years. This accounts for 40% of materials published in public domain, followed by nanoparticle synthesis (25%), continuous flow technology development (8%), catalysis (7%), polymer synthesis (5%), and the fabrication of organic electronic materials (4%). Specific to the synthesis of organic compounds, the target compounds synthesised has grown in complexity, combining multiple technologies to achieve a unique platform customised for each type of synthetic work. During the first half of the last decade, the focus of continuous flow organic synthesis was primarily on one-step transformations which are relatively straight forward, producing small organic molecules in high yields and in good quantities.[12,13,26]

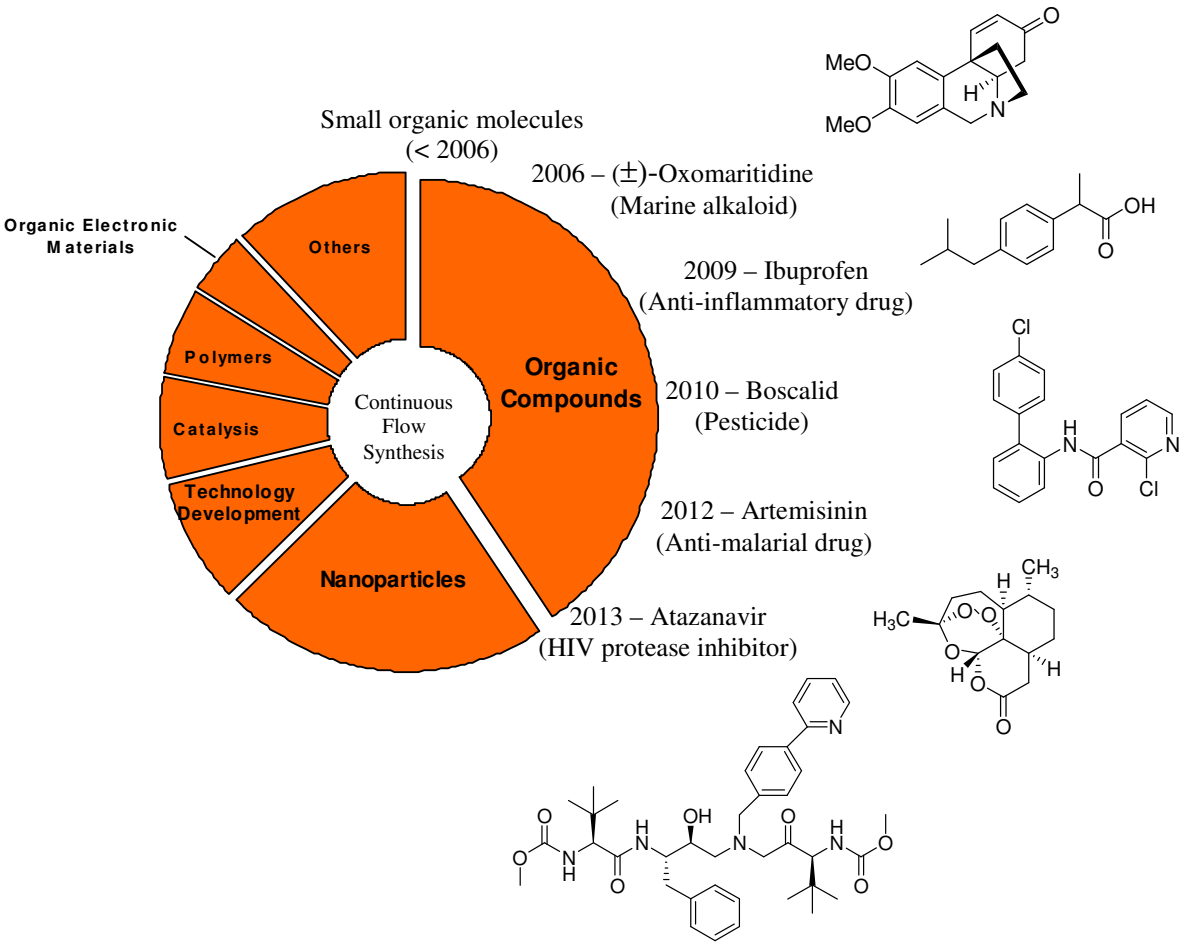

Figure 1.3 A total of 121 continuous flow synthesis publications, from 2009 to 2013, divided into six main research areas according to their respective frequencies. Notable examples of organic compounds which have been synthesised via flow chemistry are included.

The first significant step towards fully unlocking the massive potential of the continuous flow method was made in 2006 when Baxendale *et al.* demonstrated the seven-step synthesis of a marine natural product – (±)-oxomaritidine, using immobilised reagents, catalysts and scavengers.[46] This work led to more tandem transformations, connecting several steps into a sequence of multi-phase synthesis incorporating in-line analyses, work-up and purification.[47-51] With regard to other more specialised work, nanoparticle and polymer syntheses benefit enormously from the narrow channels of flow reactors, providing a stringent control on particle size and molecular weight distribution which are often problematic in batch reactions.[52,53] In addition, the development of the continuous flow method in recent years has also seen the inclusion of (i) microwave technology to promote process intensification and catalysis, as well as (ii) simulated moving-bed chromatography to link synthetic steps to the purification process.[30,54]

1.5 Overview of PhD

The objectives of this PhD project were: (i) to build a self-assembled continuous flow platform capable of addressing the synthetic requirements of a research laboratory; (ii) to transfer an existing batch chemistry to the continuous flow mode via reaction screening, optimisation and scale out; and (iii) to apply the synthesised compounds as building blocks for chemical biology investigations. The project sought to explore the themes of reaction selectivity and product scalability in continuous flow chemistry by developing new synthetic methodologies that are both practical and accessible to research chemists. The work presented in this dissertation is divided into three main parts – Introduction (Chapter 1), Research Work (Chapter 2 – 4) and Experimental (Chapter 5). A brief overview of the research work is described in the following paragraph.

Chapter 2 of this dissertation presents the selective mono-protection of di- and triamines as carbamates and enamines with three different types of protecting group. Twenty three compounds, with *N*-Boc, *N*-Fmoc and *N*-Dd*iv* protected amines of varying methylene spacer lengths, were synthesised via the continuous flow method. Moreover, six members of the library also contain ethylene glycol bridges separating the two terminal amino moieties. The stability of the N-Dd*iv* compounds to *N*→*N*' migration were also investigated. Using two of the *N*-Boc-protected compounds as starting materials, Chapter 3 examines the multi-step continuous flow synthesis of *N*-alkylglycine (peptoid) monomers, involving selective mono-alkylation, Fmoc carbamation and catalytic transfer hydrogenolysis. The first two steps were linked as a tandem sequence via the use of silica-based trisamine scavenger to remove excess alkylating agents in the reaction system. The last synthetic step was performed in a modified commercial hydrogenation platform (H-Cube). A transfer catalytic hydrogenolysis procedure was developed using 20% $Pd(OH)_2/C$ and 1,4-cyclohexadiene as the catalyst and hydrogen donor pairing.

Two different *N*-alkylglycine monomers were synthesised via the continuous flow method and used as the building blocks of oligo-*N*-alkylglycines. Chapter 4 describes the microwave-assisted solid phase synthesis of oligo-*N*-alkylglycines and their biological evaluations. Nine different *N*-alkylglycine oligomers were assembled via solid phase synthesis and they were grouped into three categories, named *Standard*, *Triethylene glycol* (*TEG*) and *Hybrid*, according to their chemical

structures. The syntheses of the TEG and hybrid peptoids were aided by microwave irradiation. All the oligomers were evaluated for their cellular permeability and cytotoxicity in different cell lines. The significance of the biological results are highlighted at end of the chapter. In all three chapters, the synthetic protocols, along with the yield of each compound, are reported and discussed.

CHAPTER 2

FLOW MEDIATED MONO PROTECTION OF DI- AND TRIAMINES

2.1 Background: Selective Protection of Amines

The use of different protecting groups to facilitate the construction of structurally complex compounds (e.g. peptides, oligosaccharides, glycolipids, etc.) has become a common strategy in the field of organic synthesis.[55] While considerable efforts have been invested towards the development of novel protecting-group-free (PGF) synthesis, a large number of existing reactions are still overwhelmingly dependent on the use of protecting groups to mask competing reactivities of multi-functional molecules.[56] Thus, the selective protection of functional groups is often regarded as a challenging aspect of synthetic work born out of sheer necessity. Mono-protected aliphatic compounds are especially important as they are commonly used as spacers, linkers or scaffolds in larger molecular assemblies.[57-59]

It is widely known that the selective mono-protection of a multi-functional molecule with two or more chemically identical moieties is difficult to achieve due to competing active sites between the unprotected substrate and the mono-protected product. Conventional synthetic practice of using one-to-one equivalent of reagent to substrate in generating the desired mono-protected compound often results in poor product yield due to the formation of the di-protected side product.[60,61] In overcoming this, different strategies have been introduced to achieve a high degree of selectivity.[62] The reactivity of protecting group precursors plays an important role in inducing reaction mono-selectivity. Pittelkow *et al.* demonstrated the use of *tert*-butyl phenyl carbonate to generate *N*-*tert*-butyloxycarbonyl protected diamines in decent yields.[63] However, the reduced reactivity of the phenyl carbonate based precursor necessitates aggressive reaction conditions to promote the carbamation reaction.

An alternative method to promote reaction selectivity was reported by Pringle via the concept of "ionic immobilisation" utilising strong cation exchange (SCX) chromatography.[64] This was preceded by the work of Das *et al.* who employed sulfonic acid functionalised silica as a heterogeneous "catalyst" to attain chemoselective protection of various amino compounds.[65] In addition, mono-acylation of cyclic diamines on solid phase has also been investigated.[66] Subsequent cleavage from the solid support leads to the formation of the mono-protected products

in good yields. However, this approach falls short in term of synthetic efficiency due to the additional synthetic steps involved (i.e. resin binding and cleavage) which limits the step economy of the reaction (Scheme 2.1).[67] The use of chemical auxiliaries such as $MgCl_2$ or $AlCl_3$, $Cu(BF_4)_2.nH_2O$, 9-borabicyclo[3.3.1]nonane (9-BBN), and HCl to induce selectivity have also been reported.[68-71] While these methods are experimentally feasible, they are limited in term of practical scalability.

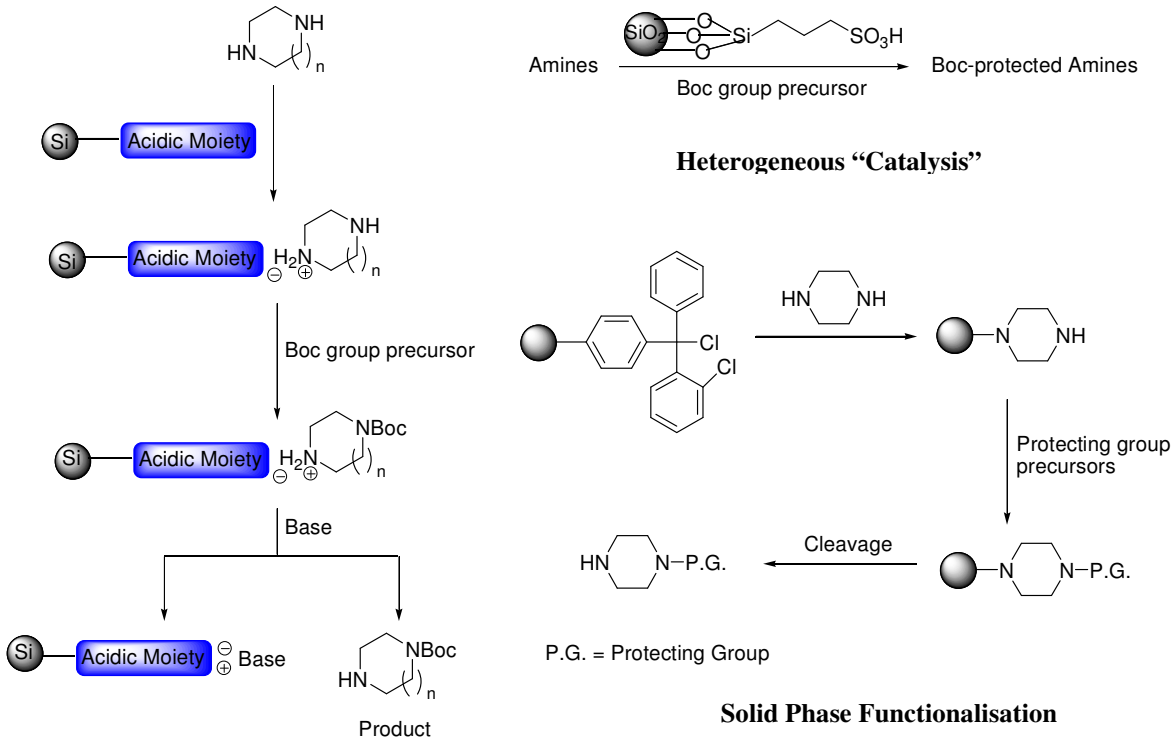

Scheme 2.1 Selective protection of amines via different strategies as reported in the literature.[64-66]

A more common solution employed in the literature involves the use of a large excess of the reaction substrates (diamines) against the limiting reagent (protecting group precursor).[72] Even though satisfactory yields (with respect to the PG precursor) of the reaction are obtained from such approach, the method itself is less than ideal due to a gross violation of atom economy.[73] Besides being economically wasteful, using a large excess of starting materials is not only environmentally unsustainable but also leads to isolation and purification challenges during final work-up. Presented with the problem of reaction selectivity in the macroscale batch environment, the selective mono-protection of di- and triamines using three different protecting groups *tert*-butyloxycarbonyl (Boc), 9-fluorenylmethyloxycarbonyl (Fmoc)

and 1-(4,4-dimethyl-2,6-dioxocyclohexylidene)isovaleryl (Dd*iv*) via continuous flow synthesis was investigated.

The Boc and Fmoc groups are popular masking moieties used in organic synthesis. The Boc group can be removed by acid-catalysed hydrolysis whereas the Fmoc group is removed by base-catalysed β-elimination.[74] On the contrary, the Dd*iv* group is a relatively recent invention which can withstand acidic and basic conditions but is readily removed via nucleophilic substitution.[75] This chapter discusses the selective continuous flow mono-protection of aliphatic acyclic di- and triamines via two different types of reaction – (i) *N*-carbamation of primary amines using Boc and Fmoc protecting groups, and (ii) enamination of primary amines with the Dd*iv* protecting group (Scheme 2.2). Di-*tert*-butyl-dicarbonate (Boc_2O) and *N*-(9-flourenylmethoxycarbonyloxy)succinimide (Fmoc-OSu) which are commercially available were chosen as the protecting group precursors to derive the series of *N*-carbamates ($-NHCO_2R$) whereas 2-(1-hydroxy-3-methylbutylidene)-5,5-dimethylcyclohexane-1,3-dione (Dd*iv*OH) was used to generate the enamine derivatives ($-NHCR_1{=}CR_2$). These reactions require markedly distinct reaction conditions due to the differing scale of reactivity of the protecting group agents.

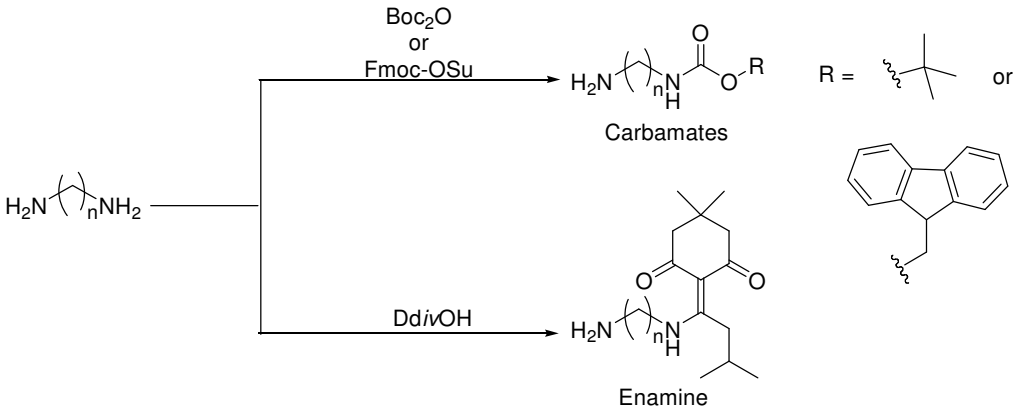

Scheme 2.2 Formation of primary amine-based *N*-carbamates and enamine.

2.2 Continuous Flow Set-Up

The reaction set-up for the continuous flow synthesis of mono-protected di- and triamines was divided into two stages (Figure 2.1). In the first stage (pre-conditioning), the reactants were brought to optimum temperature prior to mixing. During the pre-conditioning step, the two reactants (amines and protecting group

precursors) were pumped through two separate PTFE capillary tubing (0.50 mm I.D.) with identical internal volumes (0.18 mL).

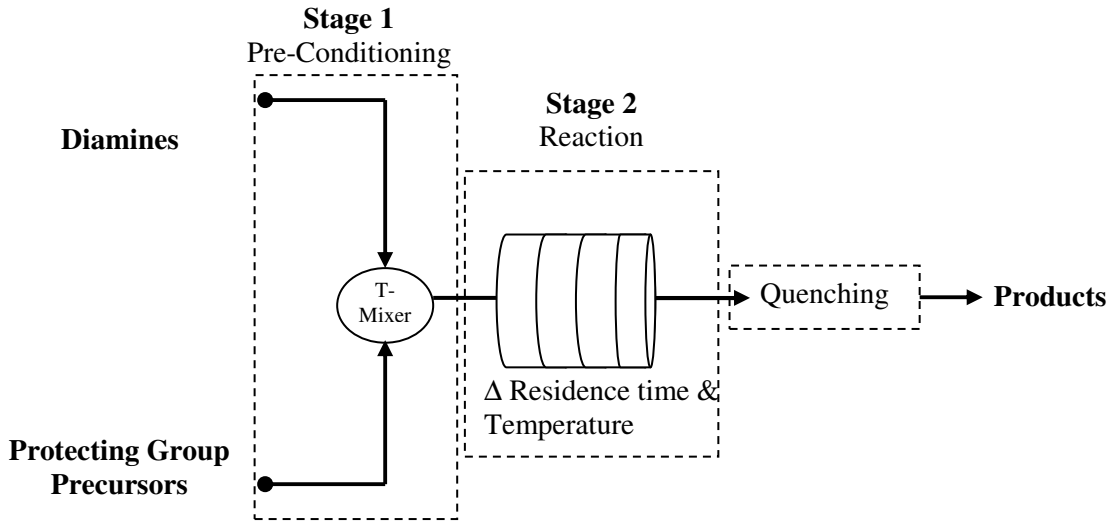

Figure 2.1 Reaction set-up for the continuous flow synthesis of mono-protected di- and triamines.

This was achieved by physically immersing the tubing in a bath set to the desired working temperature of the reaction, thus allowing starting materials to be pre-conditioned before mixing in the T-mixer. This pre-conditioning reduces the time required for the reactants to reach thermal equilibrium within the flow reactor as soon as mixing begins and promotes reproducibility. In the second stage (post mixing), the reaction proceeded along a PTFE-based flow reactor (0.50 mm I.D., 2.00 mL internal volume, 10.16 m total length). Upon exiting the flow reactor, the reaction stream was immediately quenched.

2.3 Mono-Boc Carbamation

The first point of investigation was the selective introduction of a Boc group onto a symmetrical molecule bearing a pair of terminal amino moieties using Boc_2O as the protecting group precursor. In continuous flow experiments, yields of reaction are controlled via the manipulation of (i) reaction stoichiometry, (ii) reaction temperature and (iii) residence time. Solvent screening was initially performed to determine the best solvent system for the reaction studied. This was to ensure full physical compatibility of the reaction mixture within the flow reactor.

Precipitation of materials was observed with the use of dichloromethane and 1,4-dioxane during batch synthesis, hence these solvents were deemed incompatible

with the flow set-up. Methanol proved to be the ideal solvent as it afforded complete solubility of all reactants and product mixtures. 1,6-Diaminohexane **1a** was used as the arbitrary test substrate during preliminary screenings. In order to minimise the formation of side products, reaction screenings were performed at 0°C while the residence time was fixed at 1 min. The reaction was quenched by dropping the crude stream into a collection vial filled with cold MeOH containing an excess of silica-based trisamine scavenger. This ensured no further reaction occurred between the reactants beyond the stipulated residence time in the flow reactor.

2.3.1 Reaction Stoichiometry, Temperature and Residence Time

With an initial concentration of 0.10 M for both the diamine and Boc_2O, the optimal reaction stoichiometry was determined. As the stoichiometric excess of the diamine was raised from 1.0 to 3.0 equivalents, the corresponding yield of product formation increased accordingly (entries a – j, Table 2.1). At 2.5 equivalents of diamine, a maximum yield of 70% *N*-Boc-1,6-diaminohexane **2** was found with no further improvement as more diamine was used. Furthermore, the formation of the di-protected side product **3** was noticeably suppressed (i.e. a decrease of almost six times) at higher diamine concentrations (entries a vs. j, Table 2.1). It was evident that the mono-protected species predominates when an excess of diamine was used in the reaction and the results confirmed previous published reports concerning the positive effect of stoichiometric excess of diamine on the selectivity of the reaction.[72]

Increasing the reaction temperature from 0 to 25°C had a detrimental effect on product yield with more side products formed (entries f – i, Table 2.1). A lower reaction temperature proved to be advantageous in slowing down the second nucleophilic attack. Thus, using 1.0 to 2.0 equivalents of Boc_2O to diamine, a good balance between starting material consumption (61% conversion based on diamine) and product yield (64%) was achieved (entry f, Table 2.1). Halving the residence time from 1.0 to 0.5 min had no appreciable influence on the product output (entries f vs. k, Table 2.1), while the yield dropped from 64 to 53% with an extra minute of dwell time (entries f vs. l, Table 2.1). Prolonging the residence time undoubtedly increases the probability of molecular interaction between the product and the unreacted Boc group precursor within the flow reactor. Therefore, the residence time for the reaction was kept at 1.0 min.

Table 2.1 Formation of mono-Boc-protected diamines **2**, **4** and **6** as a function of reaction stoichiometry, residence time, temperature and reactor channel's internal diameter.

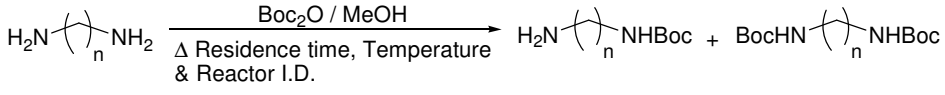

n =			
2	**1b**	**4**	**5**
4	**1c**	**6**	**7**
6	**1a**	**2**	**3**

Entry	Diamine	Equiv	Reactor I.D. (mm)	Temperature (°C)	Residence Time (min)	Isolated Yield (%)
a	**1a**	1.0	0.5	0	1.0	42 (1 : 0.56)[i]
b	1a	1.2	0.5	0	1.0	48 (1 : 0.40)
c	1a	1.4	0.5	0	1.0	54 (1 : 0.36)
d	1a	1.6	0.5	0	1.0	52 (1 : 0.34)
e	1a	1.8	0.5	0	1.0	57 (1 : 0.26)
f	1a	2.0	0.5	0	1.0	64 (1 : 0.19)
g	1a	2.0	0.5	25	1.0	53 (1 : 0.22)
h	1a	2.5	0.5	0	1.0	70 (1 : 0.18)
i	1a	2.5	0.5	25	1.0	62 (1 : 0.23)
j	1a	3.0	0.5	0	1.0	67 (1 : 0.10)
k	1a	2.0	0.5	0	0.5	63 (1 : 0.12)
l	1a	2.0	0.5	0	2.0	53 (1 : 0.13)
m	1a	2.0	1.0	0	1.0	53 (1 : 0.23)
n	1a	2.0	1.6	0	1.0	51 (1 : 0.24)
o	**1b**	2.0	0.5	0	1.0	64 (1 : 0.24)
p	1b	2.0	1.0	0	1.0	60 (1 : 0.15)
q	1b	2.0	1.6	0	1.0	50 (1 : 0.36)
r	**1c**	2.0	0.5	0	1.0	65 (1 : 0.21)
s	1c	2.0	1.0	0	1.0	66 (1 : 0.13)
t	1c	2.0	1.6	0	1.0	59 (1 : 0.38)

[i] The molar ratio of mono-Boc product to di-Boc side product.

[ii] Conditions: 0.10 M Boc_2O as the limiting reagent. MeOH as solvent.

2.3.2 Flow Reactor's Internal Diameter

The role of flow reactor's internal diameter as a distinct feature of the continuous flow process was also examined. While previous published work have utilised microreactors and micromixers to achieve selective mono-acylation and alkylation respectively, none has specifically studied the relationship between flow reactor's internal diameter and the selectivity profile of a consecutive competitive reaction within the meso-scale range.[76] Hence, a comparison of product selectivity was derived by performing the mono-protection reaction in separate tubular flow reactors of different internal diameters (i.e. 0.5, 1.0 and 1.6 mm respectively). Employing test substrate **1a**, the product yield fell by as much as 11% when the internal diameter increased from 0.5 to 1.0 mm. A further increase of 0.6 mm in the cavity size of the tubing had little consequence on the isolated yield (entries f, m & n, Table 2.1).

In order to generate additional evidence, the experiments were repeated with 1,2-diaminoethane **1b** and 1,4-diaminobutane **1c**. Based on the results obtained with the diamino compounds having shorter alkyl chain length, both the 0.5 and the 1.0 mm I.D. flow reactors produced comparable product yields in the region of 60 – 66%. Interestingly, better mono-selectivity was observed with the use a larger internal diameter (i.e. 1.0 mm I.D.) for both compounds **1b** and **1c** (entries o, p, r & s, Table 2.1). However, lower yields were obtained with a 1.6 mm I.D. flow reactor and the product to side product ratios were conspicuously in favour of the di-protected species (entries q & t, Table 2.1). Figure 2.2 provides an illustration of the results.

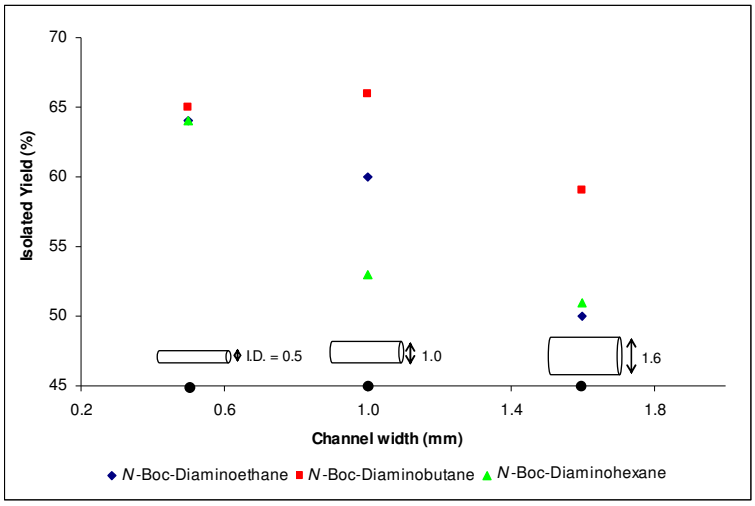

Figure 2.2 Reactor's internal diameter vs. product yield of *N*-Boc-diamines. Conditions: 2.0 equiv diamines, τ – 1.0 min, T – 0°C. Average isolated yield of three separate experiments per data point.

In general, there was a positive enhancement on the preferential formation of the mono-protected product when reactions were performed in flow reactors with smaller internal diameters. The mass transfer mechanism in the continuous flow system is governed primarily by molecular diffusion.[77] This is determined by the fluid flow behaviour within the tubular reactor as indicated by the Reynolds number (*Re*).[22] An *Re* value below 2300 represents a general laminar flow regime in which viscous forces predominate over inertial forces. Using Equation 2:

$$Re = \frac{\rho.\upsilon.D}{\mu} \qquad (\mathbf{2})$$

where $\rho_{MeOH\ at\ 0°C} = 0.81 \times 10^{3}\ kgm^{-3}$

$\upsilon = 2.00 \times 10^{-3}\ Lmin^{-1}$

$\mu_{MeOH\ at\ 0°C} = 8.17 \times 10^{-4}\ Pa.s$

The individual *Re* corresponding to the 0.5, 1.0 and 1.6 mm I.D. flow reactors are 84.16, 42.08 and 26.30 respectively.

The calculated values confirmed that non-turbulent flow prevails in all three systems but the smallest internal diameter of 0.5 mm produces a disturbed laminar flow (i.e. small vortical irregularities occurring at curved fluid path) which has a direct effect on the mixing efficiency within the flow reactor. As the starting materials converge into a single stream, a smaller internal diameter provides a shorter path of diffusion for the reacting molecules to traverse through; hence speeding up the overall mixing process which ultimately determines the homogeneity of the solution. Achieving a homogenous environment early in the reaction is essential in reducing the occurrence of side-reaction as a result of competing cascading reactions among all the reacting species.

As shown in Figure 2.3, the diamine (represented by the blue spheres) must effectively diffuse through the product layer (green spheres) as the reaction progresses, in order to react with the protecting group agent (yellow spheres). A slower rate of mixing, relative to the rate of side product formation, impedes the chemical selectivity of the reaction system. When compared to a batch environment, inefficient mechanical stirring often leads to poor solution mixing and creates localised concentration hotspots of starting materials. System inhomogeneity inevitably causes statistically biased distribution of reacting molecules at the expense of product yield.

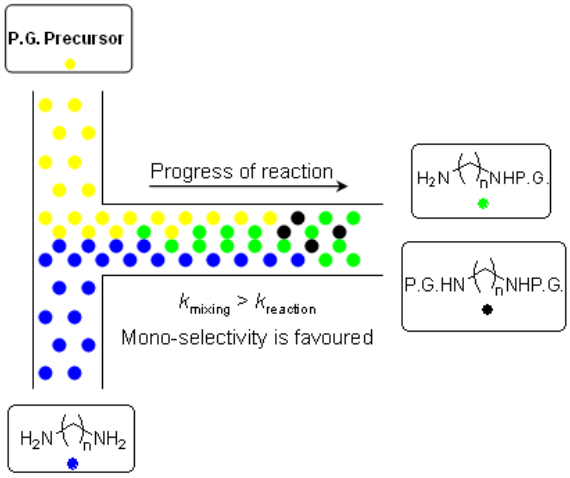

Figure 2.3 Consecutive reactions of (i) product formation (between blue and yellow spheres) and (ii) a competitive subsequent transformation of product to side product (between green and yellow spheres).

2.3.3 Synthetic Scope

Based on the optimal reaction parameters established using the test substrates aforementioned (entries f, o & r, Table 2.1), the scope of the continuous flow mono-Boc carbamation reaction was examined with a series of aliphatic acyclic di- and triamines of varying alkyl chain length and bridge motifs (Table 2.2).

For the α, ω-alkanediamines, the yields of the mono-protected species were found to be the range of 59 – 77%; demonstrating good overall selectivity but with no distinct correlation between product exclusivity and the length of the alkane chain (entries a – e, Table 2.2). In addition, a similar level of selectivity was also observed with the ethylene glycol-diamines showing a lack of influence of the ethylene glycol (EG) moiety on the behaviour of the diamino molecule (entries f & g, Table 2.2). When the continuous flow method was used to synthesise mono-Boc protected triamines, a higher yield was obtained with diethylenetriamine in comparison to 4,7,10-trioxatridecan-1,13-diamine (entries h vs. i, Table 2.2). In both cases, side products in the form of di- and tri-Boc-protected species were isolated via flash column chromatography. The presence of extra methylene groups appears to reduce the reaction selectivity as the formation of *N*,*N*,*N*-Boc-protected 4,7,10-trioxatridecan-1,13-diamine exceeded that of *N*,*N*,*N*-Boc-protected diethylenetriamine by a factor of six.

Table 2.2 Mono-Boc carbamation of di- and triamines via continuous flow synthesis.

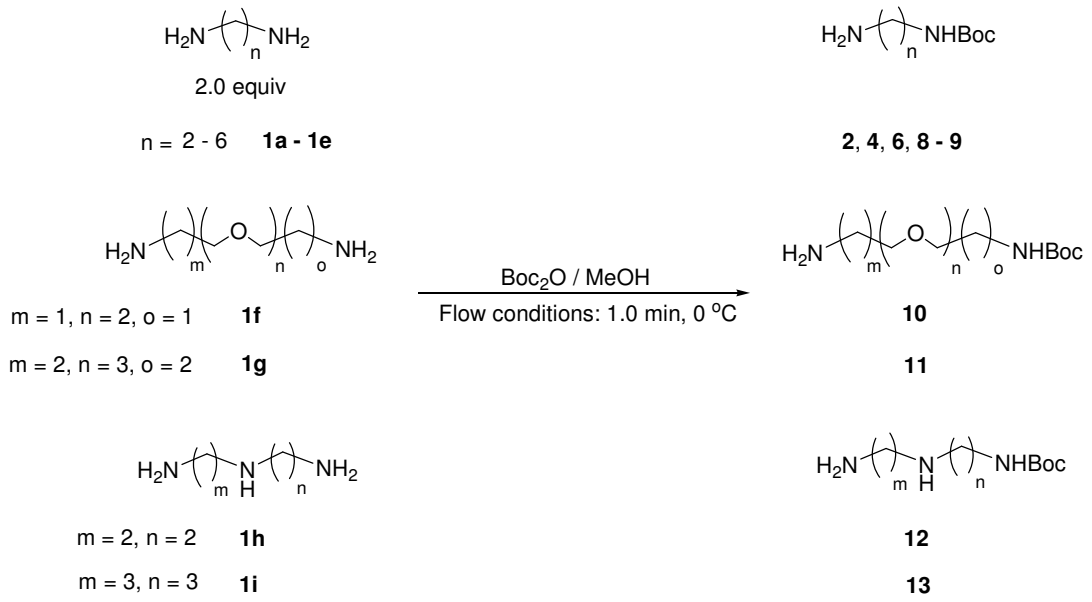

Entry	Amine	Product	Isolated Yield[i] (%)
a	**1b** 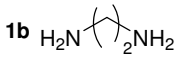	**4** 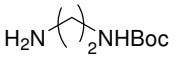	64
b	**1d** 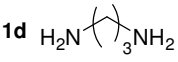	**8** 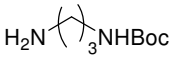	77
c	**1c** 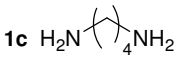	**6** 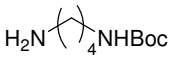	65
d	**1e** 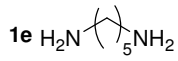	**9** 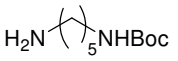	59
e	**1a** 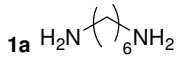	**2** 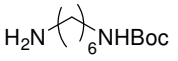	61
f	**1f** 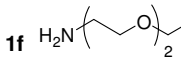	**10** 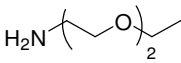	65
g	**1g** 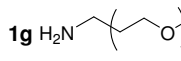	**11** 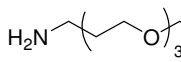	67
h	**1h** 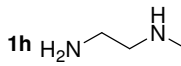	**12** 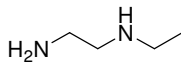	55
i	**1i** 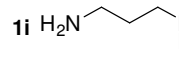	**13** 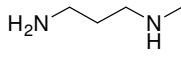	40

[i] Average isolated yield of three separate experiments per entry.

[ii] Conditions: Boc_2O (5.0 mmol) : Amine (2.00 equiv) at 0°C and 1.0 min residence time. MeOH was used as the solvent.

2.4 Mono-Fmoc Carbamation

In general, batch synthesis of *N*-Fmoc diamino compounds has proven to be remarkably problematic and there is a lack of preceding literatures on the direct synthetic access of the Fmoc-appended target molecules. The prevalent method of using a large excess of diamine over the protecting group precursor to gain mono-selectivity is not suited for mono-Fmoc protection since the Fmoc moiety is easily cleaved by free amines (i.e. working as a base in a β-elimination reaction) upon pro-longed exposure in the solution.

The most commonly used strategy thus far involves the mono-Boc protection of the diamine, followed by an Fmoc protection of the remaining free amino moiety and finally, the Boc group cleavage to give the compound of interest.[78] The three-step procedure is uneconomical and has poor atom economy due to the introduction and subsequent removal of a sacrificial protecting group.[73] This provides an excellent opportunity to demonstrate the flexibility of the continuous flow platform as it would offer superb control of reaction time in a meso-scale reaction setting.

2.4.1 Solvent and Concentration

Having established the optimal conditions for the mono-Boc carbamation of diamines, an attempt to use the same set of parameters to synthesise an analogous series of mono-protected carbamates using Fmoc as the protecting group of interest was made. Initial experiments were unsuccessful due to system blockage as a result of material precipitation within the flow reactor. The mono- and di-Fmoc-protected compounds were found to be insoluble in MeOH and instantly precipitate upon formation. Furthermore, the protecting group precursor Fmoc-OSu is rapidly hydrolysed in MeOH due to the nucleophilic nature of the solvent. Consequently, solvent screening was performed to find a suitable replacement for MeOH.

Among the polar aprotic (i.e. acetonitrile, ethyl acetate, dichloromethane, dimethylformamide and tetrahydrofuran) and non-polar (i.e. 1,4-dioxane and diethyl ether) solvents tested, only dimethylformamide afforded acceptable solubility for both the starting materials and the resulting Fmoc-protected compounds. Nonetheless, it has been observed that the solubility of diamines in DMF decreases with longer alkyl chain length and in general, a concentration of 0.10 M provided the optimal

compound solubility for all of the diamines used. As a result, the starting concentration of Fmoc-OSu was reduced to 0.05 M to retain the same stoichiometric excess of diamines to the protecting group precursor (1.0 to 2.0 equivalents). Moreover, the residence time was shortened from 1.0 to 0.5 min whilst maintaining the reaction temperature at 0°C. The reaction was quenched by dropping the crude stream into a collection vial filled with cold methanolic hydrochloric acid (– 20 ^{o}C, pH 2 – 3) [Details are illustrated in the Experimental Section as Figure 5.2a & b; page 85]. The free amino moiety was instantly protonated in the acidic solution thus preventing further reaction between the reactants.

2.4.2 Synthetic Scope

Based on the new reaction conditions, a series of mono-Fmoc protected compounds were synthesised (Table 2.3). In general, good yields ranging from 51 – 63% were obtained with the α, ω-alkanediamines with no discernible association between alkyl chain length and product mono-selectivity (entries a – d, Table 2.3). However, the use of 1,6-diaminohexane **1a** only gave a mediocre 45% yield which is lower than a statistically favourable outcome (entry e, Table 2.3). This could indicate a limitation of the method to effectively derive mono-Fmoc-alkanediamines beyond members bearing alkyl backbone longer than five methylene groups. With regard to mono-Fmoc-EG-diamines, a good selectivity was observed with a 10% yield difference between compounds bearing two and three repeating EG units (entries f vs. g, Table 2.3). Interestingly, substituting Fmoc-OSu with 9-flourenylmethoxycarbonyl chloride (Fmoc-Cl) as the protecting group precursor led to significantly lower yields (i.e. 25 – 42%) in all cases.

Table 2.3 Mono-Fmoc carbamation of diamines via continuous flow synthesis.

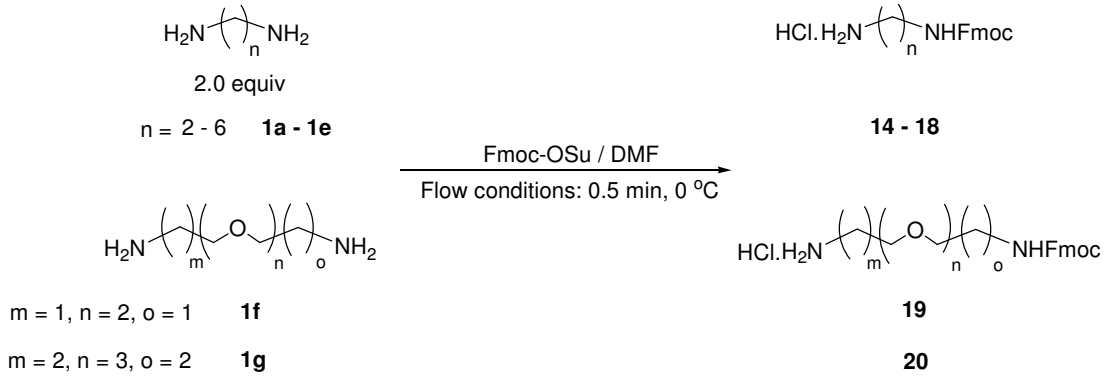

Entry	Amine	Product[i]	Isolated Yield[ii] (%)
a	**1b** $H_2N(CH_2)_2NH_2$	**14** $HCl.H_2N(CH_2)_2NHFmoc$	63
b	**1d** $H_2N(CH_2)_3NH_2$	**15** $HCl.H_2N(CH_2)_3NHFmoc$	59
c	**1c** $H_2N(CH_2)_4NH_2$	**16** $HCl.H_2N(CH_2)_4NHFmoc$	51
d	**1e** $H_2N(CH_2)_5NH_2$	**17** $HCl.H_2N(CH_2)_5NHFmoc$	62
e	**1a** $H_2N(CH_2)_6NH_2$	**18** $HCl.H_2N(CH_2)_6NHFmoc$	45
f	**1f** $H_2N(CH_2CH_2O)_2CH_2CH_2NH_2$	**19** $HCl.H_2N(CH_2CH_2O)_2CH_2CH_2NHFmoc$	61
g	**1g** $H_2N(CH_2CH_2O)_3CH_2CH_2CH_2NH_2$	**20** $HCl.H_2N(CH_2CH_2O)_3CH_2CH_2CH_2NHFmoc$	51

[i] Product exists as a hydrochloride salt due to acid quenching.

[ii] Average isolated yield of three separate experiments per entry.

[iii] Conditions: Fmoc-OSu (2.5 mmol) : Amine (2.00 equiv) at 0°C and 0.5 min residence time. DMF was used as the solvent.

2.5 Mono Enamination with the Dd*iv* Group

Whilst numerous publications have reported the selective carbamation of amines, limited progress has been made on the non-carbamate based protection route via the formation of enamine derivatives using the 1-(4,4-dimethyl-2,6-dioxocyclohexylidene)ethylene (Dde) protecting group.[79] Reactive amines that are masked as enamines are typically stable to both acidic and basic conditions, thus offering an alternative synthetic orthogonality (i.e. removal of the Dde group is

achieved via nucleophilic substitution) when used in combination with either Boc or Fmoc protecting groups.[80]

Preliminary work carried out using 1,6-diaminohexane **1a** and 2-acetyldimedone (DdeOH) produced an unstable product which rapidly rearranges after chromatographic separation.[57] Detailed investigations revealed the inherent instability of the mono-Dde protected compound as the Dde group was susceptible to nucleophilic removal of the free terminal primary amine upon product isolation. As a consequence, the Dde group freely migrates from one molecule to another resulting in the di-protected side product being the predominant species (Scheme 2.3).[81]

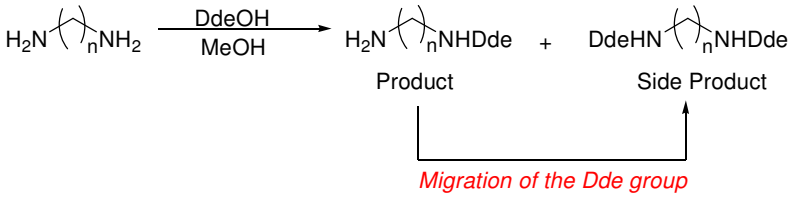

Scheme 2.3 Mono-Dde protection of diamines and the resulting Dde group migration.

In addressing the product stability issue, the protecting group precursor DdeOH was subsequently replaced with Dd*iv*OH which introduces the isovaleryl moiety adjacent to the alpha carbon (i.e. C_2) of the dimedone ring (Figure 2.4).[75]

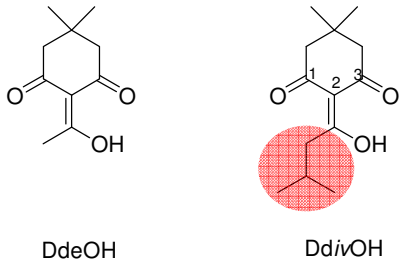

Figure 2.4 Structural difference of the Dde/Dd*iv* protecting group precursors.

Being a variant of the original Dde group, the Dd*iv* protecting group offers enhanced product stability owing to steric hindrance afforded by the isovaleryl handle. The structural modification significantly slows down the rate of protecting group migration by limiting the access of any free nucleophiles to the electrophilic β-carbon. The desired protecting group precursor was easily synthesised by reacting dimedone with pre-activated isovaleric acid to yield Dd*iv*OH.[75]

2.5.1 Temperature and Reaction Stoichiometry

Using MeOH as the reaction solvent, the best conditions for the enamination reaction were established via continuous flow screening. Taking advantage of the chromophore of the Dd*iv* group, HPLC was used as a tool to rapidly establish the favoured reaction parameters (i.e. methyl benzoate was used as an internal standard to standardise all HPLC results). The reaction was quenched by dropping the crude stream into a collection vial containing cold MeOH (–20 ^{o}C).

Among the key parameters studied, temperature was found to play the most significant role in promoting the enamination reaction. No product formation was observed below 90°C with a residence time window of two minutes. Hence, the reaction temperature was gradually increased until the mono-Dd*iv* test compound **30** was detected by HPLC analysis. When compared with the same residence time, raising the reaction temperature from 120 to 130°C consistently gave higher product yields. However, product mono-selectivity was adversely affected when the reactants were subjected to prolonged heating. At 130°C, a substantial drop in product yield was observed when the residence time was extended from one to two minutes (entries k vs. l, Table 2.4).

Hence, the exposure of reactants to elevated temperatures must be carefully controlled to avoid feeding excessive energy into the reaction system which promotes the formation of unwanted side products. With regard to reaction stoichiometry, it was shown that increasing the stoichiometric excess of the diamine from 1.2 to 2.0 equivalents improved the product mono-selectivity from 57 to 81% (entries c vs. k, Table 2.4). This demonstrates a strong positive influence of substrate concentration on the corresponding yield of the mono-Dd*iv* compound; similar to the preferential formation of mono-carbamates as discussed in earlier sections.

Table 2.4 Formation of *N*-Dd*iv*-1,6-diaminohexane **21** as a function of reaction stoichiometry, temperature and residence time.

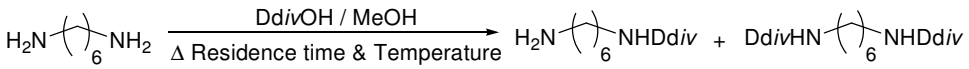

1a **21** **22**

Entry	**1a** (Equiv)	Temperature[i] (°C)	Residence Time (min)	HPLC Yield[ii] (%)
a	1.2	120	1.0	53 (1 : 0.30)[iii]
b	1.2	120	2.0	44 (1 : 0.39)
c	1.2	130	1.0	57 (1 : 0.29)
d	1.2	130	2.0	53 (1 : 0.43)
e	1.5	120	1.0	65 (1 : 0.30)
f	1.5	120	2.0	66 (1 : 0.50)
g	1.5	130	1.0	71 (1 : 0.40)
h	1.5	130	2.0	65 (1 : 0.33)
i	2.0	120	1.0	75 (1 : 0.28)
j	2.0	120	2.0	64 (1 : 0.30)
k	2.0	130	1.0	81 (1 : 0.24)
l	2.0	130	2.0	29 (1 : 2.48)

[i] System was pressurised to 5 bar.

[ii] Methyl benzoate was used as an internal standard . HPLC wavelength – 254 nm.

[iii] The integrated peak ratio of product **21** to side product **22**.

[iv] Conditions: 0.10 M Dd*iv*OH as the limiting reagent. MeOH as solvent.

2.5.2 Synthetic Scope

A series of mono-Dd*iv* protected compounds were synthesised employing the most favourable conditions found during the reaction screening stage (Table 2.5). Excellent yields (i.e. 91 & 80% respectively) were obtained with shorter members of the α, ω-alkanediamine family (entries a & b, Table 2.5). This suggests the tangible influence of a steric field exerted by the Dd*iv* group within its vicinity; thus restricting the access of the remaining free terminal amine to another Dd*iv*OH molecule.

As the backbone length increases, less of the spatial hindrance effect is transferred across the alkyl bridge resulting in a steady decline of product mono-selectivity (entries c – e, Table 2.5). Nonetheless, the inference excludes EG-diamines as a higher product yield (i.e. 71%) was obtained with a diamine molecule bearing three repeating EG units vis-à-vis its shorter analogue (entries f vs. g, Table 2.5). In order to determine the stability of the mono-Dd*iv* compounds, their half lives were

measured via HPLC analysis. With initial concentrations of 1.1 – 2.2 mM, pure mono-Dd*iv* compounds were heated to 80°C for 16.5 h. Based on the calibration curves of product concentration against time, the corresponding half lives for the compounds studied were between 8.4 and 25.4 h at 80°C (Table 2.6).

Table 2.5 Mono-Dd*iv* enamination of diamines via continuous flow synthesis.

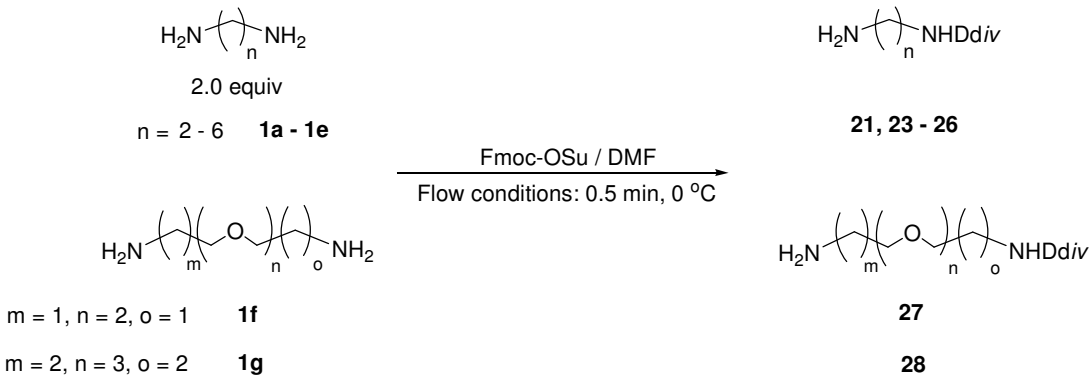

Entry	Amine	Product	Isolated Yield[i] (%)
a	**1b** $H_2N(CH_2)_2NH_2$	**23** $H_2N(CH_2)_2NHDdiv$	91
b	**1d** $H_2N(CH_2)_3NH_2$	**24** $H_2N(CH_2)_3NHDdiv$	80
c	**1c** $H_2N(CH_2)_4NH_2$	**25** $H_2N(CH_2)_4NHDdiv$	72
d	**1e** $H_2N(CH_2)_5NH_2$	**26** $H_2N(CH_2)_5NHDdiv$	72
e	**1a** $H_2N(CH_2)_6NH_2$	**21** $H_2N(CH_2)_6NHDdiv$	58
f	**1f** $H_2N(CH_2CH_2O)_2CH_2CH_2NH_2$	**27** $H_2N(CH_2CH_2O)_2CH_2CH_2NHDdiv$	63
g	**1g** $H_2N(CH_2CH_2O)_3CH_2CH_2CH_2NH_2$	**28** $H_2N(CH_2CH_2O)_3CH_2CH_2CH_2NHDdiv$	71

[i] Average isolated yield of three separate experiments per entry.

[ii] Conditions: Dd*iv*OH (5.0 mmol) : Amine (2.00 equiv) at 130°C and 1.0 min residence time. MeOH was used as the solvent.

Table 2.6 Solution half lives of *N*-Dd*iv*-diamines at 80°C.

Entry	Product	$[Conc,]_{initial}$ [i] (mM)	$t_{1/2}$ at 80°C (h)
a	**23** 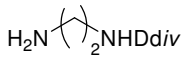	1.6	8.4
b	**24** 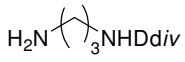	2.2	8.4
c	**25** 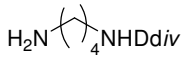	1.6	12.0
d	**26** 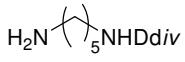	1.5	15.1
e	**21** 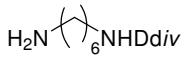	1.4	25.4
f	**27** 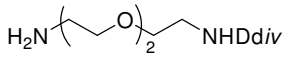	1.8	9.0
g	**28** 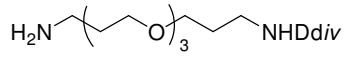	1.1	12.1

[i] Compounds were dissolved in MeOH.

2.6 Summary

A composite library of twenty three selectively mono-protected aliphatic acyclic di- and triamines was synthesised via continuous flow (Table 2.7). Members of the library, bearing three different orthogonally compatible protecting groups – Boc, Fmoc and Dd*iv*, were generated in good to excellent yields (i.e. 45 – 91%) using a meso-scale continuous flow reactor. As a result of enhanced mixing and efficient physical transport within a meso-scale environment, the continuous flow method demonstrates a high level of reaction selectivity control through a combination of spatial and temporal manipulation as opposed to conventional applications of catalysts or chemical auxiliaries. Using protecting group precursors which are commercially available (Boc_2O and Fmoc-OSu) as well as easily accessible synthetically (Dd*iv*OH), the newly developed procedure provides an economical alternative to existing synthetic routes which are costly and restrictive in scale.

Owing to the flexibility of the continuous flow system, optimal reaction conditions for a specific reaction can be easily adjusted as a function of fluid flow rate and bath temperature. In general, short residence time and low reaction temperature (i.e. 1 min at 0°C) favour the carbamation reaction whereas enamination of the diamines necessitates a considerably higher working temperature (i.e. 1 min at

130°C). As Dd*iv*OH is sterically hindered, a significantly higher reaction temperature is required to increase the rate of effective molecular collisions to facilitate the enamination reaction. With the continuous flow method, the reaction can be easily scaled out by increasing the length of experimental output without any further optimisation once the ideal conditions have been identified. This was successfully demonstrated on a 20.0 g scale continuous flow synthesis of *N*-Boc-1,6-diaminohexane **2** using the same experimental set-up and reaction parameters as described in Section 2.3.

Table 2.7 Continuous flow synthesis of mono-protected di- and tri-amines. P.G. denotes protecting group.

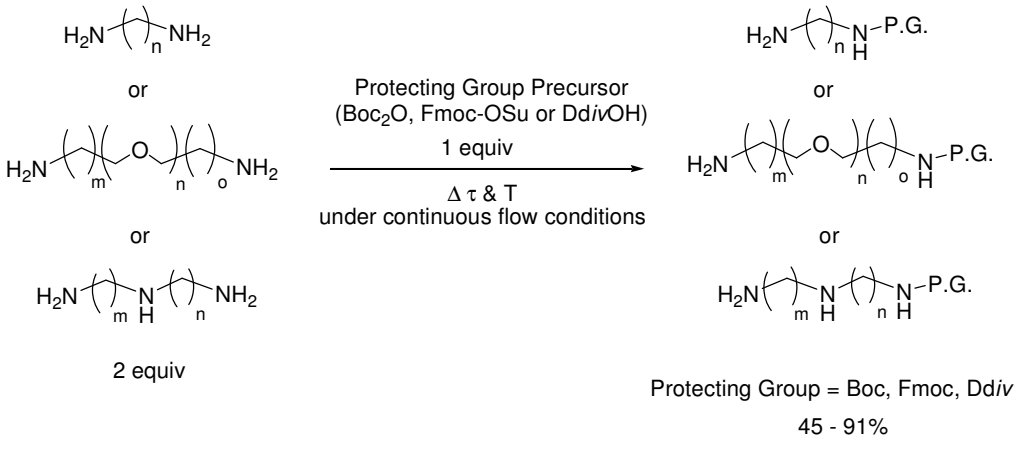

Entry	Amines	Isolated Yield (%)[i]		
		P.G. = Boc[ii]	P.G. = Fmoc[iii]	P.G. = Dd*iv*[iv]
a	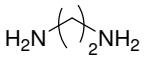	64	63	91
b	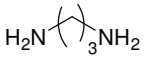	77	59	80
c	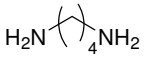	65	51	72
d	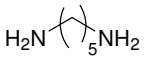	59	62	72
e	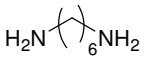	61	45	58
f	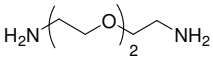	65	61	63
g	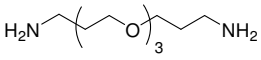	67	51	71
h	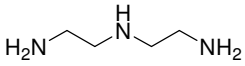	55	-	-
i	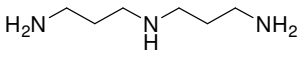	40	-	-

[i] Average isolated yield of three separate experiments per entry.

[ii] Conditions: Boc_2O (5.0 mmol) : Amine (2.00 equiv) at 0°C and 1.0 min residence time. MeOH was used as the solvent.

[iii] Conditions: Fmoc-OSu (2.5 mmol) : Amine (2.00 equiv) at 0°C and 0.5 min residence time. DMF was used as the solvent.

[iv] Conditions: Dd*iv*OH (5.0 mmol) : Amine (2.00 equiv) at 130°C and 1.0 min residence time. MeOH was used as the solvent.

CHAPTER 3

MULTI-STEP CONTINUOUS FLOW SYNTHESIS OF MONOMERS FOR PEPTOID SYNTHESIS

3.1 Background: Peptidomimetics

Peptides are superb ligands for proteins and they have immense potential as tools and agents for biological investigations.[82] Unfortunately, they can have limited *in vivo* application due to poor pharmacokinetic properties and susceptibility to proteolytic degradation.[83] As a consequence, the discovery of compounds mimicking the functions of conventional peptides but with better metabolic stability has led to the development of peptidomimetics.[84] The term *peptoid* was originally introduced by Farmer and Ariëns in 1982 to describe a broad class of peptidomimetics which exhibit the biological functionality of peptides but are structurally distinct from α-peptides.[85] In this thesis, the definition of peptoids refers explicitly to *N*-alkylglycine oligomers (Figure 3.1).[86]

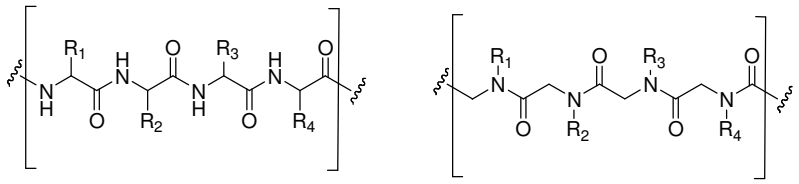

Figure 3.1 Generic structures of a conventional α-peptide compared to an oligo-*N*-substituted glycine or peptoid ($R_{1\text{-}4}$ represent side chains).

3.1.1 Peptoids as Molecular Transporters

Cellular delivery of biologically relevant cargos (e.g. genes, proteins, drugs and imaging probes) via complexation or conjugation with a transporter is of tremendous importance in cell biology.[87-91] It has great potential in medicinal applications involving the assisted delivery of synthetic probes and therapeutic agents into target cells. As a result, the development of molecular transporters that provide the highest level of cellular uptake for a broad selection of synthetic- and bio-cargos has attracted considerable attention. The role of peptoids in facilitating cellular uptake and delivery is well known and it is discussed in this section.

A breakthrough was made in the late 1980s when researchers correlated the presence of the trans-activator of transcription (Tat) protein to increased viral transcription and replication activities in HIV-infected cells.[92] Subsequent work led to the isolation of a short sequence of polypeptide, RKKRRQRRR (residues 49 to 57), identified as the primary region responsible for the translocation of the Tat protein across the plasma membrane, an amphiphilic lipid bilayer which limits the movement of molecules between the intercellular space and the cell cytoplasm.[93] The hydrophilic head group bears a negatively charged phosphate moiety whereas fatty acids make up the hydrophobic tails of the plasma membrane. In order for molecular transporters to effectively penetrate the cell membrane, they must interact with both the hydrophilic and the hydrophobic segments of the lipid bilayer.

The aforementioned sequence of basic amino acids comprising of arginines (R), lycines (K) and glutamine (Q) became the first generation of transporters known as cell penetrating peptides (CPPs).[94] They are essentially short chain peptides capable of translocating the cell membrane with remarkable efficiency. In most cases, highly permeable CPPs contain more hydrophilic residues than hydrophobic ones.[95] Peptides with side chains bearing amino or guanidinium moieties generally demonstrate high cellular internalisation even though the uptake efficiency and organelle specificity are markedly influenced by the amino acid residues involved. In intercellular environments, the peripheral amines are protonated and this promotes the interaction between the cationic side chains and the hydrophilic head groups of the cell membrane. This initial electrostatic interface eventually leads to the encapsulation of the transporters. The actual mechanism of uptake remains unclear even though recent reviews have proposed a dual pathway mechanism involving both endocytosis (active transport) and direct translocation (passive diffusion).[96,97]

Although the use of CPPs as molecular vehicles has attracted a substantial following, they are susceptible to enzymatic degradation which compromises their use as ideal transporters. As such, re-engineered analogues of CPPs which remove the proteolytic vulnerability of α-peptides but retain their cell penetrating properties have been introduced. The relocation of side chain from the α-carbon to the α-amino group prevents enzymatic recognition of the resulting *N*-alkylglycine oligomers and greatly improves their bioavailability. While stereocentres are clearly absent in peptoids, chirality is unnecessary for cellular uptake as confirmed through CPP models and studies.[98,99] It has been reported that peptoids can exhibit a three- to thirty-fold

increase in permeability compared to their peptide analogues.[95] Multiple publications have elucidated the structural characteristics of cell penetrating peptoids (CPPos) that are responsible for their impressive cell penetrating abilities.[59,95,100-102]

In general, a high density of positive charge on the side chains is identified as the hallmark of efficient molecular transporters. Nevertheless, it is not the sole determining feature as ensuing investigations have revealed other factors influencing the rate of transporter uptake. When analysing their performance, four key physicochemical properties should be taken into consideration. These include (i) lipophilicity, (ii) polar surface area (i.e. the sum of Van der Waals surface area of oxygen and nitrogen atoms, including the attached hydrogens), (iii) hydrogen bonding capacity (i.e. sum of hydrogen bond acceptors and donors), as well as (iv) side chain composition.[95] Based on the work of Kodadek *et al.*, the tertiary amides of the oligomer backbone has been attributed as the primary reason for the enhanced cellular penetration ability of peptoids. The absence of the highly polar amide hydrogens on the backbone results in lower polar surface area (PSA) in peptoids (Figure 3.2). Decreased polarity benefits cellular internalisation as formation of a hydration shell surrounding the peptoid molecule is minimised.

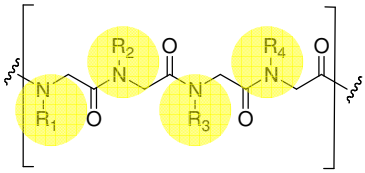

Figure 3.2 Peptoids have lower solvent accessible surface areas of heteroatoms due to the lack of amide hydrogens on their backbone.

It is hypothesised that oligo-*N*-alkyl glycines require lower desolvation energy to move from an aqueous environment (the interstitial compartment) to the fatty interior of the plasma membrane. The lower number of available hydrogen bond donors is also important as this reduces the hydrogen bond donor-acceptor interactions between the peptoid backbone and the hydrophilic head groups of the lipid bilayer. With regard to side chain composition, Wender *et al.* deduced that non-rigid and unhindered straight chain methylene spacers (between the head group and the peptoid backbone) play a decisive role in promoting translocation activity.[98] Increasing the distance between the peripheral head group and the oligomer backbone resulted in the enhancement of transporter uptake. Interestingly, peptoids bearing side

chains with guanidinium head group provided better penetration results in comparison to other types of cationic moieties but they are generally more toxic.[101,102] In addition to the preceding discussion, molecular size, volume and rigidity of peptoid structures also have minor influence on the efficacy of their cellular translocation.

Based on existing literature, there is a general consensus that amphiphilicity (i.e. the hydrophilic and hydrophobic properties of a molecule) of molecular transporters dictate their overall cell permeability. Cationic systems are fundamentally the architectural starting point in the process of designing optimum transporters. The performance of these cationic oligomers can be improved by fine tuning their amphiphatic characteristics via the incorporation of different side chain motifs.[103] In most cases, CPPos possess a homogeneous sequence of alkyl or aryl side chains even though oligomers with an alternating sequence of alkyl-aryl side chains have also been reported.[59,88] However, a conspicuous absence among the commonly used side chain motifs is the ethylene glycol (EG) moiety. The inclusion of polyethylene glycol (PEG) into dendrimeric systems has been shown to decrease the cytotoxicity of gene delivery vehicles.[104,105] Furthermore, PEGylation of dendritic polymers enhances their solubility and prolongs their circulation time in the bloodstream.[106] This provided the motivation to incorporate ethylene glycol-based side chains into peptoid transporters as these structures could potentially provide enhanced cellular penetration ability.

3.2 Background: Peptoid Monomers

In essence, peptoids are synthetically engineered polymers made of repeating *N*-substituted glycine units. Peptoids are typically synthesised via solid phase peptide synthesis (SPPS) involving the stepwise addition of the desired monomers.[86,107] The SPPS method is well suited to laboratory scale synthesis and has good synthetic efficiency up to approximately 50 residues.[108] The SPPS strategy has been widely adopted by many research laboratories.[59,98,109] Moreover, a high level of purity of the target peptoids can be obtained using an optimised synthetic route which negates further downstream purification.[110]

Gaining access to structurally creative peptoids necessitates the availability of *N*-substituted glycine monomers. These structurally diverse monomers are responsible for the unique properties observed on peptoids and the structure-activity relationship of peptoids has been well elucidated by several different research groups.[87,88,95,111]

Published work has described a diverse range of monomers over the years; consisting of alkyl or aryl side chains with acidic, basic or neutral moieties. The architecture of these monomers can generally be simplified into two main parts – the glycine core and the chemically decorated side chain which is connected to the glycine amine (Figure 3.3). Two different synthetic approaches can be used to assemble a target monomer.

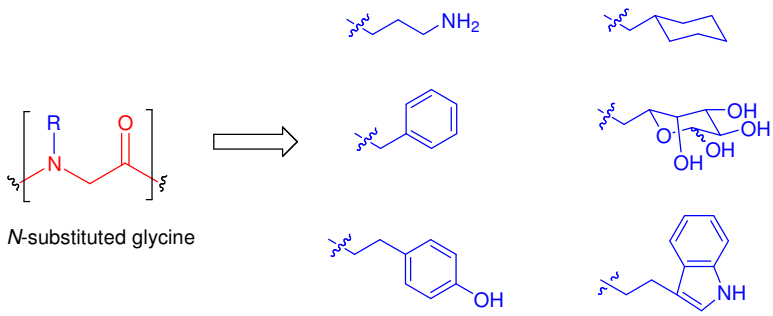

Figure 3.3 Glycine core of a peptoid monomer (in red) and selected examples of side chains, R (in blue), as reported in the literature.[88]

The first method involves constructing the monomer through a series of sequential steps employing solution phase chemistry to give the desired monomeric building block (Figure 3.4a).[110,112] The end product is then used in solid phase analogous to the role of amino acids in solid phase peptide synthesis. The alternative strategy uses a "sub-monomer" method which directly builds the monomer, unit by unit, on solid phase through a repetitive cycle of amide coupling and nucleophilic substitution utilising submonomers (Figure 3.4b).[113] The availability of a vast library of commercially available reagents highlights the unique advantage of the sub-monomer approach. Furthermore, it circumvents the need for a main chain protecting group as haloacetic acid ($BrCH_2CO_2H$) directly couples to the amine after pre-activation with a carbodiimide.

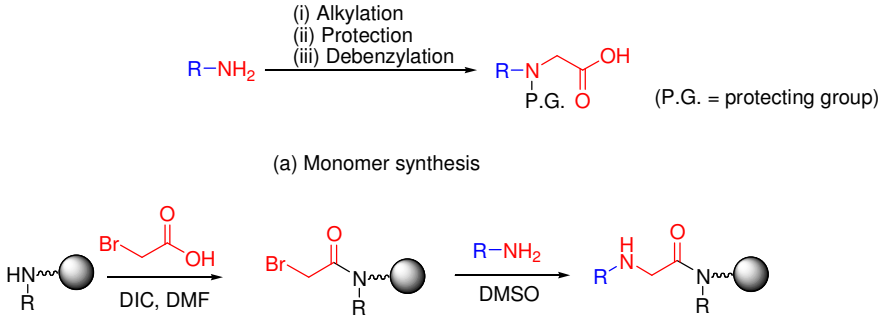

Figure 3.4 Comparison of the monomer vs. sub-monomer methods.[112,113]

Subsequently, the second half of the sub-monomer is introduced via a nucleophilic substitution reaction with a primary amine displacing the halogen and generating a new secondary amine which allows the propagation of the target compound. Both strategies were introduced by Zuckerman *et al.* and have since been extensively adapted by other research groups.[114] The sub-monomer method negates the need for pre-made monomers and is intuitively easier to apply. However, side reactions could lead to poor yields and low purity of the target compound.

On the contrary, the use of peptoid monomers during SPPS involves the iterative cycle of main chain protecting group cleavage and amide coupling. Each monomer is fundamentally a protected *N*–substituted glycine unit which proliferates the peptoid chain. Prior to the invention of the sub-monomer method, Zuckerman *et al.* synthesised multiple monomers to be used in peptoid assembly. However, the productivity of their synthetic endeavours was the rate limiting factor in generating enough compounds to be used for subsequent downstream processes.[114] As a consequence, the development of an alternative synthetic method which could address the shortcomings of existing solution phase chemistry would undoubtedly provide a much needed answer to rapidly produce motif-specific monomers in high yields.

3.3 Background: Batch Synthesis of Peptoid Monomers

The optimisation work presented in this chapter discusses the synthesis of the *N*-Fmoc-(6-Boc-aminohexyl)glycine monomer. Bradley *et al.* developed a four-step route which begins with the mono-Boc protection of 1,6-diaminohexane (Scheme 3.1).[115] The *N*-Boc-protected compound was then mono-alkylated with ethyl bromoacetate, followed by saponification to liberate the acid moiety. The last step involves an Fmoc carbamation of the secondary amine using Fmoc-OSu which gives the desired compound. The Boc and Fmoc protecting groups are appended to the monomer to facilitate peptoid chain assembly on solid support using an Fmoc-SPPS strategy, with the Boc group removed in the final step. The procedure suffered from a relatively moderate yielding alkylation reaction (55%) and a low yield for the ester saponification and Fmoc carbamation steps (40%).

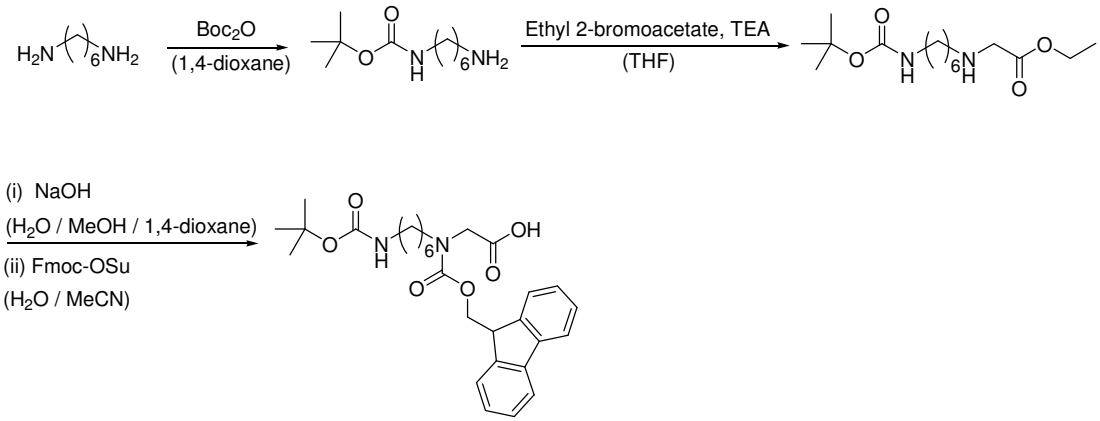

Scheme 3.1 A sequential synthesis of the *N*-Fmoc-(6-Boc-aminohexyl)glycine monomer.[115]

The aforementioned synthetic route was later re-optimised by substituting ethyl 2-bromoacetate with benzyl 2-bromoacetate to allow replacement of the saponification step with a hydrogenation procedure (Scheme 3.2).[112] While the first two steps remain unchanged, the Fmoc carbamation is performed immediately after the alkylation reaction in the new sequence. The liberation of the acid functionality is achieved by palladium-catalysed hydrogenolysis to remove the benzyl protecting group, thus giving the target monomer. The mono-protection step was carried out with a large excess of the diamine substrate over the protecting group pre-cursor. Although the procedure is well established and gives seemingly good results, it is synthetically

inefficient (i.e. 6 equivalents of diamines to the limiting reagent). Chapter 2 of this thesis was dedicated to the selective mono-protection of di- and triamines.

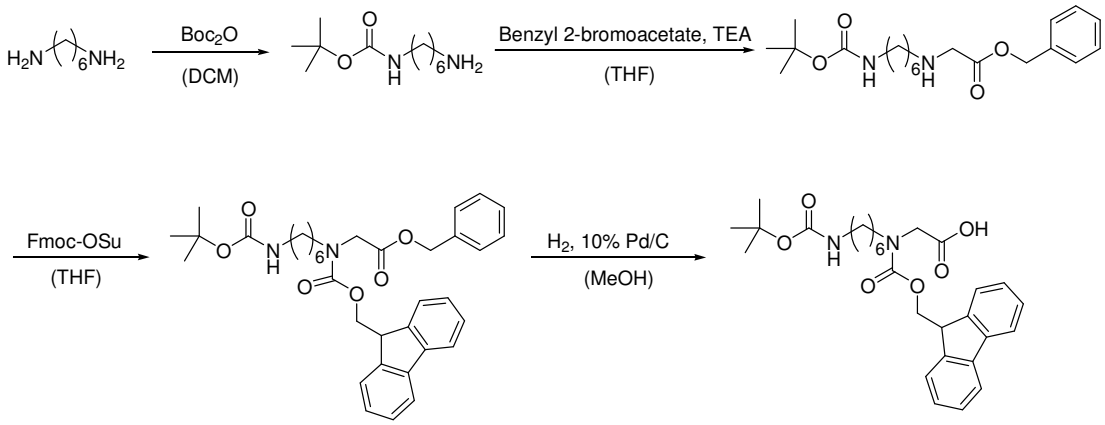

Scheme 3.2 An alternative route leading to the *N*-Fmoc-(6-Boc-aminohexyl)glycine monomer.[112]

In the original route, an inorganic base was added to hydrolyse the ester but careful control of the succeeding reaction condition was necessary to prevent the formation of an anhydride between the Fmoc protecting group precursor and the free acid (Scheme 3.1, step [iii]). The modified strategy introduced the use of benzyl 2-bromoacetate as the alkylating agent of choice as the benzyl ($-CH_2Ph$) protecting group can be easily removed by a catalytic hydrogenolysis process. This eliminated the saponification reaction which then allowed the base labile protecting group to be introduced following the mono-alkylation of the free primary amine. Changing the reaction sequence proved to be highly beneficial as the Fmoc carbamation step demonstrated improved reaction yields. However, the final step of Pd-catalysed batch hydrogenolysis proved to be challenging due to several reasons.

The Fmoc group can be susceptible to hydrogenolytic cleavage upon prolonged exposure to palladium and hydrogen.[74] In a batch environment, the contact time between substrate, reagent and catalyst is immensely difficult to control. Furthermore, there are inherent safety concerns when scaling up the reaction due to the reactivity of hydrogen in the presence of the palladium catalyst. As a consequence of the drawbacks highlighted, developing a more refined method of sequential synthesis is highly attractive in lieu of the continued use of batch chemistry. The continuous flow method provides an ideal platform in offering new opportunities to improve the overall efficiency of the peptoid monomer synthesis.

3.3.1 Pre-Flow Model Reaction

A direct transfer of reaction conditions from batch mode to the flow platform is typically not possible due to the risk of solvent incompatibility, among other things, which promotes material precipitation during the reaction.[32] Hence, reaction screening was initially performed in batch to observe the behaviour of each transformation in the three-step sequence (Scheme 3.3). The monomer synthesis begins with *N*-Boc-1,6-diaminohexane **2** which serves as the N^{ω}-protected side chain of the monomer unit. Using benzyl 2-bromoacetate as the alkylating agent and triethylamine as the base, spontaneous material precipitation (i.e. TEA-bromide salt) was observed in single- or mixed-solvent systems of 1,4-dioxane, DCM and THF. Acetonitrile provided complete solubility of the reaction mixture and gave the mono-alkylated compound **29a** in a modest yield of 59% after isolation.

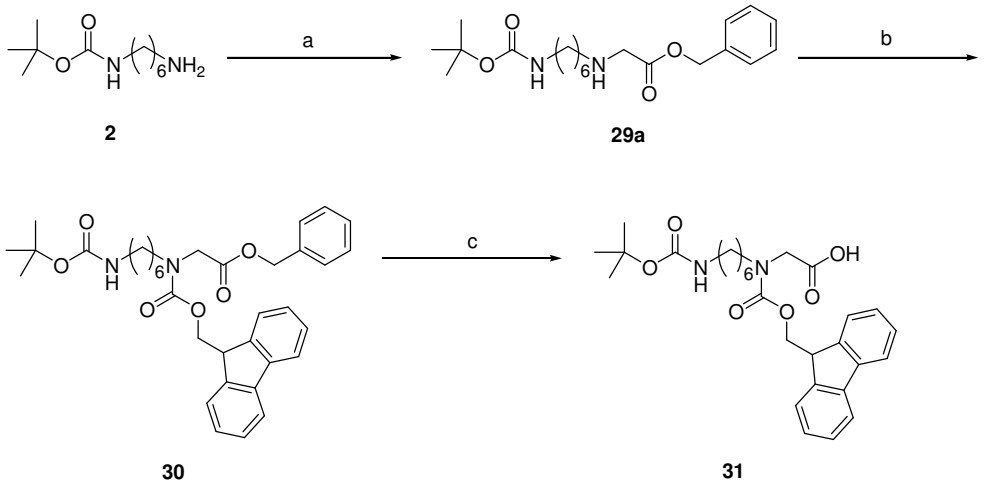

Scheme 3.3 Batch synthesis of monomer **31**. Reagents and conditions: (a) benzyl 2-bromoacetate (1 equiv), TEA (3 equiv), MeCN, 18 h, 59%; (b) Fmoc-OSu (1 equiv), MeCN, 18 h, 98%; (c) NH_4HCO_2 (2.5 equiv), 10% Pd/C (8.0 mol%), EtOH, 19 min, 54%.

Subsequently, the mono-alkylated compound was reacted with Fmoc-OSu to give the Fmoc-protected benzyl acetate **30.** Even though material solubility ceased to be a problem at this stage, performing the reaction in DCM gave 78% yield whereas the use of MeCN gave close to quantitative yield post chromatographic purification. The final step of benzyl group removal utilising heterogeneous Pd-catalysed transfer hydrogenolysis was performed in ethanol; employing ammonium formate and 10% Pd/C as the hydrogen donor / catalyst pairing.[116] At a catalyst loading value of 8.0 mol%, the reaction was complete within 19 min (based on HPLC analysis) and gave

the monomer **31** in a final purified yield of 54%. In-house experiments also confirmed published reports of the lability of the Fmoc group under hydrogenolysis conditions.[117,118] Hence, the delicate control of reaction time is a prerequisite in preventing the unwanted removal of the Fmoc protecting group from the monomer.

3.4 Selective Alkylation in Flow

The following section focuses on the continuous flow synthesis of benzyl 2-(6-Boc-hexylamino)acetate **29a** (Scheme 3.4). In general, the alkylation reaction in batch produces inconsistent results as a consequence of over-alkylation. Due to an inductive effect, the secondary amine product is innately more nucleophilic compared to its pre-cursor. Upon formation of the mono-alkylated compound, a consecutive competitive reaction takes place leading to the generation of the di-alkylated species. Hence, the explicit goal of the alkylation reaction in flow was to achieve a high degree of mono-alkylation and minimising excessive di-alkylation. In the following discussion, the progress of the alkylation reaction was monitored via HPLC and the best parameters were quickly established based on the screening results.

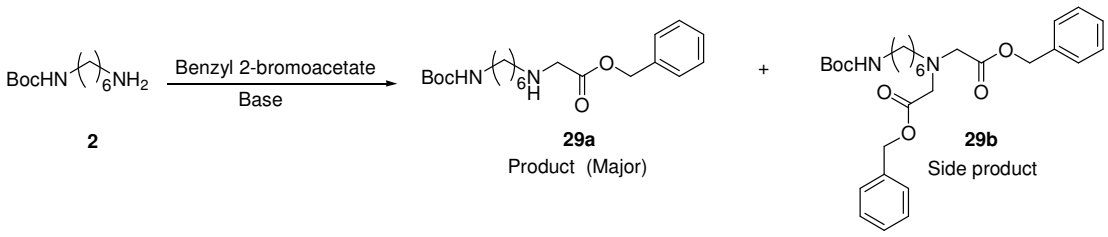

Scheme 3.4 Alkylation of *N*-Boc-1,6-diaminohexane **2** leads to the formation of the product **29a** and a competing side product **29b**.

3.4.1 Solvents

As the nucleophilic attack occurs on the halogen-bearing carbon, a bromide anion is liberated and it readily abstracts a proton from the quaternary nitrogen centre. Thus, a mole of hydrogen bromide is generated and serves as a source of acid in the reaction mixture. In order to prevent the protonation of the nucleophile, an organic base is typically used to neutralise the acidic species. As a result, the base-halide salt spontaneously crashes out in non-compatible solvent systems as described in Section 3.3.1. Performing the alkylation reaction in the continuous flow set-up necessitates the

use of a polar medium and four different organic solvents – DCM, DMF and MeCN (polar aprotic) as well as MeOH (polar protic), were tested.

Material precipitation was only observed in DCM while the rest afforded complete solubility due to their increased polarity. Using three equivalents of DIPEA and a substrate concentration of 40 mM, MeCN gave a higher product yield compared to DMF (i.e. 85 vs. 69% based on HPLC analysis) when the reaction was carried out under flow conditions (τ – 3 min and T – 100°C). In addition, MeCN also produced a better ratio of product to side product relative to the values obtained in DMF (Entries b vs. c, Table 3.1). Unsurprisingly, MeOH gave a dismal 14% yield using the same reaction conditions (Entry a, Table 3.1). The nucleophilic solvent is unsuited for the reaction as it reacts readily with the alkylating agent leading to a loss of reactant.

3.4.2 Residence Time and Temperature

The residence time was initially set at 3 min as very low starting material conversion was observed below this duration. A window of reaction temperatures between 80 to 130°C were tested and the maximum yield was observed between 100 and 110°C (Figure 3.5). Using MeCN as the solvent, the working pressure of the system exceeded 2 bar at 107°C and increasing the temperature beyond 110°C had a detrimental effect on the yield of the reaction. The alkylation step did not benefit from a pro-longed exposure to high reaction temperature as increasing the residence time by an extra two minutes at 90°C led to a drop in reaction yield. This observation was later confirmed with other elevated temperature set points. Thus, an obvious trend emerged from this study correlating shorter residence time at higher temperature with better mono-alkylation yields.

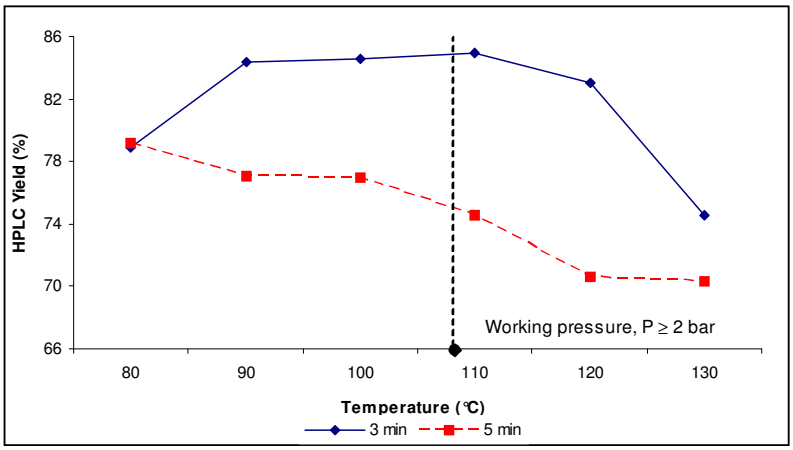

Figure 3.5 Continuous flow alkylation of *N*-Boc-1,6-diaminohexane **2** with a 3 vs. 5 min residence time.

3.4.3 Base and Substrate Concentration

Having established the optimal residence time and reaction temperature, other reaction parameters were evaluated. In the alkylation reaction, an excess of organic base was used to prevent deactivation of the nucleophile. Three equivalents of selected organic bases were tested for their effectiveness in the reaction. Both 1,8-diazabicycloundec-7-ene (DBU) and piperidine gave very low yields in the alkylation reaction (Entries d & e, Table 3.1). A highly probable cause is the reaction between the alkylating agent and the organic bases which occurs preferentially over the nucleophilic attack of the primary amine substrate. While piperidine is a known nucleophile, an amidine base such as DBU is typically classified as non-nucleophilic. However, in-house experiments confirmed published findings with regard to the less conspicuous nucleophilic nature of DBU.[119] As such, two tertiary amine bases (TEA and DIPEA) which are sterically hindered, were chosen for further testing. Interestingly, DIPEA afforded a better yield compared to TEA (i.e. 85 vs. 69%) using the same reaction conditions (Entries c vs. f, Table 3.1).

As the productivity of a flow reaction is correlated to the substrate concentration, the molarity of *N*-Boc-1,6-diaminohexane **2** was increased from 40 to 100 mM in anticipation of retaining the high mono-alkylated yield. Unfortunately, the reaction yield dropped by 15% with only a slight change in the product to side product ratio in favour of the di-alkylated species (Entry h, Table 3.1). The results indicated that the conversion of starting material to product was less effective at increased concentrations. Thus, in order to generate a larger quantity of the desired

compound, an optimised flow reaction should simply be allowed to run longer with minimal adjustment to its substrate concentration. When seen from a method design perspective, it was interesting to note that a lower product yield was observed when both reagent and substrate were not subjected to the pre-heating treatment described in Section 2.2 of Chapter 2 (Entry g, Table 3.1).

3.4.4 Flow versus Batch and Microwave Methods

A series of comparison was made between the continuous flow experiments and several variations of the alkylation reaction in batch mode. Firstly, the alkylation reaction was subjected to microwave irradiation to mimic the high thermal transfer efficiency of a flow set-up. At 68% yield, rapid heating to the desired working temperature using microwave irradiation appeared to favour the formation of the mono-alkylated product over the side product (Entry i, Table 3.1). It is postulated that the rapid heating afforded by microwave irradiation generates a uniform thermal profile within the reaction system as opposed to the formation of localised hot spots when the reaction system was subjected to a normal heating process.[120]

This was supported by the evidence obtained from another set of experiment which employed conventional heating using a standard laboratory oil bath. In addition to a less favourable product to side product ratio, the product yield was 8% lower compared to the microwave irradiated reaction (Entry j, Table 3.1). Further investigations revealed that in a room temperature reaction that was left to stir for 24 h, the side product formation was almost two and half times more than that observed in the microwave reaction. However, prolonging the reaction at room temperature did increase the product yield by as much as 12% as the extended time drives the reaction to completion (Entry k, Table 3.1).

Table 3.1 Formation of benzyl 2-(6-Boc-hexylamino)acetate **29a** as a function of various reaction parameters.

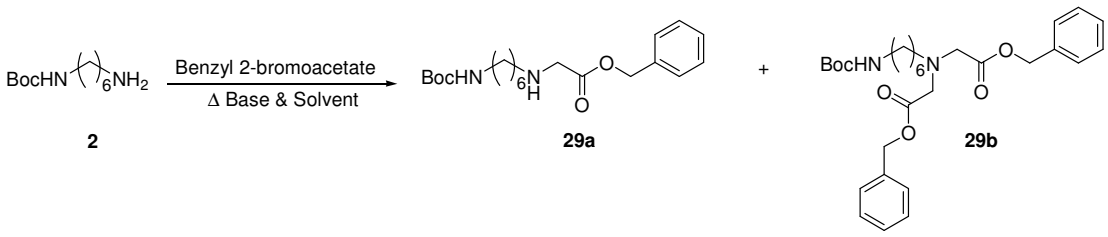

2 **29a** **29b**

Entry	Method	Solvent	Base	Conditions[i] ([Substrate] / Heating mode)	HPLC Yield **29a**[ii] (%)
a	Flow	MeOH	DIPEA	[40 mM], reactor in oil bath	14
b	Flow	DMF	DIPEA	[40 mM], reactor in oil bath	69 (1 : 0.16)[iii]
c	Flow	MeCN	DIPEA	[40 mM], reactor in oil bath	85 (1 : 0.10)
d	Flow	MeCN	Piperidine	[40 mM], reactor in oil bath	6
e	Flow	MeCN	DBU	[40 mM], reactor in oil bath	10
f	Flow	MeCN	TEA	[40 mM], reactor in oil bath	69 (1: 0.06)
g	Flow	MeCN	DIPEA	[40 mM], no pre-heating	69 (1 : 0.08)
h	Flow	MeCN	DIPEA	[100 mM], reactor in oil bath	70 (1 : 0.11)
i	Batch	MeCN	DIPEA	[40 mM], μwave irradiation	68 (1 : 0.05)
j	Batch	MeCN	DIPEA	[40 mM], tube in oil bath	60 (1 : 0.09)
k	Batch	MeCN	DIPEA	[40 mM], 24 h at r.t.	80 (1 : 0.12)

[i] Scale of each experiment – 20 μmol. Conditions: τ – 3 min, T – 100°C, Flow reactor volume – 2 mL

[ii] Methyl benzoate was used as an internal standard. HPLC wavelength – 254 nm.

[iii] The integrated peak ratio of product **29a** to side product **29b**.

Based on the results presented, the continuous flow method provided the optimum solution in deriving the mono-alkylated compound with good yield as well as superior speed of access. Hence, using the optimised conditions, the reaction was scaled out with a 4 mL flow reactor to produce ~ 1.00 g of the mono-alkylated compound **29a** at 67% isolated yield in approximately five hours (Scheme 3.5). An analogue of the compound, bearing a triethylene glycol (TEG) bridge between two terminal amino moieties **32**, was also produced in similar scale at 60% purified yield.

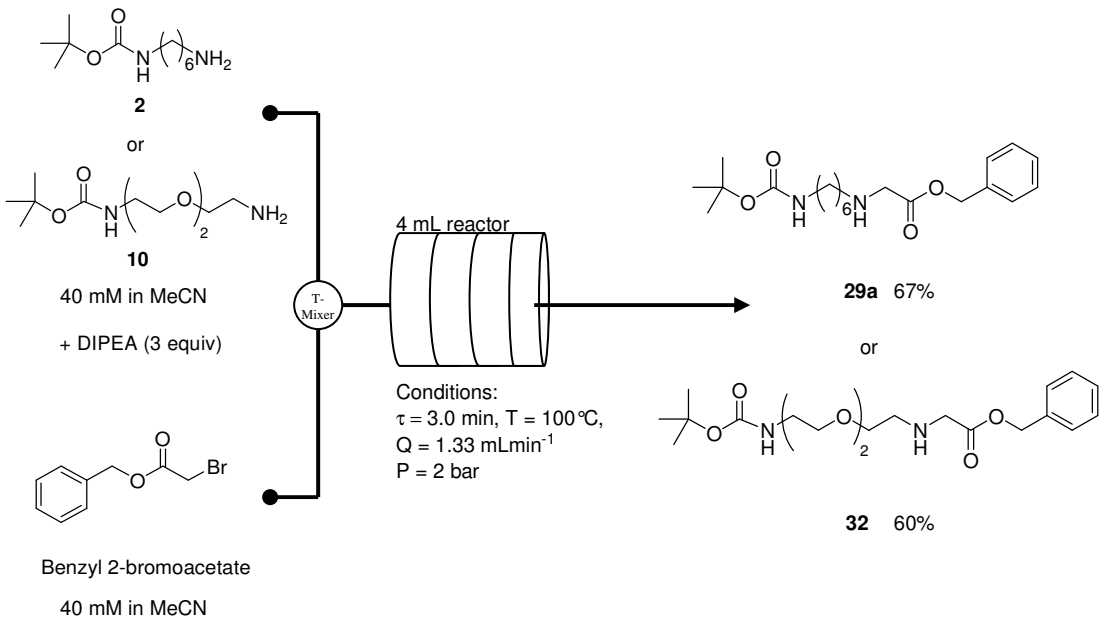

Scheme 3.5 Single step flow alkylation of *N*-Boc-diamino compounds **2** or **10** to give the mono-alkylated products **29a** or **32**.

3.5 In-Line Scavenging of Excess Alkylating Agent

The continuous flow alkylation reaction was performed in a single step. It was vital to quench the reaction stream, post flow reactor, in order to remove the excess alkylating reagent. The crude solution was collected into a flask containing scavenging resin which captures the unreacted alkylating agent prior to reaction work-up. The crude mixture was purified by flash column chromatography to give the isolated product. While this approach is useful in a single step transformation, a sequential continuous flow reaction requires an in-line scavenging procedure which could scavenge the alkylating agent from the first exiting stream before being fed into the next reaction.[121] This would remove the need for an intermediate process of column purification after the first reaction stage and allow the integration of two cascading steps (alkylation and Fmoc carbamation).

Two different silica-based scavengers, Si-Thiol (loading value: 1.43 $mmolg^{-1}$) and Si-Trisamine (loading value: 1.58 $mmolg^{-1}$), were chosen as potential candidates due to the silica core's inert stability and non-swelling properties in organic solvents (Figure 3.6). Both scavengers were packed into their respective columns and tested for their scavenging efficiency. In a typical set-up, an exiting stream from the alkylation reaction (after the back-pressure regulator) was connected directly to the

scavenging column (Scheme 3.6). The efficiency of each scavenger species was then determined based on the HPLC analysis of the reaction stream post scavenging.

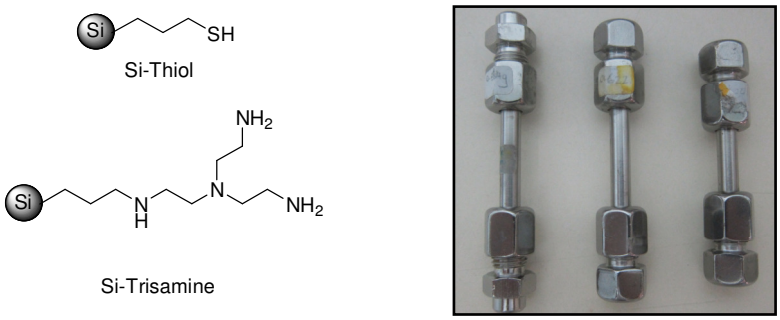

Figure 3.6 (Left) Silica-based thiol (Silicycle's Siliabond) and tris-amine (Biotage's ISOLUTE) scavengers; (Right) Columns packed with scavenger resin (diameter x length: 0.5 x 5.0 / 6.0 cm).

Based on qualitative analysis, the Si-Trisamine scavengers were more effective in removing the excess alkylating agent relative to the mercaptan particles under the same reaction conditions. This could be a consequence of the deactivated sulfhydryl moiety which slowly undergoes oxidation at ambient conditions. As a result, Si-Trisamine was chosen as the in-line scavenger for the two-step transformation process. For an alkylation reaction at 4.9 mmol scale, a column measuring 0.5 x 6.0 cm (diameter x length) packed with 0.62 g of Si-Trisamine scavengers was used to remove unreacted alkylating agent from the exiting reaction stream. Hence, roughly 0.60 g of trisamine scavengers is consumed for every gram of product made.

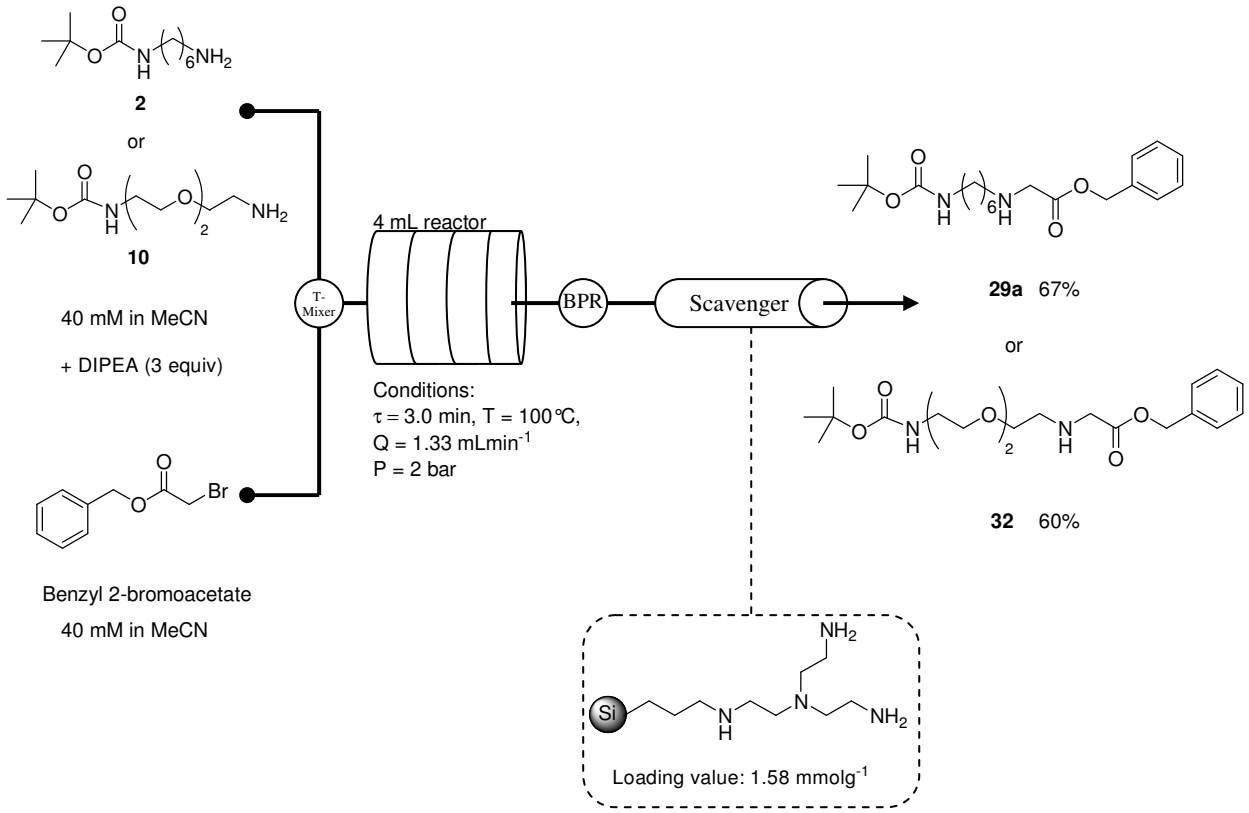

Scheme 3.6 In-line scavenging protocol of unreacted alkylating reagent.

3.6 Fmoc Carbamation in Flow

Prior to performing the two-step sequential transformation (linking alkylation to Fmoc carbamation directly), the one step synthesis of the Fmoc-protected compound **30** was attempted in flow (Scheme 3.7). In a direct adaption of the reagent used in batch synthesis, Fmoc-OSu was used as the protecting group precursor to introduce the Fmoc synthon and the reaction was performed at room temperature in MeCN. With a substrate concentration of 20 mM and one equivalent of Fmoc-OSu, a minimum of 3 min was required to facilitate the complete conversion of the mono-alkylated compound **29a** to its Fmoc-protected analogue **30**. After reaction work-up, the Fmoc-protected compound was obtained in excellent yield at 98%. Changing the solvent system proved to be detrimental to the product yield as DCM only gave 78% yield whereas an equal mixture of 1,4-dioxane and DCM led to a further 16% slide in the purified yield. Likewise, the TEG analogue **33** also gave close to quantitative yield when synthesised via the continuous flow method.

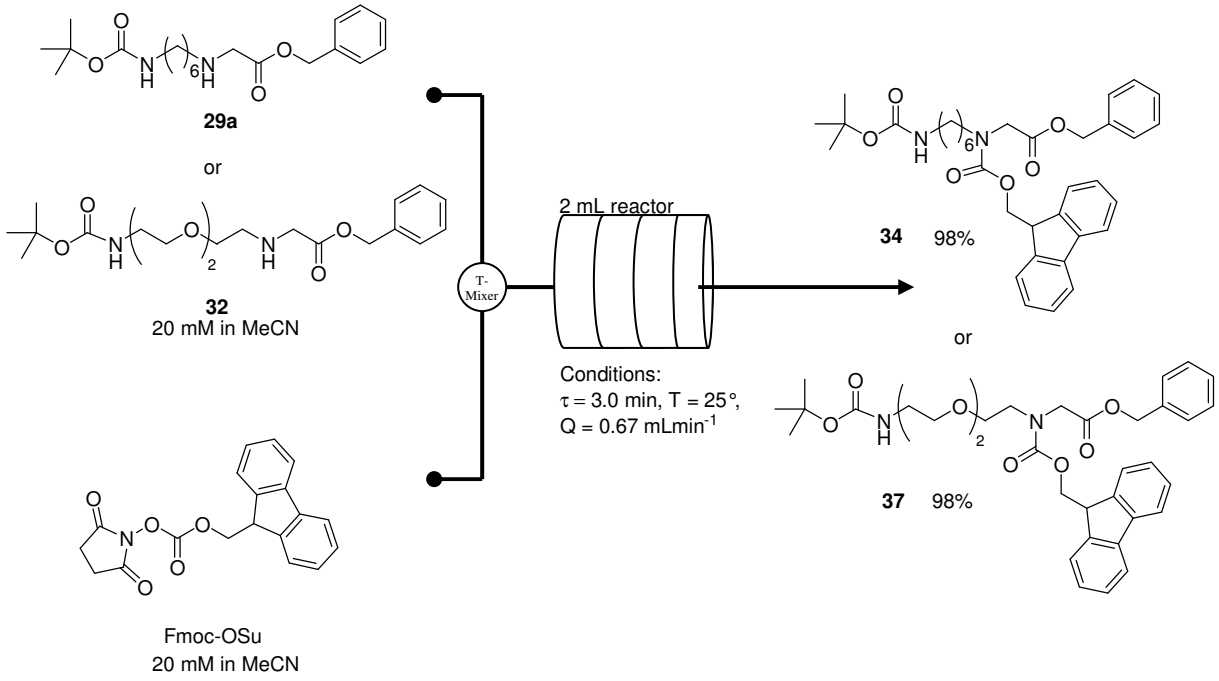

Scheme 3.7 Single step flow carbamation of N^{α}-alkyl-N^{ω}-Boc-diamines **29a** and **32** to give the Fmoc-protected compounds **30** and **33**.

3.7 Tandem Alkylation and Fmoc Carbamation in Flow

The goal of the sequential continuous flow reaction was to remove the intermediate purification step which is both labour intensive and time consuming. The ability to link two cascading reactions into a single transformation sequence is highly appealing as it increases the synthetic efficiency of the overall transformation. The removal of the flash chromatography procedure has the distinct advantage of reduced material consumption. Nonetheless, in order to merge two different synthetic transformations into a single sequence, the exiting stream of the first reaction must be fully compatible with the reaction conditions of the subsequent conversion. As such, the overall conversion must be viewed as a continuous process which demands complete reagent solubility and minimal occurrence of unwanted side reactions.

In reviewing the two-step transformation of the *N*-Boc-protected diamines to their Fmoc-protected alkyl analogues, the requirement of chromatographic purification between the first and the second stage was addressed by introducing a silica-based trisamine scavenging column to remove the excess alkylating agent (Section 3.5). However, the use of DIPEA during the alkylation step carries the risk of initiating the Fmoc group cleavage in the succeeding downstream reaction. As a

result, the original design of a seemingly straight forward synthetic route had to be revised accordingly. A decision was made to switch the Fmoc precursor to FmocCl. The nucleophilic attack on the protecting group precursor would liberate a chloride anion which forms an equivalent of hydrochloric acid. Under normal conditions, the acid would protonate the secondary amine and thus, deactivates the nucleophile. However, as the first reaction stream contains an excess of DIPEA, the base would neutralise the acid readily and protects the nucleophile from *in situ* passivation.

Armed with the modified sequence, the two-step transformation was carried out as depicted in Scheme 3.8. It is important to note that a cooling process (using water bath) was introduced after the scavenging protocol to cool down the first reaction stream prior to the second stage mixing (Details are illustrated in the Experimental Section as Figure 5.8; page 112). With an equal residence time of 3.0 min for both the alkylation and Fmoc carbamation steps, respectively; the syntheses of **30** and its TEG analogue **33** gave 69 and 62% yields over two steps. In a scale-out reaction spanning slightly over six hours, 1.4 g of the Fmoc-protected benzyl acetate **30** was produced from 4.9 mmol of *N*-Boc-1,6-diaminohexane **2**. The experiment was also successfully repeated on a similar scale using *N*-Boc-1,8-diaminotriethylene glycol **10** as the precursor molecule to produce the Fmoc-protected TEG compound **33**.

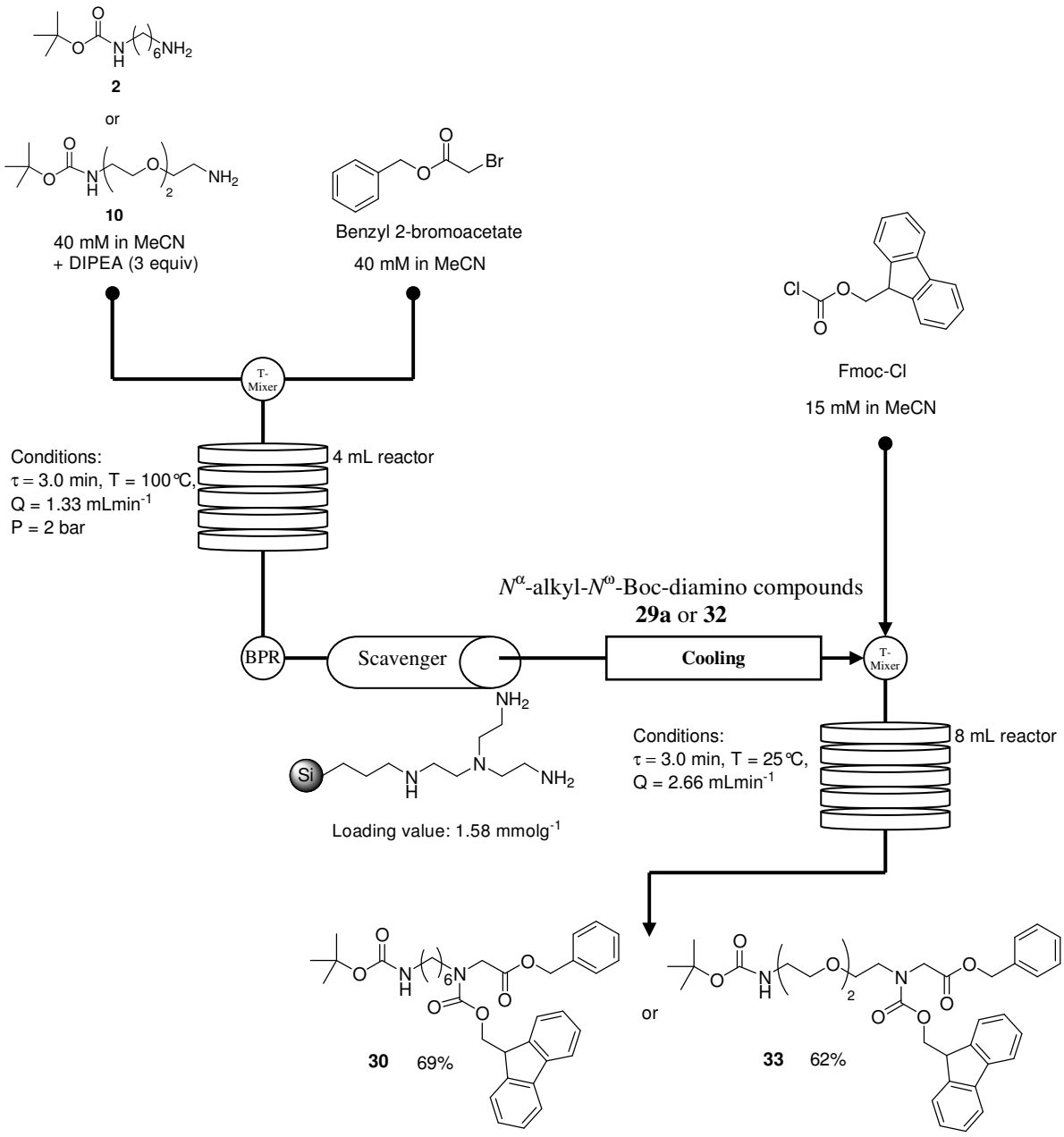

Scheme 3.8 Tandem alkylation and Fmoc carbamation as a continuous sequence.

3.8 Catalytic Hydrogenolysis in Flow

The last stage of the monomer synthesis involves the catalytic hydrogenolysis of the Fmoc-protected benzyl acetate compound **30** to derive its debenzylated analogue **31**. The heterogeneous catalysis reaction typically uses a solid supported transition metal as the catalyst and a source of molecular hydrogen is required to facilitate the chemical transformation.[122] The versatility of the palladium metal is well described in the literature and it remains as the one of the most popular transition metals in

promoting a wide range of chemical reactions.[123,124] Specific to the hydrogenolysis reaction, an interesting side reaction has been detected during the batch synthesis of the target peptoid monomer (Scheme 3.9).

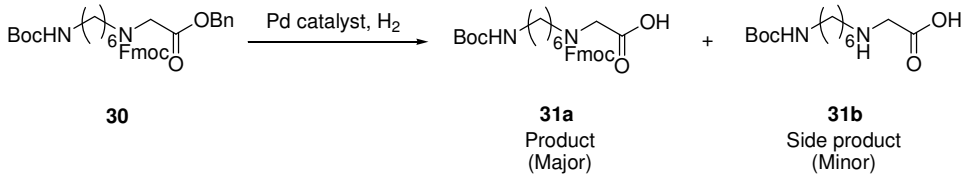

30 **31a** Product (Major) **31b** Side product (Minor)

Scheme 3.9 Palladium-catalysed debenzylation and its side reaction.

It has been found that the Fmoc protecting group is labile towards palladium-catalysed hydrogenolysis. While the removal of the benzyl group remains as the primary effect of the reaction, the Fmoc group is unwittingly cleaved depending on the reactivity of the catalyst, the duration of reaction and the substrate concentration. Similar observations have been reported in the literature and the side reaction affects both the conventional method of performing hydrogenolysis (i.e. hydrogen gas with catalyst) as well as catalytic transfer hydrogenation (i.e. the generation of molecular hydrogen *in situ* via a hydrogen donor).[118,125] In order for hydrogenolytic cleavage to take place, a suitable leaving group (e.g. carboxylate anions) must be present and the resulting carbenium ion must also be sufficiently stabilised.[126]

The preferential cleavage of the benzyl group over the Fmoc group could occur as a result of steric limitation exerted by the large fluorenyl ring. As the catalytic cycle takes place on the palladium metal, the substrate must be correctly aligned to the catalyst surface in order for the hydrogen transfer process to occur.[127] As the fluorenyl moiety is more bulky relative to the benzyl group, achieving the correct molecular orientation would be mechanistically harder. As a result, a particular interest in performing the catalytic flow hydrogenolysis is to generate a high degree of selectivity during the reaction *sans* Fmoc group removal. It was hypothesised that facile manipulation of contact time between the catalyst and the substrate could be exploited to promote a high level of reaction selectivity during the transformation process.

In addition, other types of transition metal catalysts which have been reported to be effective in encouraging selective hydrogenolysis were also tested for their efficacy in promoting the debenzylation reaction.[128] A decision was made to develop

transfer hydrogenation in flow due the practical aspects of instrumentation. Microwave-assisted catalytic hydrogenolysis was also attempted in order to derive a comparison between flow transfer hydrogenolysis and the microwave method.

3.8.1 Continuous Flow Transfer Hydrogenolysis

The continuous flow transfer hydrogenolysis reaction was performed using ThalesNano's CatCart catalysts. Each cartridge measures 30 mm in length with a diameter of 4 mm and has an average weight loading of 150 mg (i.e. mass of solid supported catalyst).[129] It is conveniently inserted into a hollow aluminium chamber which can be digitally heated to the desired working temperature (Figure 3.8). Specific to the hydrogenolysis reaction, an ethanolic stream of reactants containing the substrate and hydrogen donor was passed through the CatCart to effect chemical transformation. Several hydrogen donor and catalyst pairings were investigated for their efficacy in facilitating the reaction. Cost friendly hydrogen donor sources such as ammonium formate and 1,4-cyclohexadiene were the main candidates tested during early stage screenings.[130,131]

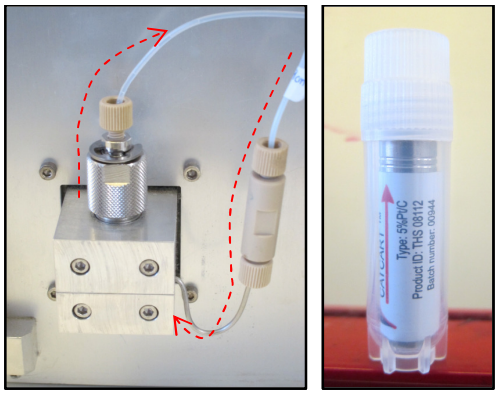

Figure 3.8 (Left) Aluminium heating chamber and the unidirectional flow stream; (Right) CatCart's packed catalyst.

Initially, ammonium formate and 10% Pd/C were chosen as the hydrogen donor and catalyst pairing to mirror the catalytic system used in the analogous batch reaction described in Section 3.3.1. Unfortunately, a serious fluctuation in system pressure was detected when ammonium formate was used as the hydrogen donor. It has been established that the crystalline compound spontaneously decomposes into ammonia, carbon dioxide and hydrogen gas when exposed to palladium metal.[132] The evolution of gaseous by-products proved to be detrimental as the reaction stream's

flow rate was adversely affected leading to pump failure during reaction. Furthermore, the presence of ammonia increases the risk of side product formation as the Fmoc group is susceptible to basic cleavage.[133] As a consequence, the hydrogen donor was replaced with 1,4-cyclohexadiene which gives a mole of H_2 per donor molecule as well as benzene, an inert by-product.[134]

Using **30** as the test substrate and 2.5 equivalents of 1,4-cyclohexadiene as the hydrogen donor, a series of experiments was performed employing two separate catalyst systems – 10% Pd/C and 20% $Pd(OH)_2/C$ (Pearlman's catalyst).[135] Palladium metal actively promotes hydrogenolysis whilst discouraging aromatic ring's saturation and carbon supported catalysts are reportedly more reactive as a result of increased active surface area.[126,136] Three different substrate concentrations (i.e. 15, 30 and 50 mM) were prepared and each was tested with 10% Pd/C as the catalyst. An experiment performed at room temperature with 15 mM of substrate concentration and 1.00 $mLmin^{-1}$ flow rate gave a poor 23% product yield based on HPLC analysis (Entry a, Table 3.2).

Table 3.2 The efficiency of Pd-catalysed flow transfer hydrogenolysis as a function of catalyst system and substrate concentration.

30 **31a** **31b**

Entry	Catalyst	[**30**][i] (mM)	HPLC Yield **31a**[ii] (%)
a	10% Pd/C	15	23[iii]
b	10% Pd/C	15	78 (1 : 0.25)[iv]
c	10% Pd/C	30	69 (1 : 0.15)
d	10% Pd/C	50	54 (1 : 0.10)
e	20% $Pd(OH)_2/C$	15	96 (1 : 0.00)
f	20% $Pd(OH)_2/C$	30	82 (1 : 0.08)
g	20% $Pd(OH)_2/C$	50	70 (1 : 0.10)

[i] Conditions: H_2 donor – 2.5 equiv of 1,4-cyclohexadiene; Solvent – EtOH; Q – 1.00 $mLmin^{-1}$; T - 40°C; Scale – 7.5 µmol.

[ii] Aniline was used as internal standard. HPLC wavelength – 254 nm.

[iii] T - 25°C

[iv] The integrated peak ratio of product **31a** to side product **31b**.

Increasing the temperature by 15°C significantly enhanced the rate of reaction as 78% of product **31a** was detected. However, an unwanted side reaction was also observed as one fifth of the converted starting material underwent Fmoc cleavage to give the side product **31b** (Entry b, Table 3.2). At higher substrate concentrations, starting material conversion became less effective despite seeing a reduced formation of side product (Entries c & d, Table 3.2). Even though the catalyst gave decent yields across the range of concentrations studied, an attempt to scale out the reaction exposed a serious underlying problem of material retention. In a scale out experiment, saturation of the catalyst system was observed after 20 min (i.e. ~ 14% of total reaction progress) as only starting material was detected in the exiting stream. Interestingly, a sample collected from the post-run flushing stream with pure hydrogen donor solution revealed the presence of the product, mixed with starting material.

Performing a pro-longed flushing protocol did little to remove the starting material as it was strongly adsorbed on the packed catalyst. Continuous flushing of the cartridge with copious amount of solvent was tremendously wasteful and time consuming. Furthermore, it was shown that using the 10% Pd/C packed cartridge resulted in elevated system pressure; fluctuating between 9 to 11 bar during the reaction. Hence, it is highly probable that the unknown degree of matrix porosity within each type of CatCart catalyst plays a significant role in the retention of substrate and product. In addressing the material retention issue, the packed cartridge was subsequently replaced with CatCart's version of Pearlman's catalyst. When performing experiments using the 20% $Pd(OH)_2/C$ catalyst, it was immediately evident that the system pressure generated by the reaction stream was noticeably lower (i.e. 1 bar consistently) compared to the previous catalyst used. This suggests a much higher matrix porosity within the CatCart and thus, could potentially reduce the retention of materials in the packed cartridge. On a side note, Pd metal leaching was not investigated in this study.

Similarly, 1,4-cyclohexadiene was used as the hydrogen donor and the reaction stream flow rate was kept unchanged at 1.00 $mLmin^{-1}$. It was evident that the overall results were much better with Pearlman's catalyst compared to 10% Pd/C. At 15 mM of substrate concentration, 96% of product formation was measured by HPLC. More importantly, no side product was seen within the limit of detection (Entry e,

Table 3.2). Even though product yield was negatively affected by increasing the substrate concentration, an impressive 70% yield was still recorded at a concentration of 50 mM (Entry g, Table 3.2). More importantly, the product to side product ratios at lower substrate concentrations were better than their corresponding values using 10% Pd/C as the catalyst (Entries e & f vs. 2 & 3, Table 3.2). Using the optimised conditions, ~ 1.00 g of the debenzylated product **31a** and its TEG analogue **34** were scaled out at 70 and 68% isolated yields, respectively, in slightly more than three hours (Scheme 3.10).

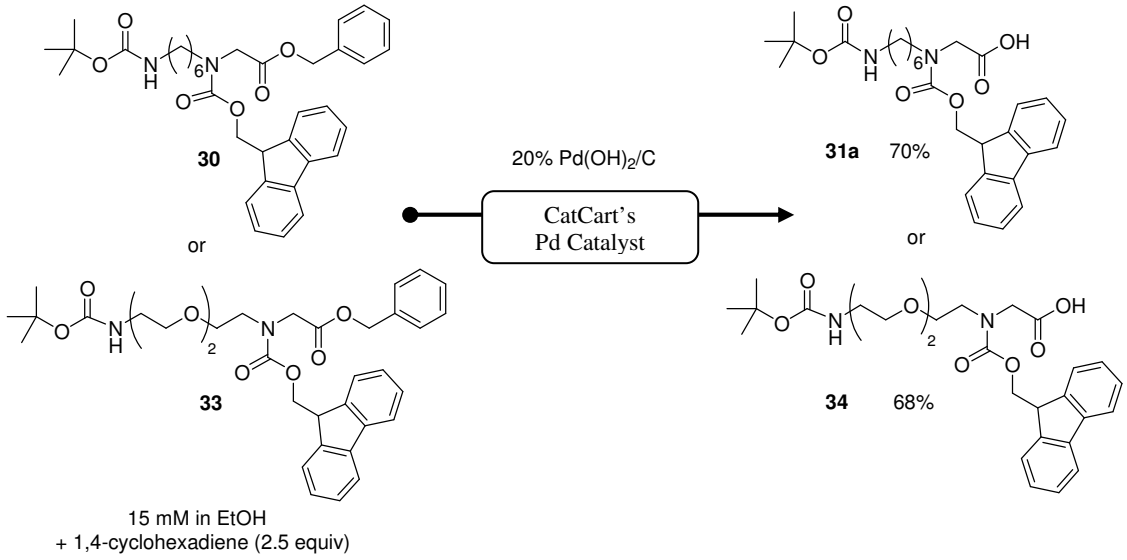

Scheme 3.10 Continuous flow transfer hydrogenolysis.

Based on the results obtained, it can be concluded that the efficiency of flow transfer hydrogenolysis is highly dependent on the temperature of the reaction as well as the substrate concentration (Figure 3.9). While a fair comparison of synthetic efficiency between catalytic transfer hydrogenolysis carried out in batch versus the flow method is not entirely possible due to the vastly different mode of reaction, it is speculated that the increased efficiency witnessed in flow catalysis is greatly facilitated by a pseudo-stoichiometric effect. This is due to the availability of an overwhelming excess of catalyst when a unidirectional stream of reactants flows through the packed cartridge. Nonetheless, without the right catalyst system, consistency is difficult to achieve in flow transfer hydrogenolysis as a consequence of material retention which affects the steady state flow of a reaction stream. As a side note, CatCart's 5% Pt/C and 5% Ru/Al_2O_3 failed to derive the desired product despite claims of their ability to promote the debenzylation process in batch chemistry.[128]

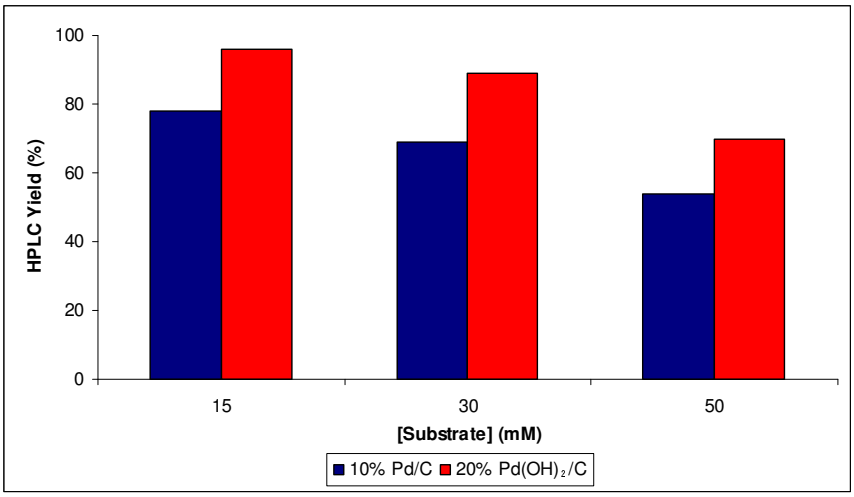

Figure 3.9 Efficacy of catalysts is dependent on substrate concentration.

3.8.2 Microwave-Assisted Catalytic Hydrogenolysis

Several publications have advocated the use of microwave instruments to achieve high synthetic productivity with improved speed and efficiency.[137-139] A series of experiments were conducted to compare the results obtained from the catalytic flow method against the microwave approach. The experiments were performed using a CEM Discover SP microwave unit coupled to a Parker's hydrogen generator (Figure 3.10). The hydrogen gas was channelled into the microwave module via a gas addition unit which regulates the amount of hydrogen gas available for reaction. Based on the manufacturer's recommendation, the substrate **30** was prepared at a concentration of 0.25 M and 10% Pd/C was used as the catalyst.

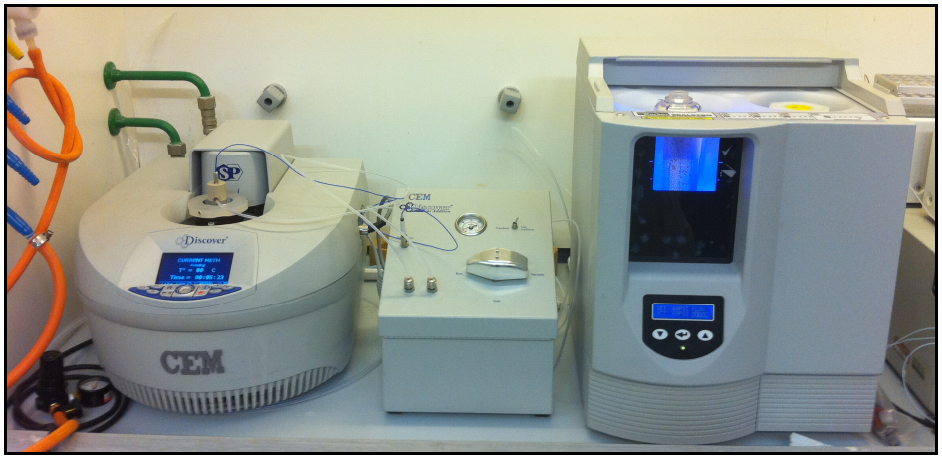

Figure 3.10 (From left to right) CEM Discover SP microwave unit coupled to a gas addition unit and a hydrogen gas generator.

Using 4.5 mol% of catalyst loading, the reaction gave a limited 26% yield of the debenzylated product **31a** when irradiated under microwave conditions for 2 min (Entry a, Table 3.3). When the reaction time was extended to 10 min at 80°C, the yield increased substantially to 87%; accompanied by the occurrence of Fmoc cleavage. Subjecting the same reaction to a further 3 min irradiation time caused a 12% decline in product yield as more of the side product was produced (Entries b & c, Table 3.3). When the scale of the experiment was increased by two and a half times, the reaction which was microwave irradiated for 12 min at 80°C gave only 41% of product yield (Entry d, Table 3.3). Prolonging the reaction time by an extra 8 min, in addition to increasing the hydrogen gas pressure to 60 psi, produced a much better result at 60% yield after chromatographic purification (Entry e, Table 3.3).

Table 3.3 Debenzylation via hydrogenolysis under microwave conditions.

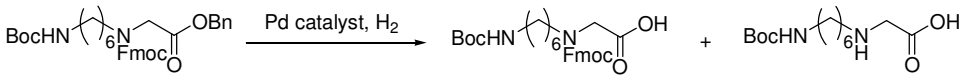

30 **31a** **31b**

Entry	Scale of **30** (mmol)	Conditions[i]	HPLC Yield **31a**[ii] (%)
a	0.48	2 min, 55°C, 50 psi	26
b	0.48	10 min, 80°C, 50 psi	87 (1 : 0.15)[iii]
c	0.48	13 min, 80°C, 50 psi	75 (1 : 0.33)
d	1.20	12 min, 80°C, 50 psi	41 (1 : 0.02)
e	1.20	20 min, 80°C, 60 psi	87 (1 : 0.18)
			60[iv]

[i] Conditions: Catalyst – 10% Pd/C (4.5 mol%); Solvent – EtOH

[ii] Aniline was used as internal standard. HPLC wavelength – 254 nm.

[iii] The integrated peak ratio of product **31a** to side product **31b**.

[iv] Isolated yield.

Despite its proven functionality in assisting the hydrogenolysis reaction, the microwave method suffers from common limitations associated with batch chemistry. At comparable substrate concentrations, the formation of side product is conspicuously more prominent in reactions which had undergone microwave irradiation. This could be attributed to the excessive contact time between the active palladium catalysts and the starting material which is tremendously difficult to control in a batch environment. Besides, the productivity of synthesis is also limited by the maximum volume of reactants that can be accommodated by the reaction vessel

during each cycle of microwave irradiation. Hence, scaling up an optimised reaction would be impractical as it involves reiterative irradiation of individual vessels serially. In comparison, the scaling out strategy in flow offers a continuous mode of processing which sidesteps the use of expensive instrumentations. As such, adapting the flow strategy could greatly benefit synthetic laboratories seeking a systematic process of rapidly screening, optimising and scaling out target compounds, all on the same platform.

3.9 Summary

In conclusion, the multi-step synthesis of peptoid monomers has been successfully achieved via the continuous flow method (Figure 3.15). In addition to synthesising the *N*-Fmoc-(6-Boc-aminohexyl)glycine monomer **31a**, a novel analogue of the monomer bearing a triethylene glycol bridge motif, *N*-Fmoc-((2-(2-Boc-aminoethoxy)ethoxy)ethyl)glycine **34** was also synthesised via the same optimised route. Even though direct optimisation of reaction conditions is not always possible due to physical incompatibility of materials in the flow reactor, the flow method demonstrated great flexibility in providing quick access to valuable synthetic compounds. Based on the work discussed in this chapter, the peptoid monomers were synthesised in three steps; starting from the selective alkylation of *N*-Boc protected diamines, followed by an Fmoc carbamation reaction and lastly, Pd-catalysed hydrogenolysis. The first two steps were successfully linked as a tandem reaction which gave yields exceeding 60%.

The sequential reaction removed an intermediate purification requirement by introducing an in-line scavenging protocol. Silica-based trisamine scavengers were used to remove unreacted alkylating agent from the first reaction stream before being fed into the second reaction. The scavengers exhibited excellent durability and approximately 0.60 g of scavengers is consumed for every gram of mono-alkylated compound produced. Lastly, transfer hydrogenolysis was performed using 20% $Pd(OH)_2/C$ and 1,4-cyclohexadiene as the catalyst and hydrogen donor pairing. Good yields (68 – 70%) were obtained for the monomer **31a** and its ethylene glycol analogue **34**. Even though Fmoc cleavage was still observed in flow transfer hydrogenolysis, its occurrence was greatly reduced compared to batch chemistry as a result of minimised contact time between the active catalyst and the substrates.

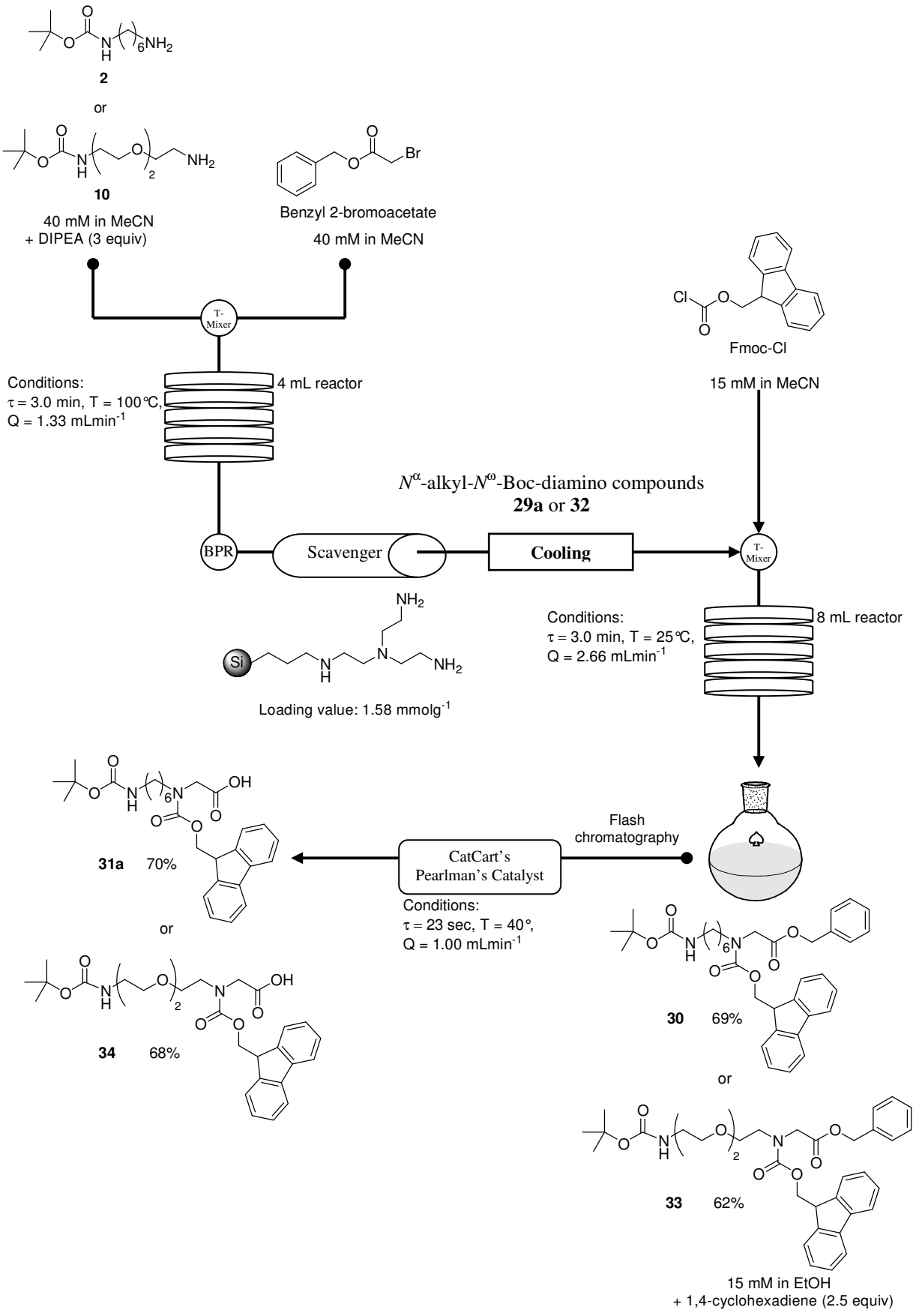

Scheme 3.11 Multi-step continuous flow synthesis of the *N*-Fmoc-(6-Boc-aminohexyl)glycine monomer **31a** and its triethylene glycol analogue, *N*-Fmoc-((2-(2-Boc-aminoethoxy)ethoxy)ethyl)glycine **34**.

CHAPTER 4

MICROWAVE-ASSISTED SOLID PHASE SYNTHESIS OF PEPTOIDS AND THEIR BIOLOGICAL EVALUATION

4.1 Solid Phase Synthesis of Peptoids

This chapter examines the assembly of three different types of peptoids via solid phase peptide synthesis (SPPS). They include (i) oligo-*N*-(6-aminohexyl)glycines (hereafter known as **standard peptoids**), (ii) oligo-*N*-((2-(2-aminoethoxy)ethoxy)ethyl)glycines (**triethylene glycol [TEG] peptoids**), and (iii) oligomers of alternating standard and TEG monomers (**hybrid peptoids**) (Figure 4.1). The solid phase method uses polymeric resins as the solid support on which the target compounds were constructed. The resins were functionalised with an appropriate linker prior to the synthesis of the oligo-*N*-alkylglycines. The work presented in this chapter used an Fmoc strategy to assemble the desired peptoids. The monomers *N*-Fmoc-(6-Boc-aminohexyl)glycine **31a** and *N*-Fmoc-((2-(2-Boc-aminoethoxy)ethoxy)ethyl)glycine **34**, were synthesised with fully orthogonal protecting groups by continuous flow synthesis as discussed in Chapter 3.

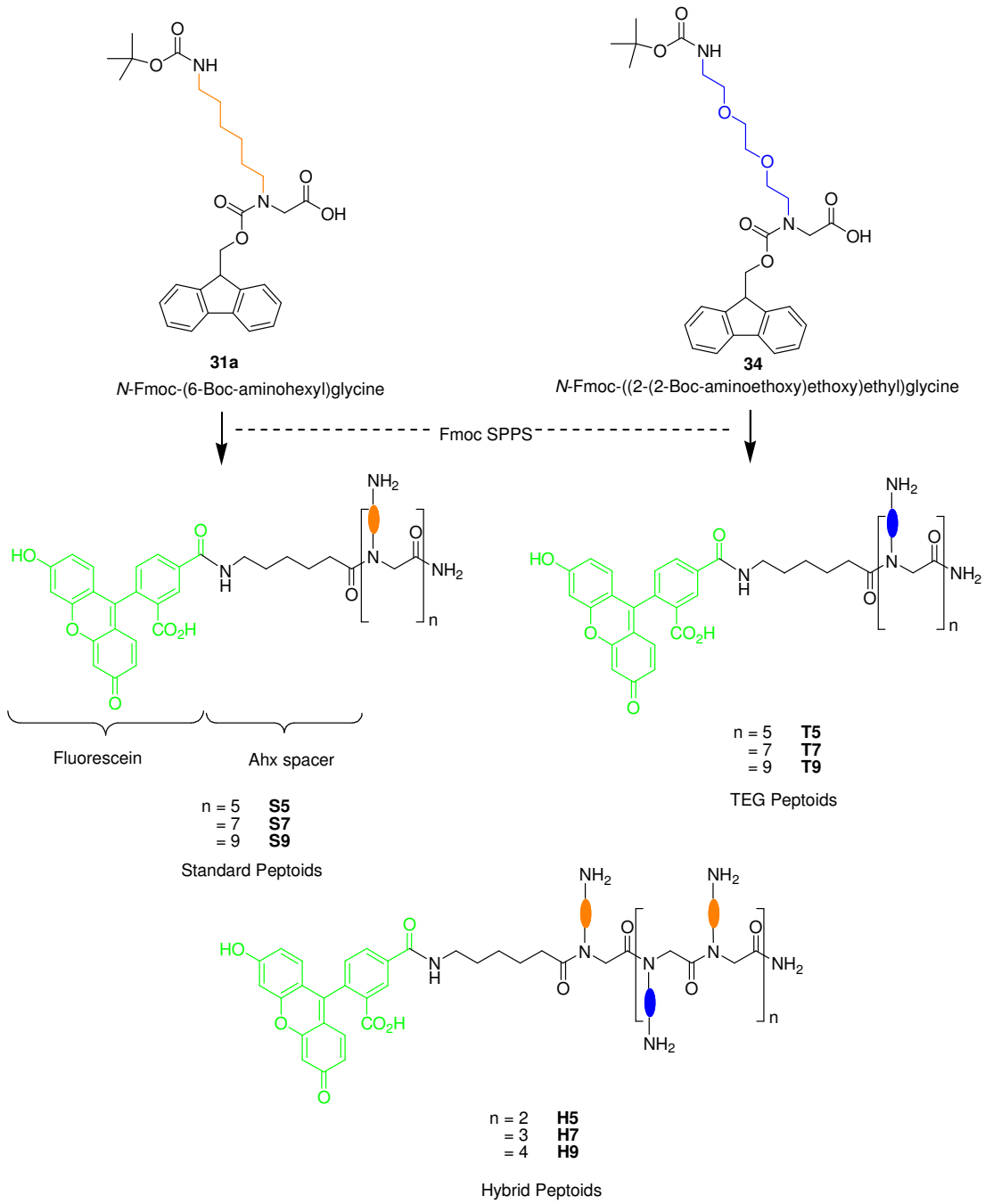

Figure 4.1 *N*-alkylglycine monomers **31a** and **34** were used to construct the standard, Triethylene Glycol (TEG) and hybrid peptoids via Fmoc-based SPPS.

In order to study the comparative cellular uptake efficiency of these molecular transporters, a nine-member collection of fluorescently labelled peptoids with varying backbone lengths (i.e. penta-, hepta- and nona-mers) and side chain compositions (i.e. homogeneous single-type residue vs. alternating dual-type residues) were synthesised. The peptoids share a generic template consisting of a fluorescent dye (5(6)-carboxyfluorescein) and the peptoid, linked by the 6-aminohexanoic acid (Ahx) spacer. The cytotoxicity and cell permeability of these oligomers were evaluated on

three different cell lines – human embryonic kidney (HEK293), human cervical carcinoma (HeLa) and Chinese hamster ovary (CHO) cells. The cytotoxicity assay, flow cytometry and confocal microscopy results of the peptoids are discussed in Section 4.2.

4.1.1 Rink Amide Functionalisation of Aminomethyl Polystyrene Resins

The construction of oligo-*N*-alkylglycines began with the selection of an appropriate solid support. Aminomethyl polystyrene (PS) resins were chosen due to their popularity in SPPS. Robust PS resins are commercially available and have good swelling properties and compatibility with the organic solvents used during SPPS synthesis (i.e. DCM, DMF and MeOH).

A Rink amide linker was coupled to the solid support as a prelude to the assembly of the peptoids, with the acid labile linker giving a primary amide at the *C*-terminal position following acid cleavage. At a concentration of 0.37 M, three equivalents of the Rink amide linker, ethyl 2-cyano-2-(hydroxyimino)acetate (Oxyma) and *N*,*N*-diisopropylcarbodiimide (DIC) were dissolved in DMF and added to the aminomethyl PS resins (loading value: 1.23 mmolg^{-1}) (Scheme 4.1). Oxyma was used as an additive to give an active ester.[140] It is an alternative to the traditionally used hydroxybenzotriazole (HOBt) which has recently caused some safety concerns. The oxime-based reagent was used throughout the SPPS.

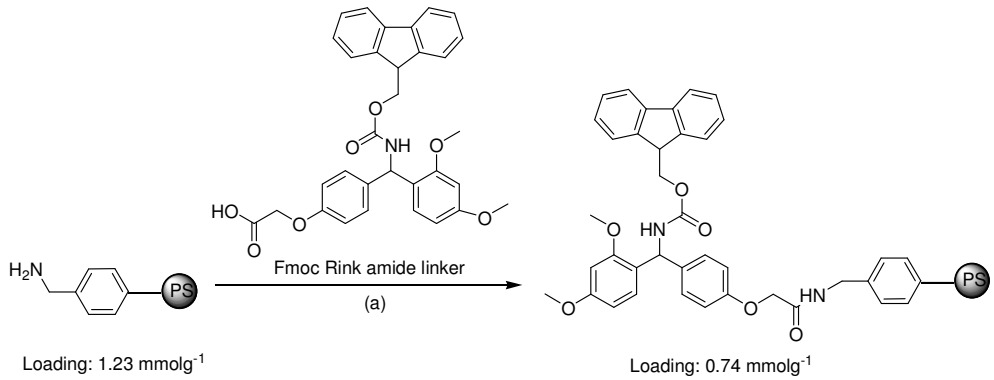

Scheme 4.1 Functionalisation of aminomethyl PS resins with the acid labile Rink amide linker. (a) DIC (3 equiv), Oxyma (3 equiv), 0.37 M in DMF, 1.5 h.

4.1.2 Solid Phase Synthesis of Standard Peptoids

Three "standard" peptoids of five, seven and nine residues (**S5**, **S7** and **S9**) were synthesised using established SPPS procedures (Scheme 4.2). The linker's Fmoc protecting group was removed to liberate the primary amine functionality using 20% piperidine in DMF. Subsequently, monomer **31a** was coupled using Oxyma and DIC (0.15 M). The progress of reaction was monitored by a qualitative ninhydrin test.

Upon confirming the first residue had been successfully attached, a reiterative cycle of Fmoc-deprotection and amide coupling was performed until the desired backbone length was achieved. Due to the unmasked amine being a secondary amine, the deprotection and coupling steps were monitored with chloranil tests. When the main chain length reached > 5 residues, the reactions were heated to 60^{o}C for 15 min, followed by an extended 15 min of mechanical agitation at room temperature to enhance the coupling efficiency of those residues which were otherwise severely affected by steric hindrance.

Once the desired length was achieved, an Ahx spacer was conjugated to the final residue and then capped with 5(6)-carboxyfluorescein to produce the final dye-labelled oligo-*N*-alkylglycine. The spacer was incorporated as a bridge between the fluorescein dye and the naked peptoid to prevent possible interference of fluorophore activity by the oligomer. The final compound was cleaved from the linker using a cleavage cocktail of 95% trifluoroacetic acid (TFA) : 2.5% triisopropylsilane (TIS) : 2.5% H_2O. TIS and water are commonly added into the mixture as scavengers to "mop-up" reactive electrophiles that are generated during the acidic cleavage. Post cleavage work-up led to the isolation of the target compounds. All three peptoids were successfully synthesised in good yields and their identities confirmed by MALDI-TOF mass spectrometry.

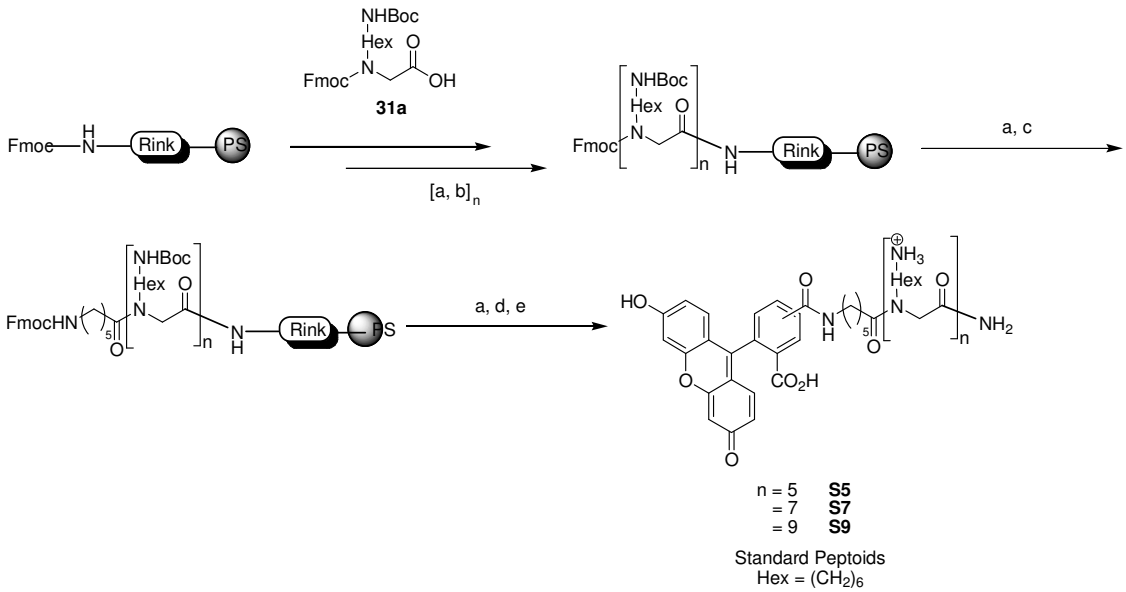

Scheme 4.2 Synthesis of fluorescein-labelled standard peptoids **S5**, **S7** and **S9**. (a) 20% piperidine in DMF (2 x 15 min); (b) monomer **31a** (2 equiv), DIC (2 equiv), Oxyma (2 equiv), 0.15 M in DMF, 30 min (**S5**) and 60°C, 15 min, followed by r.t. for 15 min (**S7** and **S9**); (c) *N*-Fmoc-6-aminohexanoic acid (2 equiv), reagents and conditions as in (b); (d) 5(6)-carboxyfluorescein (2 equiv), reagents and conditions as in (b); (e) TFA, 2.5% TIS, 2.5% H_2O, 3 h.

4.1.3 Microwave-Assisted Solid Phase Synthesis of TEG Peptoids

The standard pentamer peptoid **S5** was conveniently synthesised through SPPS performed at ambient conditions whereas the syntheses of heptamer **S7** and nonamer **S9** required additional heating. However, constructing oligomers bearing the TEG motif necessitated the use of microwave heating to assemble the desired target compounds. Initial attempts to synthesise the TEG peptoids using monomer **34** under the conditions reported in Section 4.1.2 proved futile and no product was isolated.

Multiple attempts to remove the Fmoc group on the fifth coupled residue, employing standard Fmoc cleavage protocol, were unsuccessful. The use of elevated reaction temperature and extended incubation time (i.e. 60°C for 30 min) were equally disappointing. In addition, the use of a stronger cleavage cocktail (i.e. 2% DBU : 2% piperidine in DMF) under various physical conditions also gave no visible signs of Fmoc removal. Aggregation of the peptoid structure was suspected to be the main reason behind the failure of the Fmoc deprotection step. This could be attributed to the increased bulkiness of the overall structure as a result of multiple ethylene glycol units on the side chains. Hence, a more effective method of N^{α}-Fmoc deprotection was needed. In addressing this issue, the synthesis of the TEG peptoids was attempted in a

microwave synthesiser (Scheme 4.3). The coupling mixture was prepared at 0.14 M with a 3 : 1 ratio of DMF : DCM as the solvent system of choice. The addition of 25% DCM facilitated solid support swelling, decreasing steric crowding on the resin.

Starting with the first residue, the Fmoc group deprotection was accomplished via microwave irradiation (60°C for 10 min) using 20% piperidine in DMF. The procedure was performed twice during each stage of deprotection. Subsequently, the amide coupling reaction was microwave irradiated for 25 min at 70°C. During the propagation of the oligomer's backbone, the reiterative cycles of Fmoc-deprotection and amide coupling were all carried out under microwave conditions. This included the conjugation of the Ahx spacer as well as attachment of fluorescein. The TEG peptoids **T5**, **T7** and **T9** were isolated successfully following acidic cleavage in moderate yields. This was a major breakthrough as each step of synthesis proceeded smoothly as confirmed by qualitative chloranil tests. It was clear that the N^{α}-Fmoc deprotection step benefited tremendously from the microwave-assisted heating. The unique interaction between the electromagnetic field and the solvent molecules in a microwave reaction system effectively produces a narrow thermal distribution not seen in conductive heating. This uniform thermal profile is believed to significantly enhance the reaction kinetics of the coupling process.[141,142]

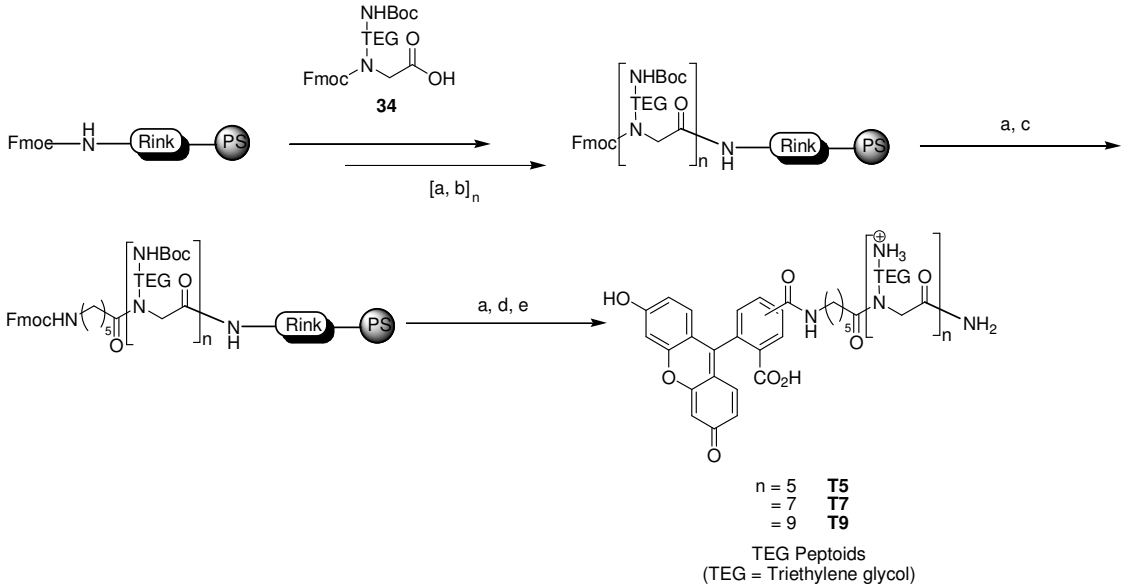

Scheme 4.3 Synthesis of fluorescein-labelled TEG peptoids **T5**, **T7** and **T9**. (a) 20% piperidine in DMF (2 x 60°C, 10 min, μwave); (b) monomer **34** (2 equiv), DIC (2 equiv), Oxyma (2 equiv), 0.14 M in 3 : 1 of DMF : DCM, μwave, 70°C, 25 min; (c) *N*-Fmoc-6-aminohexanoic acid (2 equiv), reagents and conditions as in (b); (d) 5(6)-carboxyfluorescein (2 equiv), reagents and conditions as in (b); (e) TFA, 2.5% TIS, 2.5% H_2O, 3 h.

4.1.4 Microwave-Assisted Solid Phase Synthesis of Hybrid Peptoids

The synthesis of peptoids with an alternating sequence of different monomers has been attempted previously but an oligomer featuring the combination of *N*-(6-aminohexyl)glycine **31a** and *N*-((2-(2-aminoethoxy)ethoxy)ethyl)glycine **34** is unreported. A structure bearing alternating side chains of hexyl- (i.e. six methylene units) and TEG-spacers represents a new hybrid system. The physicochemical properties of the hybrid oligomers are expected to be considerably different from either the standard or the TEG peptoids. In an effort to correlate the cellular penetration efficiency of molecular transporters with their structural amphiphilicity, these hybrid systems appear to be the ideal synthetic model for such evaluation.

Using the same microwave-assisted synthesis protocol described in Section 4.1.3, the hybrid peptoids **H5**, **H7** and **H9** were synthesised accordingly (5 – 12 yields) [Scheme 4.4]. Monomer **31a** was attached to the Rink linker, serving as a reference point for the propagation of the peptoid backbone. The pentamer **H5** was relatively accessible in comparison to the heptamer **H7** and the nonamer **H9**, as despite the use of microwave irradiation, the cleavage of the N^{α}-Fmoc group was severely problematic once the backbone length of the oligomer ≥ 8 coupled residues. It was found that the deprotection of the Fmoc group belonging to (i) the Ahx spacer on the heptamer (Fmoc-**Ahx**-[$Hex_7TEG_6Hex_5TEG_4Hex_3TEG_2Hex_1$]-PS) and (ii) the last TEG residue on the octamer (Fmoc-**TEG_8**-[$Hex_7TEG_6Hex_5TEG_4Hex_3TEG_2Hex_1$]-PS) was unsuccessful even under forceful microwave heating.

While the exact reason for the failure of the Fmoc deprotection step remains unknown, oligomer aggregation was believed to be responsible for the experimental observation. The combination of hexyl and TEG side chains could produce multiple intra- and intermolecular interactions involving the solid-supported constituents. In addition, the ethylene glycol moieties are expected to interact with solvent molecules within their vicinity, thus forming a "solvation shell" around the peptoid. As a result, aggregation of the oligomer (which could potentially generate secondary structures), as well as the solvent shell effect, effectively limit the access of piperidine to the Fmoc cleavage site. Hence, the cleavage solution was changed from 20% piperidine in DMF to a more potent mixture of 2% DBU : 2% piperidine in DMF.

The DBU / piperidine pairing has been advocated as the Fmoc cleavage cocktail of choice when working with difficult peptide sequences. The addition of piperidine is necessary to enable the scavenging of the dibenzofulvene by-product. The mixture was added to the resins and microwave irradiated at 60°C for 10 min. The solution was then drained and a fresh portion of the cleavage mixture was added to the resin. In order to drive the deprotection reaction to completion, the concentration of the mixture was increased to 4% DBU : 4% piperidine in DMF and microwave irradiated for a second time. The modified deprotection step gave encouraging results as qualitative tests indicated the successful removal of the Fmoc protecting group. While all three hybrid peptoids were successfully isolated post cleavage work up, the final yields of the heptamer **H7** and nonamer **H9** were disappointingly low. Nonetheless, the microwave-assisted protocol could be optimised for future synthesis of the hybrid oligomers and serious consideration should be given to the use of lower loading PEG-based resins (e.g. ChemMatrix).

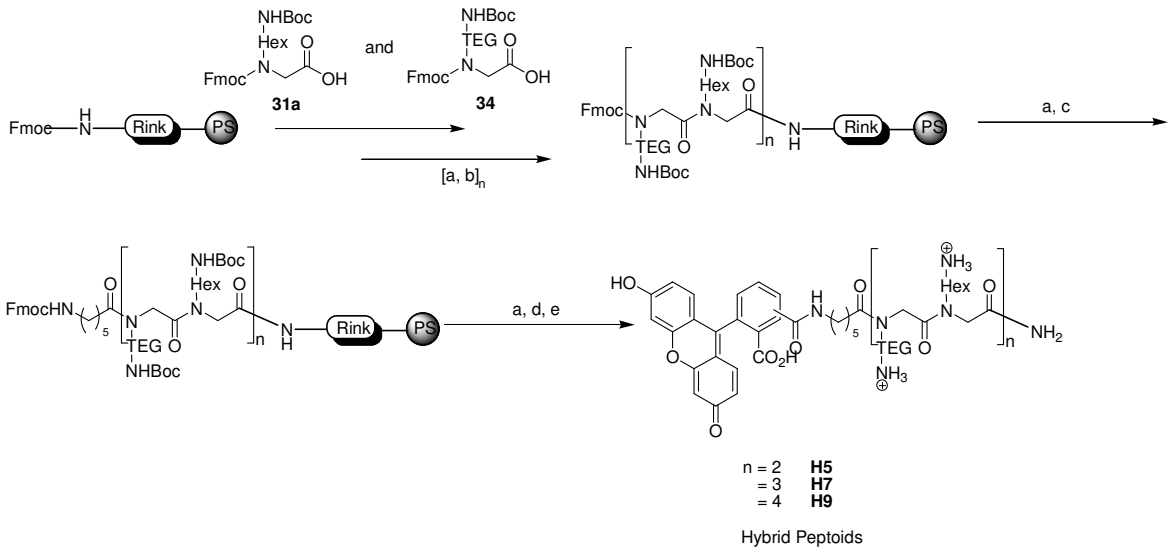

Scheme 4.4 Synthesis of fluorescein-labelled hybrid peptoids **H5**, **H7** and **H9**. (a) 20% piperidine in DMF (2 x 60°C, 10 min, μwave) (*up to heptamer*) & 2% DBU : 2% piperidine in DMF in DMF (60°C, 10 min, μwave) followed by 4% DBU : 4% piperidine in DMF (60°C, 10 min, μwave) (*octamer and beyond*); (b) monomers **31a** and **34** in a successive manner (2 equiv), DIC (2 equiv), Oxyma (2 equiv), 0.14 M in 3 : 1 of DMF : DCM, μwave, 70°C, 25 min; (c) *N*-Fmoc-6-aminohexanoic acid (2 equiv), reagents and conditions as in (b); (d) 5(6)-carboxyfluorescein (2 equiv), reagents and conditions as in (b); (e) TFA, 2.5% TIS, 2.5% H_2O, 3 h.

4.2 Biological Evaluation of Peptoid Transporters

4.2.1 Purification of the Peptoids

After the post cleavage work-up, the peptoids were purified via semi-preparative HPLC prior to biological evaluations. The attachment of 5(6)-carboxyfluorescein enables the flow cytometry and confocal microscopy investigations of the peptoids with cells.[143] Based on the best peak separation of the crude peptoid as identified by analytical HPLC, a corresponding semi-preparative method was created for the purpose of compound purification; with the compound analysed via LC-MS and MALDI-TOF MS (Figure 4.2). The isolated fractions of the target compound were combined and lyophilised to give a solid for **S5**, **S7** and **S9**; and a viscous oil for **T5**, **T7** and **T9**, and **H5**, **H7** and **H9**.

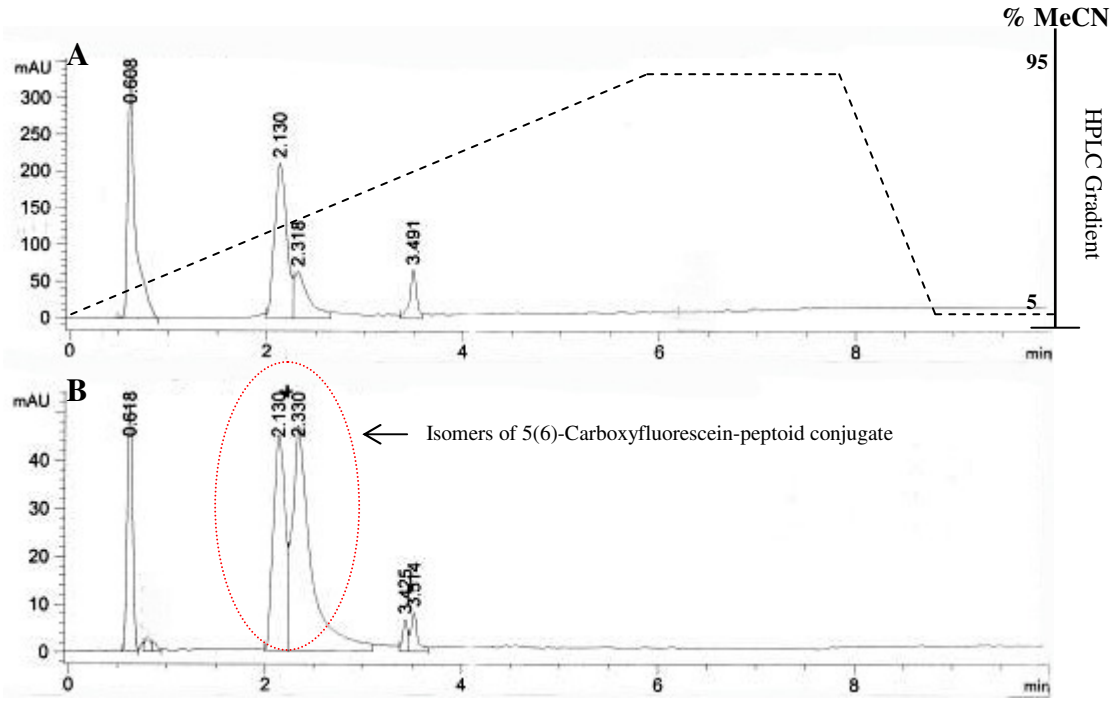

Figure 4.2 Chromatographic separation of the crude peptoid **S5** (t_R: 2.1 – 2.3 min) via analytical HPLC. The chromatography process was carried out using Dionex's Acclaim 120 column (C18, 5 µm, 120 Å, 4.6 x 150.0 mm) in a 30 minute gradient from 5 to 95% MeCN (with 0.1% HCO_2H in H_2O) at a flow rate of 1.0 $mLmin^{-1}$. The circled double peaks represent isomers of 5(6)-carboxyfluorescein-peptoid conjugate. HPLC wavelength: 254 nm (A) and 495 nm (B).

4.2.2 Cytotoxicity

Each compound was dissolved in water and its concentration determined using UV /Vis spectroscopy based on the extinction coefficient of 5(6)-carboxyfluorescein (i.e. 2.9 x 10^4) at 475 nm.[144] The biological assays were performed by Dr. Ana Maria Perez-Lopez and the results are reported and discussed in this thesis.

The cytotoxicity of the standard, TEG and hybrid peptoids was evaluated with two different colorimetric agents, 3-(4,5-dimethylthiazol-2-yl)-2,5-diphenyltetrazolium bromide (MTT) and propidium iodide (PI) (Figure 4.3).[145,146] The tests are complementary as the formazan-based assay measures the enzymatic activity of viable cells whereas the PI assay only stains the DNA of membrane-damaged cells. Hence, the different mechanisms of action involved for each dye can be used to independently validate the cell viability results.

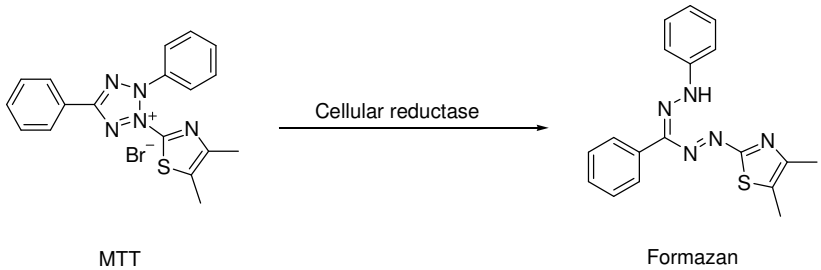

(a) MTT Assay

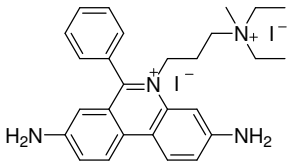

(b) Propidium iodide

Figure 4.3 Chemical structures of 3-(4,5-dimethylthiazol-2-yl)-2,5-diphenyltetrazolium bromide (MTT) (λ_{abs}: 570 nm) and the corresponding formazan (a); and propidium iodide (λ_{max} excitation: 535 nm & λ_{max} emission: 617 nm) (b) used for cytotoxicity assays.

For the cytotoxicity assays, the concentration of the peptoids was set at 10 μM and were added to HeLa cells; and incubated for 24 hours. The assay showed that all the peptoids were non-cytotoxic with cell viability measurements ≥ 80% (Figure 4.4). The increasing backbone length of the oligomers did not appear to cause any significant cell death, confirming previous reports on the non-cytotoxicity of standard peptoids and generating new information regarding the newly synthesised TEG and

hybrid oligomers.[112] The PI assay was performed via flow cytometry and it also showed excellent cell proliferation after 24 hours with measurements showing ≥ 90% cell viability (Figure 4.5). As both the MTT and PI assays were carried out independently of each other, it was reasonable to conclude that all the oligomers were non-toxic to HeLa cells at the concentration tested.

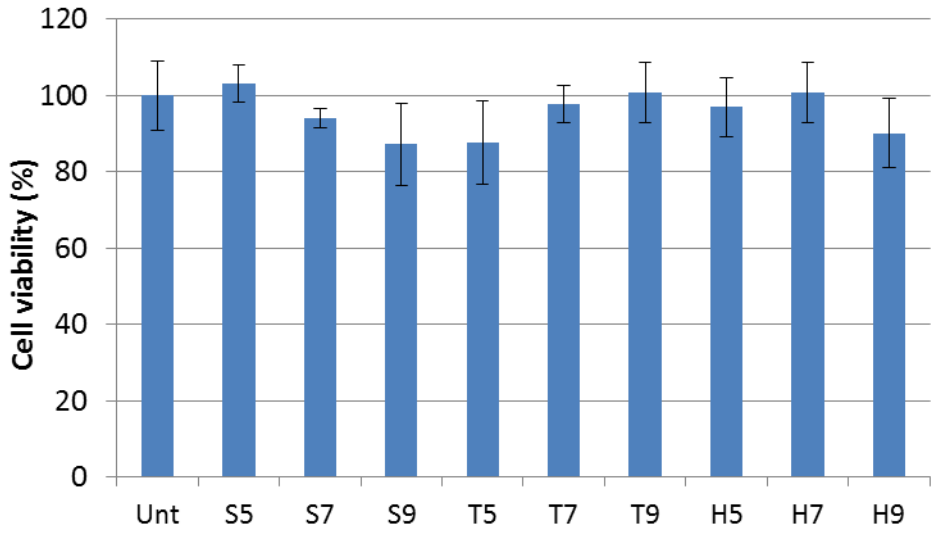

Figure 4.4 MTT cell proliferation assay of standard, TEG and hybrid peptoids on HeLa cells. 1 x 10^4 cells per well (in 96-well plate) were treated with 10 µM of each peptoid for 24 h at 37°C (n = 3). Absorbance was measured at 570 nm. 'Unt' on the x-axis denotes untreated cells.

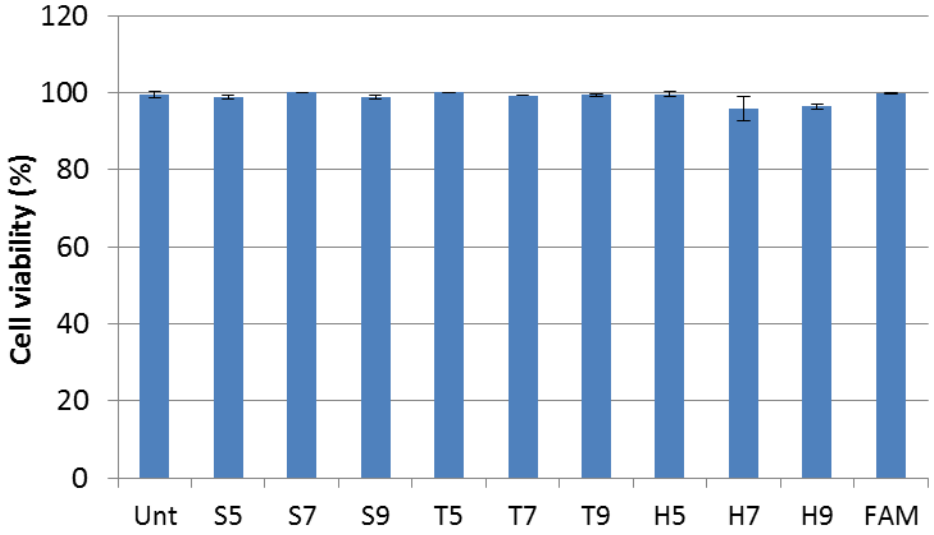

Figure 4.5 PI cell viability assay of standard, TEG and hybrid peptoids on HeLa cells. 3 x 10^4 cells per well (in 48-well plate) were treated with 10 µM of each peptoid for 24 h at 37°C (n = 2). Fluorescence was measured via flow cytometry with excitation and emission wavelengths of 535 and 617 nm, respectively.

4.2.3 Cellular Uptake Efficiency

The cellular uptake analysis was performed via flow cytometry. When the fluorescein-conjugated peptoids are internalised by cultured cells, the cells are distinctively labelled and their unique fluorescence signal can be tracked.[147-149] In general, the cellular uptake efficiency was tested on three different cell lines: HEK293, HeLa and CHO cells (in triplicate).

At each sampling point, the cells were washed and re-suspended in phosphate buffered saline (PBS) solution and analysed via flow cytometry. Trypan blue was added to the suspension to quench any extracellular or membrane-associated fluorescence.[150] The fluorescence characteristic of each cell sample was measured, quantified and ultimately converted into a measurement of relative fluorescence intensity (RFI), which is a function of the mean fluorescence of labelled-cells relative to a population of untreated cells.

4.2.3.1 Oligomer Length

Based on previous research, homo-oligomers of *N*-(6-aminohexyl)glycines were shown to be capable of effecting cellular internalisation.[112] A nonamer peptoid, being the largest member amongst the reported collection, was the most efficient molecular transporter. It was established that the longest oligomer backbone correlates with the best cellular uptake of peptoids. As such, the total number of positively charged moieties (i.e. protonated side chain amines) on the peptoid strongly influences the internalisation of the molecule.

In this study, all the standard peptoids **S5**, **S7** and **S9** were internalised by the different cell types tested at a concentration of 10 μM. With HeLa, HEK293 and CHO cells, the nonamer **S9** was approximately five times more efficient than the pentamer **S5** (Figure 4.6, A – C). More specifically, signal saturation was observed in HeLa and CHO cells after 5 hours. The results obtained from this investigation confirmed previous studies which highlighted the cellular penetration efficacy of **S9** as the most effective transporter. Therefore, this was used as a positive control to provide a basis of comparison when discussing the cellular uptake efficiency of the TEG and hybrid peptoids.

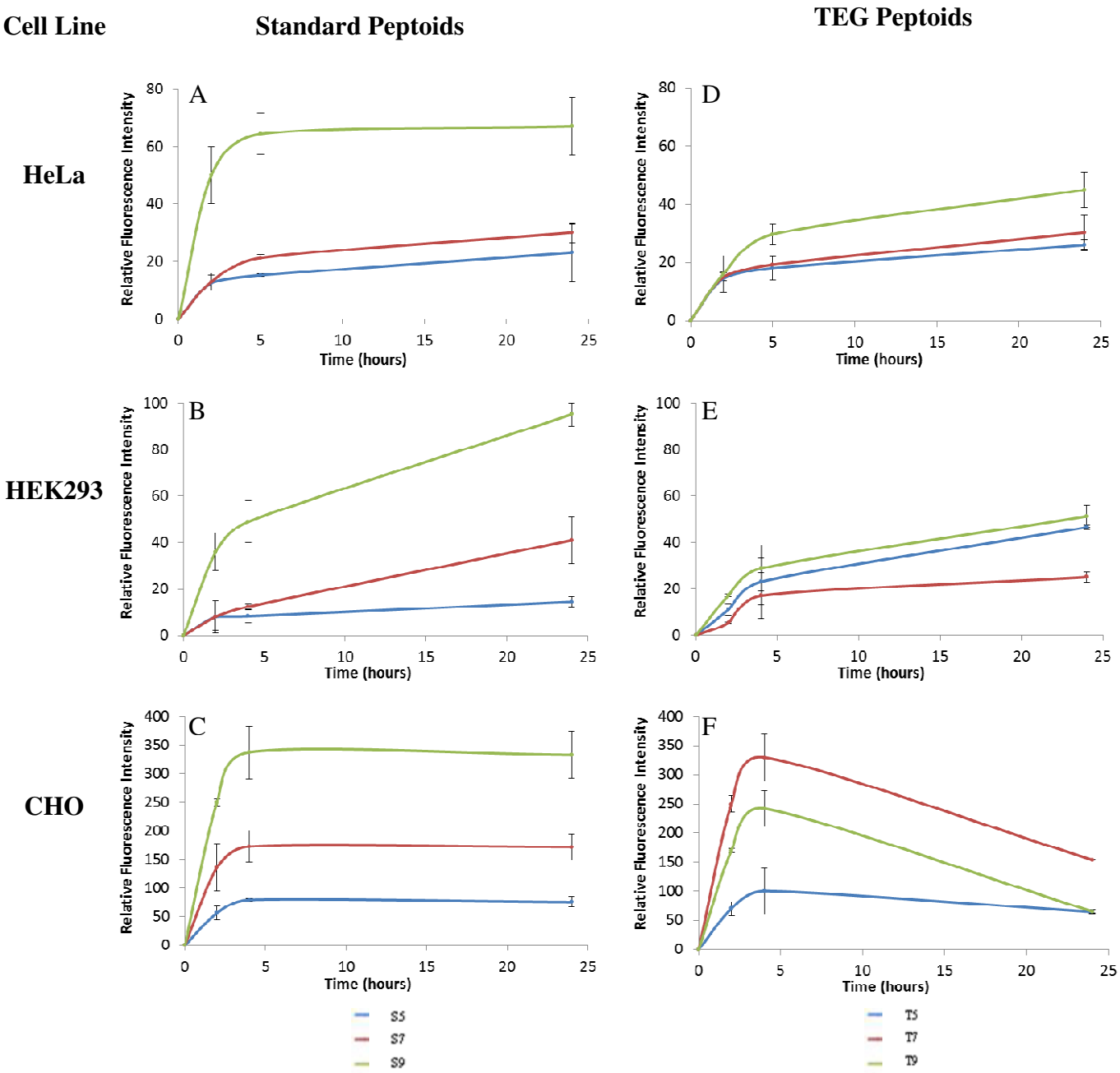

Figure 4.6 Cellular uptake assays of standard (A – C) and TEG (D – F) peptoids in HeLa, HEK293 and CHO cells. 3 x 10^4 cells per well (in 48-well plate) were treated with 10 μM of each peptoid for 2, 5 and 24 h at 37°C (n = 6). Fluorescence was measured via flow cytometry at an excitation wavelength of 488 nm, and emission monitored with a 530 / 30 band-pass filter.

The TEG peptoids **T5**, **T7** and **T9** are inherently more hydrophilic compared to the standard homo-oligomers due to the presence of multiple ethylene glycol units on the side chains. The oxygen atoms are hydrogen bond acceptors which increase the degree of solvation of the transporter. It was hypothesised that (i) a longer oligomer backbone would produce a higher rate of cellular uptake, thus corroborating observations seen in standard peptoids; and (ii) the enhancement of molecular

solubility could lead to an increased translocation of the TEG peptoids, therefore surpassing the performance of the standard homo-oligomers (*Note: This point is discussed in Section 4.2.3.2 – Side Chain Motif*). Interestingly, both hypotheses were proven inaccurate as the experimental findings revealed unusual characteristics of the TEG peptoids. In HeLa cells, the nonamer **T9** was indeed the most efficient transporter, registering almost twice the fluorescence intensity of the shortest peptoid (**T9** > **T7** > **T5**) (Figure 4.6, D). However, there was no discernible difference in term of uptake efficiency of the TEG peptoids in HEK293 cells when experimental error was taken into consideration (Figure 4.6, E).

In CHO cells, the cellular uptake efficiency of the heptamer **T7** was higher than the nonamer **T9**, breaking the general presumption that links longer peptoid backbone with increased cellular internalisation (**T7** > **T9** > **T5**) (Figure 4.6, F). Repeated experiments produced similar results and thus, implied specific transporter affinity towards different types of cell lines. A decrease in the fluorescence signals of **T5**, **T7** and **T9** was observed after 24 hours and it was highly probable that the fluorescein-conjugated peptoids were leaking from the labelled cells.[151] Prolonged incubation of cultured cells with the TEG peptoids could cause supersaturation of cells, leading to an efflux of the peptoid from the interior of the cells. Based on these findings, the cellular penetration efficacy of the TEG homo-oligomers is intrinsically more cell specific in comparison to the standard peptoids.

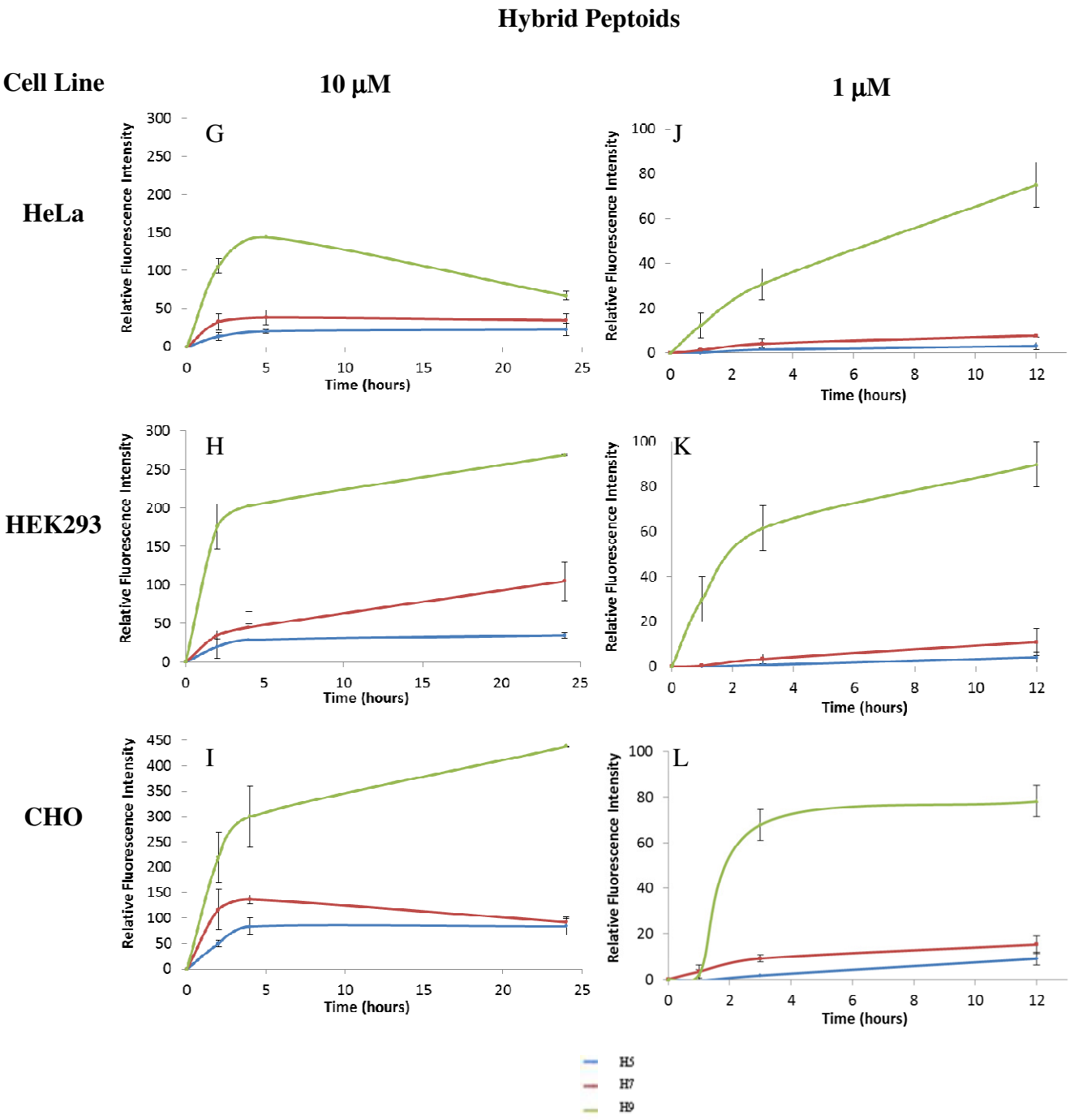

Figure 4.7 Cellular uptake assays of hybrid peptoids at 10 µM (G – I) and 1 µM (J - L) in HeLa, HEK293 and CHO cells. 3 x 10^4 cells per well (in 48-well plate) were treated with the specified concentration of each peptoid for a pre-determined duration at 37°C (n = 6). Fluorescence was measured via flow cytometry at an excitation wavelength of 488 nm, and emission monitored with a 530 / 30 band-pass filter.

Compared to the TEG peptoids, the cellular uptake efficiency of the hybrid hetero-oligomers **H5**, **H7** and **H9** was clearly dependent on their backbone length. Comparing all three hybrid peptoids, the heptamer **H7** was better than **H5** in

translocating the cellular membrane but the nonamer **H9** displayed truly remarkable penetration efficiency as a transporter. Across different cell types, it registered an average fluorescence intensity of almost seven times to that of the pentamer **H5** after 5 hours of incubation at 10 μM (**H9** > **H7** > **H5**) (Figure 4.7, G – I).

Specific to HeLa cells, a reduction in the fluorescence intensity of the nonamer **H9** was recorded after 24 hours (Figure 4.7, G). The internalised transporter molecules could escape from within the cells as a result of overloading and the phenomenon was postulated to be concentration dependent. Consequently, the concentration of the peptoid medium was decreased by ten-fold to 1 μM in subsequent experiments. At 1 μM, no fluorescence decrease was detected in any of the experiments. In HeLa cells, the uptake of **H9** was approximately thirty times better than **H5** after 3 hours (Figure 4.7, J). The excellent performance of the hybrid nonamer **H9** was also reproduced in both HEK293 and CHO cells (Figure 4.7, K & L).

4.2.3.2 Side Chain Motif

Based on the results presented in the previous section, it was evident that the nonamers **S9**, **T9** and **H9** were the best transporters from each category of peptoid synthesised. A direct comparison of all three nonamers was made to evaluate the relationship between the side chain motif and the cellular internalisation efficiency of these transporters.

At a concentration of 10 μM, the penetration efficiency of **H9** was approximately four times better than the standard peptoid **S9** after 2 hours of incubation in HEK293 cells. Meanwhile, the TEG nonamer **T9** was the least effective agent as its measured fluorescence intensity was eleven times less than **H9** under similar conditions (Figure 4.8, M). When the starting concentration was reduced by ten-fold to 1 μM, the efficacy of **H9** in translocating the cellular membrane was even more remarkable as the hetero-oligomer was sixteen times more permeable than **S9** at a similar concentration.

In HeLa cells, the fluorescence intensity of the hybrid peptoid **H9** (i.e. at 10 μM) was about thrice of the standard homo-oligomer **S9**. Unsurprisingly, the TEG nonamer **T9** lagged behind **H9** by a factor of five, indicating poor transporter efficiency in the cervical carcinoma cells (Figure 4.8, N). More importantly, the

permeability of **H9** at 1 µM (i.e. in both HEK293 and HeLa cells) was comparable to the performance of **S9** at 10 µM (within experimental error). According to confocal microscope analysis, **H9** was approximately seven-fold more permeable than **S9** based on the intensity measured from a sample cell at 1 µM (Figure 4.9). Such high level of cellular permeability at low transporter concentration has not been previously reported.

Results obtained from CHO cells were also consistent with the aforementioned findings confirming the exceptional performance of **H9**. On average, **H9** was twice as permeable as **S9** and thrice as good as **T9** in CHO cells (Figure 4.8, O). However, the efficacy of the hybrid peptoid in these cells was less pronounced at the lower end of the tested concentrations. In general, the hybrid nonamer **H9** was undisputedly the most efficient peptoid; with all cells 100% labelled within 2 hours of incubation at low micromolar concentrations (**H9 > S9 > T9**).

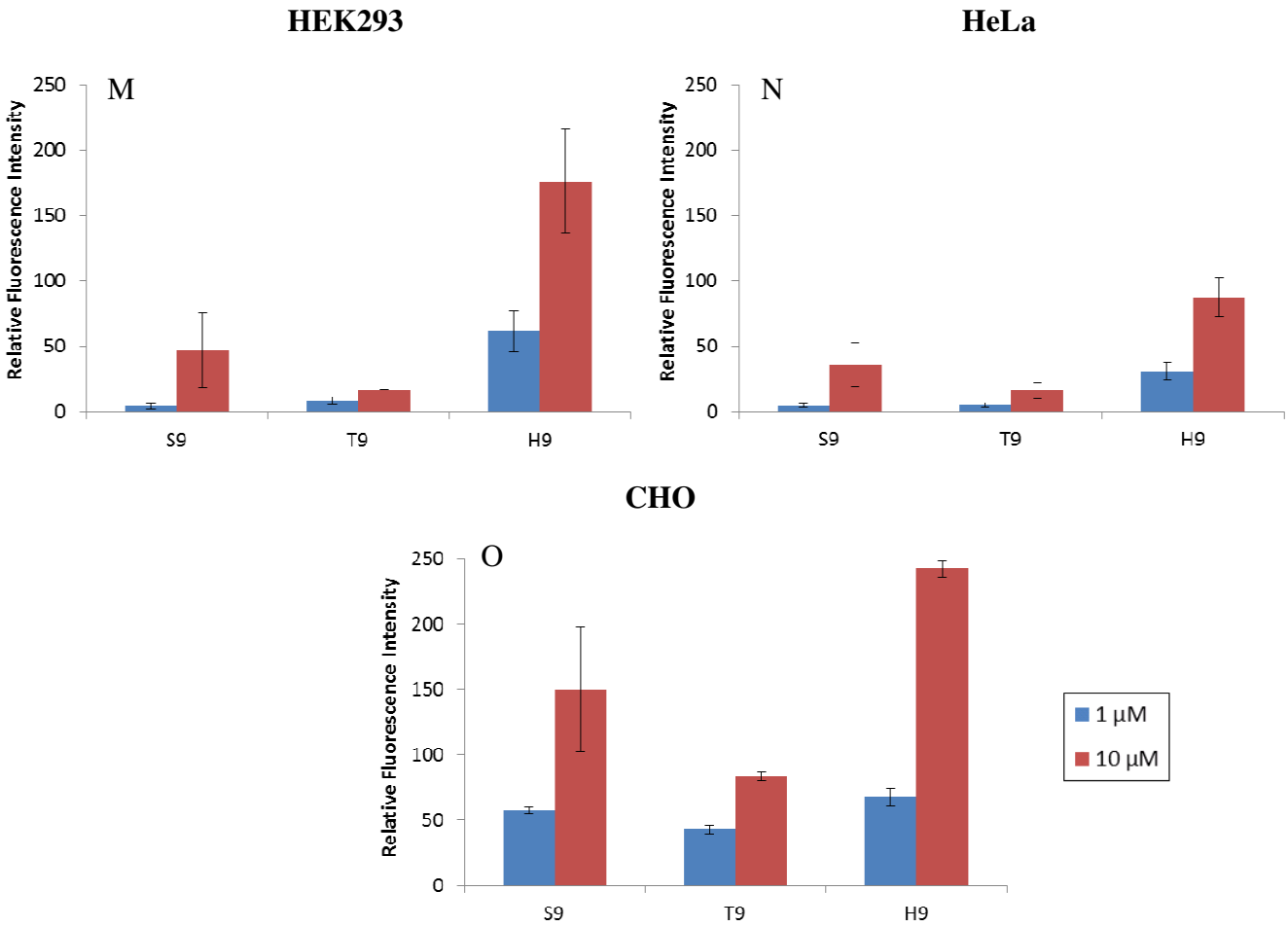

Figure 4.8 A comparison of cellular uptake efficiency of nonamer peptoids **S9**, **T9** and **H9** with different side chain motifs in HEK293, HeLa and CHO cells. 3 x 10^4 cells per well (in 48-well plate) were treated with the specified concentration of each peptoid for 2 h at 37°C (n = 6). Fluorescence was measured via flow cytometry at an excitation wavelength of 488 nm, and emission monitored with a 530 / 30 band-pass filter.

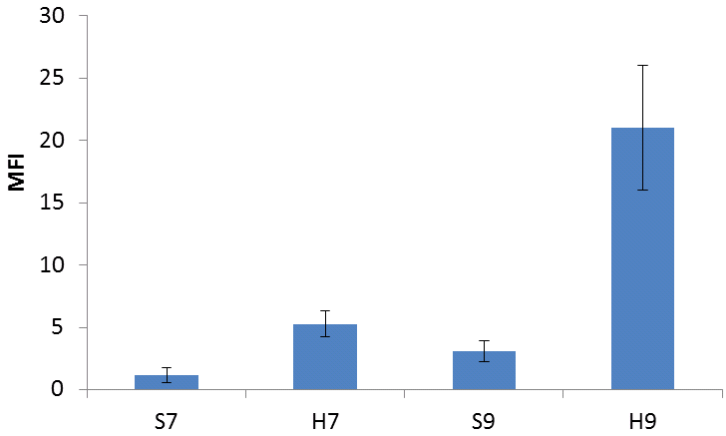

Figure 4.9 Confocal microscope analysis of HeLa cells. 4 x 10^5 were seeded onto glass cover slip (6-well plate) and incubated with **S7**, **S9**, **H7** and **H9** at 1 μM for 12 h at 37°C (n = 6). Cells were fixed with paraformaldehyde (4% w/v in PBS), treated with Hoechst 33342 (1% w/v in PBS) and imaged at λ_{ex}: 407 nm and 488 nm respectively. MFI denotes mean fluorescence intensity and the captured image was analysed with Leica's LAS AF software.

An analysis of the chemical structure of the modified peptoids provides important clues regarding the role of the added ethylene glycol units. On the TEG nonamer **T9**, there are a total of nine side chain units on each transporter molecule. Each side chain carries two ether groups, all of which can serve as hydrogen bond acceptors. This is expected to increase the solubility of the TEG peptoid significantly due to improved interaction between the transporter and its aqueous environment. While enhanced solubility was expected to increase the cell permeability of the transporter, experimental results revealed that the presence of excessive hydrogen bond acceptors negatively affected the cell permeability of the TEG peptoid. Furthermore, **T9** being the largest member in the collection (i.e. with a molecular weight of 2182.51 Da) could slow down the internalisation process due to its molecular size.

It was obvious that the standard nonamer **S9** outperformed the TEG nonamer **T9** in all three cell types tested. A plausible explanation lies in the dynamic interaction between the peptoid and the lipid bilayer cell membrane. The initial ionic interaction between the TEG peptoid's cationic side chains and the negatively charged head groups of the plasma membrane could be reduced by a "water shell" surrounding the triethylene glycol side chains. It is also possible that the process of internalisation is disrupted once the transporter reaches the lipophilic inner fold of the cell membrane. The highly hydrophilic side chains of the transporter might be

incompatible with the hydrophobic tails of the lipid bilayer, thus impeding the penetration of the transporter molecules.

In contrast, the hybrid peptoid **H9** displayed excellent cell penetrating behaviour relative to both the standard and TEG oligomers. This infers that achieving a delicate balance between molecular solubility and lipophilicity is essential in improving the cellular uptake efficiency of peptoid transporters. With a 4 : 5 ratio of *N*-((2-(2-aminoethoxy)ethoxy)ethyl) to *N*-(6-aminohexyl) side chains, the hybrid nonamer could possess an ideal proportion of structural amphiphilicity. The hybrid transporter is expected to be more soluble than standard peptoids but retains sufficient lipophilic characteristics to aid the mechanism of internalisation. Nonetheless, other factors contributing to the enhanced performance of the hybrid transporter could not be ascertained based on current data.

It has been reported that a six-residue peptoid (i.e. a shorter analogue of the nonamer peptoid **S9**) with *N*-(4-aminobutyl) side chains adopts a pseudo-helical structure in water with an all-*cis* amide conformation and such structural conformation is functionally important for certain CPPs to translocate the cell membrane.[152,153] Therefore, there is a possibility that the hybrid nonamer espoused a unique structural conformation which facilitates the process of internalisation. In-depth structural investigations are required to elaborate the intricacies the hybrid transporter.

The locality of the hybrid peptoids, once internalised, was of special interest due to their distinct amphiphilic characteristics. Thus, confocal microscopy was used to image the internalised transporters. Figure 4.10 shows a series of images taken from HeLa cells after incubation with hybrid heptamer **H7** at 1 μM for 12 hours (Figure 4.10, P). Based on the images, the peptoid could be seen in vesicular pockets (i.e. peripheral bright fluorescence clusters) surrounding the cell nuclei (Figure 4.10, R). The cytosol of cells was also clearly stained with green fluorescence implying a release of the transporter from the endosomes over time. The nucleus (stained with the blue *bis*-benzimide dye) showed no indication of peptoid internalisation (Figure 4.10, Q). The locality of the internalised hybrid transporter is consistent with previously observed confocal images of standard peptoids.[112] In general, no extraordinary organelle specificity was observed with the hybrid peptoids.

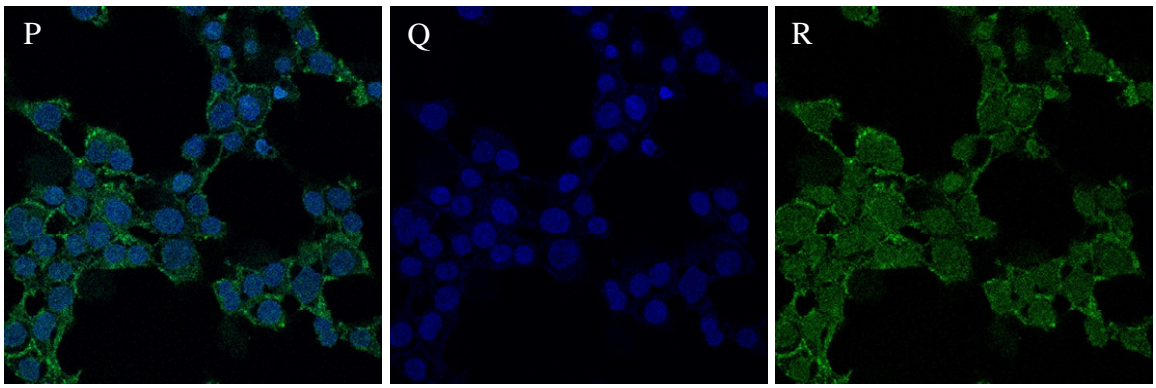

Figure 4.10 Confocal microscope image of HeLa cells. 4 x 10^5 were seeded onto glass cover slip (6-well plate) and incubated with hybrid peptoid **H7** at 1 μM for 12 h at 37°C (n = 6). Cells were fixed with paraformaldehyde (4% w/v in PBS), treated with Hoechst 33342 (1% w/v in PBS) and imaged at λ_{ex}: 407 nm (Q) and 488 nm (R), respectively. (P) represents a transposition of images from the respective channel.

4.3 Summary

A total of nine peptoids, from three different structural categories, were synthesised via solid phase synthesis. These include the homo-oligomers of (i) *N*-(6-aminohexyl)glycines (standard peptoids) and (ii) *N*-((2-(2-aminoethoxy)ethoxy)ethyl)glycines (TEG peptoids), as well as the hetero-oligomer of alternating standard and TEG residues (hybrid peptoids). 5(6)-carboxyfluorescein was used as a fluorescence tracker in monitoring the cellular activity of the peptoids via flow cytometry. Under normal synthetic conditions, it was discovered that the N^{α}-Fmoc group deprotection of the TEG and hybrid peptoids was problematic when the length of the oligomer backbone was ≥ five monomer units. Therefore, the TEG and hybrid peptoids were assembled using microwave-assisted SPPS which provided access to the novel architectures. Three members of each peptoid category – pentamer, heptamer and nonamer, were synthesised for biological evaluations.

The peptoids were evaluated for their cytotoxicity and cellular uptake efficiency in three different cell lines (HEK293, HeLa and CHO). Based on the results of MTT and PI assays, all the peptoids were observed to be non-cytotoxic at a concentration of 10 μM as evidenced by the relatively high HeLa cell viability. In general, the standard and hybrid peptoids demonstrated positive correlation between translocation efficiency and the length of oligomer backbone (nonamer > heptamer > pentamer). However, the TEG peptoids were more cell specific; displaying markedly different permeability in the different cells tested. While all nine peptoids showed

cellular internalisation, the hybrid nonamer was the best transporter. Experimental findings showed that HEK293 and HeLa cells were successfully labelled by the hybrid nonamer **H9** after 2 hours of incubation at a concentration of 1 μM; demonstrating comparable internalisation efficiency to the standard nonamer **S9** at a much higher concentration (i.e. 10 μM). The superior performance of the hybrid peptoid is believed to stem from its amphiphilic characteristics, achieving a good balance between enhanced solubility through the addition of multiple ethylene glycol units and retaining sufficient lipophilic characteristic via the six methylene spacer-side chains.

CHAPTER 5

EXPERIMENTAL

5.1 General Information

5.1.1 Chemicals

All solvents, reagents, catalysts and resins were obtained from commercial suppliers and used without purification, unless otherwise stated.

5.1.2 Instruments

^{1}H and ^{13}C NMR spectra were recorded on an automated Bruker AVA 500 (500 and 125 MHz, respectively) in the indicated solvents at 298 K. Chemical shifts (δ) are quoted in parts per million (ppm) relative to the residual solvent and all coupling constants (*J*) were measured in Hertz (Hz).

Electrospray mass spectrometry analysis was performed on an Agilent 1100 series LC-MS system. Mass spectra were acquired via a VG Platform Single Quadrupole Electrospray Ionisation (ESI) mass spectrometer. High Resolution Mass Spectrometry (HR-MS) was performed using Bruker 3.0 T Apex II spectrometer.

Analytical HPLC was conducted on an Agilent 1100 series HPLC system coupled to a Polymer Lab PL-ELS 1000 Evaporative Light Scattering (ELS) detector with UV detection at 220, 254, 260, 282 and 495 nm. Supelco's Discovery® C18 (50 mm x 2.1 mm x 5 μm) column was used. Elution was performed with Solvent A (0.1% formic acid in HPLC-grade deionised water) and Solvent B (0.1% formic acid in HPLC-grade MeOH / MeCN) at 1 $mLmin^{-1}$ with a gradient of 5 to 95% B over 3 min, followed by 2 min isocratic at 95% B and ending with a gradient of 95 to 5% B over 1 min.

Infrared (IR) spectra were recorded on a Fourier Transform IR Bruker Tensor 27 spectrometer. All samples were run neat and frequencies were reported in cm^{-1}. Only frequencies corresponding to significant functional groups are reported.

Microwave reaction was carried out by irradiating the reaction mixture in a Biotage Initiator Microwave Synthesiser at 2.45 GHz.

Live cells were monitored using a Leica fluorescence microscope (20x) under bright light and 488 nm excitation. Flow cytometry analysis was carried out on a Becton Dickinson (BD) FACS Aria® cytometer using FACSDiva® or FlowJo software. The absorbance of 96-well plates was read on a Benchmark Bio-Rad microplate reader at 570 nm using the Microplate Manager 4.0 software. Confocal images were taken on a Leica SP5 confocal microscope and Zeiss 510 Meta software was used for digital acquisition. Deconvolution was carried out using AutoQuant X software.

5.2 Flow Instrumentation

The flow experiments were performed on a self-assembled continuous flow set-up. The main components of the flow system are represented schematically in Figure 5.1.

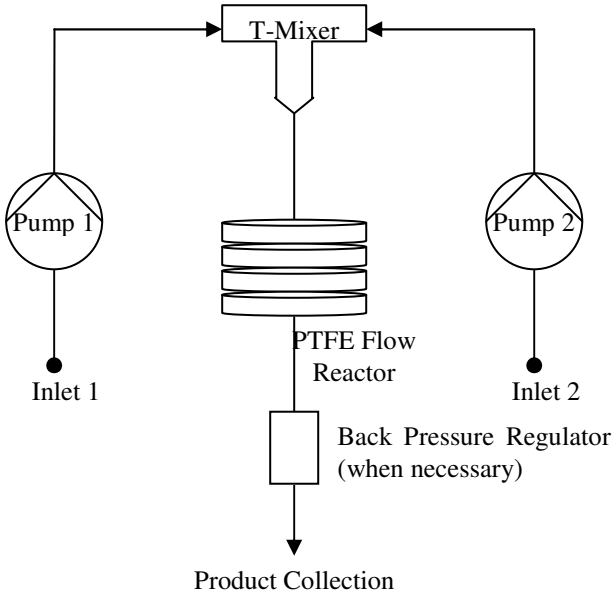

Figure 5.1 General schematic of the continuous flow set-up.

Two or more HPLC pumps were used to deliver the reactants continuously into the flow reactor. Each pump was equipped with a pressure transducer to monitor the pressure of the flow system during reactions. Material precipitation within the flow reactor could easily be detected when the pressure of the system suddenly increases at a constant total flow rate. A simple T-mixer (commercially available) with an internal bore of 0.80 mm was used to mix two separate feed streams and the mixture was channelled into the flow reactor.

The coil reactor was made of PTFE tubing (0.50 mm I.D.) with an internal volume of 2.00, 4.00 or 8.00 mL. PTFE tubing was chosen as it is chemically inert, corrosion resistant towards a broad range of solvents, acids and bases as well as being highly lubricious (with a low coefficient of friction). In order to perform reactions at elevated temperatures, an adjustable back pressure regulator (BPR) was installed to pressurise the flow system. Standard HPLC fittings were used to connect each individual component to create a fully functional reaction platform. Detailed specifications of the system are listed in Table 5.1.

Table 5.1 System specifications of the continuous flow set-up.

Component	Specification
HPLC Pump	**Pump**: Knauer Smartline Pump 100 **Pumphead:** 10 mL with ceramic inlays (with pressure transducer) **Flow range**: 0.001 – 10.000 $mLmin^{-1}$ **Delivery system**: Double-piston pump with main and auxiliary piston **Dimension**: 110 x 130 x 250 mm (W x H x D) **Flow accuracy**: < 1.0% at 1 $mLmin^{-1}$, 12 MPa **Flow precision**: < 0.5% at 1 $mLmin^{-1}$, 12 MPa
Reagent Inlet	**Material**: PTFE tubing (1.00 mm I.D.)
Mixer	**Configuration**: T-Mixer **Material**: PEEK **Bore size**: 0.80 mm
Flow Reactor	**Material**: PTFE tubings (0.50 mm I.D.) **Operating Temperature**: -270 to 260^{o}C
Back Pressure Regulator	**Diaphragm**: Spring-loaded FFKM (perfluorinated rubber) **Housing**: PEEK **Membrane**: Polyimide **Operating Pressure**: 1 – 20 bar
Product Outlet	**Material**: PTFE tubing (0.50 mm I.D.)

5.3 Experimental for Chapter 2

5.3.1 Flow Mediated Mono-Boc Carbamation

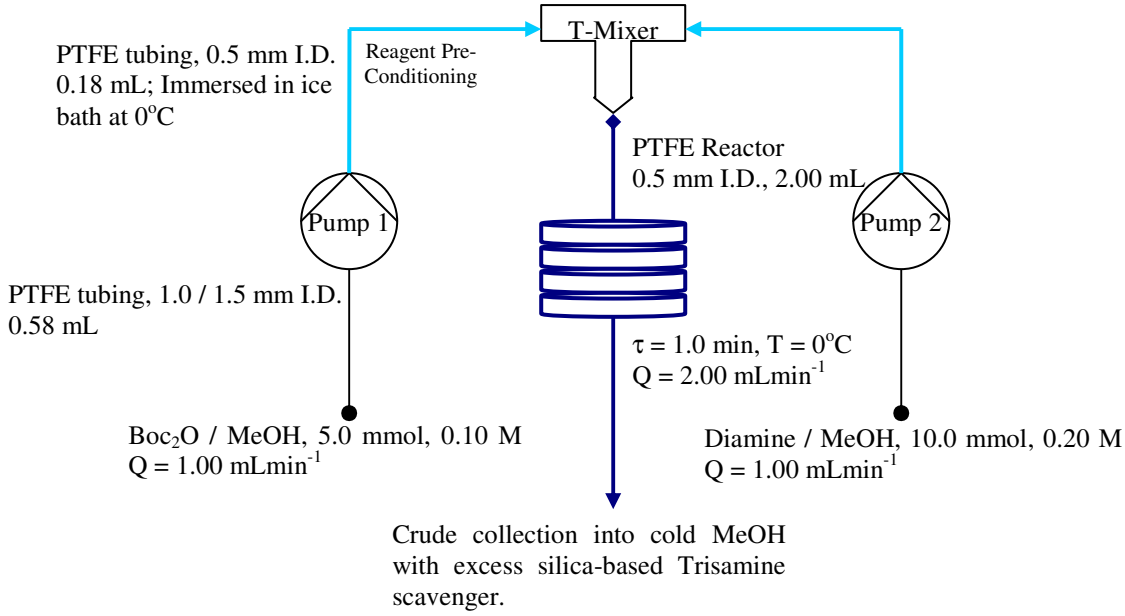

Figure 5.2a Mono-Boc carbamation via continuous flow synthesis.

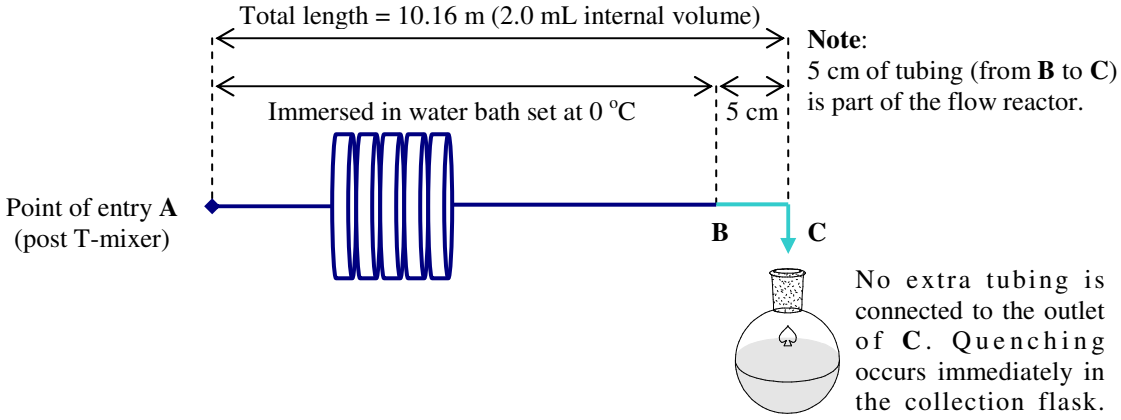

Figure 5.2b Flow reaction stream from point of entry **A** to point of exit **C**, and the subsequent quenching. Residence time is calculated based on the total time spent from **A** to **C** at a constant 2.0 mL reactor volume.

Flow Screening Procedure:

Diamines **1a**, **1b** or **1c** (0.10 M, 10 mL) and Boc_2O (0.10 M, 10 mL) in MeOH were fed continuously into a PTFE reactor (0.50, 1.00 or 1.50 mm I.D., 2.00 mL total volume) immersed in a water bath set to the desired working temperature (0 or 25°C). The reactants were introduced via two separate pre-conditioning segments of PTFE

tubing (0.5 mm I.D., 0.18 mL volume) immersed in a temperature adjusted bath. The reactants converged in the T-mixer and the stoichiometry as well as residence time of the reaction were determined by adjusting the individual flow rates of the HPLC pumps. The reaction stream (20 mL) was collected at steady state after 1.5 reactor volume, into a flask filled with cold MeOH (80 mL, – 20°C) containing an excess of trisamine scavenger (0.63 g, 1.0 mmol; assuming 50% mono-Boc carbamation efficiency). The solution was filtered and the filtrate concentrated *in vacuo*. The crude mixture was purified via flash column chromatography (silica gel, 90:10 DCM / MeOH with 0.1% TEA) and the product yields reported accordingly.

General Scale-Out Procedure:

Diamines and triamines **1a – 1i** (0.10 M, 50 mL) and Boc_2O (0.20 M, 50 mL) in MeOH were fed continuously into a PTFE reactor (0.50 mm I.D., 2.00 mL total volume) immersed in an ice bath (0°C). The reactants were introduced via two separate pre-conditioning segments (temperature set at 0°C) of PTFE tubing (0.5 mm I.D., 0.18 mL volume). The reactants converged in the T-mixer and the total flow rate of reaction stream was fixed at 2.00 $mLmin^{-1}$ to give a residence time of 1.0 min. The reaction stream (100 mL) was collected at steady state after 1.5 reactor volume, into a flask filled with cold MeOH (200 mL, –20°C) containing an excess of trisamine scavenger (3.00 g, 4.7 mmol; assuming 50% mono-Boc carbamation efficiency) under rigorous stirring. The solution was filtered and the filtrate concentrated *in vacuo*. The crude mixture was purified via flash column chromatography (silica gel, 90:10 DCM / MeOH with 0.1% TEA) to give:

***tert*-Butyl *N*-(2-aminoethyl)carbamate (4)**

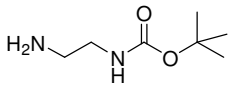

Yield: 0.51g (64%); yellow oil

IR (neat): ν (cm^{-1}) = 3294, 2976, 1687, 1519; ^{1}H NMR (500 MHz, $CDCl_3$): δ [ppm] = 1.43 [s, 9H, $(CH_3)_3$], 2.04 (s, 2H, NH_2), 2.81 (t, *J* = 5.9 Hz, 2H, NH_2CH_2), 3.20 (q, *J* = 5.6 Hz, 2H, CH_2NH), 4.99 (br s, 1H, NH); ^{13}C NMR (125 MHz, $CDCl_3$): δ [ppm] = 28.40 [$(CH_3)_3$], 40.37 (NH_2CH_2), 41.63 (CH_2NH), 79.07 [$OC(CH_3)_3$], 156.02

(NH**C**O_2C); LC-MS (ESI^+): m/z (%) =161.2 (100) $[M+H]^+$; HR-MS ($C_7H_{16}N_2O_2$): calc: 160.1206; found: 160.1202. Spectral data are consistent with the literature.[I]

***tert*-Butyl *N*-(3-aminopropyl)carbamate (8)**

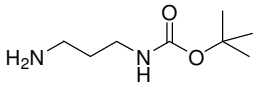

Yield: 0.67 g (77%); yellow oil

IR (neat): ν (cm^{-1}) = 3383, 2967, 2918, 1687, 1518, 1163; ^{1}H NMR (500 MHz, $CDCl_3$): δ [ppm] = 1.43 [s, 9H, (C**H**$_3$)$_3$], 1.60 – 1.64 (m, 2H, NH_2CH_2C**H**$_2$$CH_2NH$), 2.16 (s, 2H, N**H**$_2$), 2.76 (t, *J* = 6.6 Hz, 2H, NH_2C**H**$_2$), 3.19 – 3.23 (m, 2H, C**H**$_2$NH), 4.90 (br s, 1H, N**H**); ^{13}C NMR (125 MHz, $CDCl_3$): δ [ppm] = 28.40 [(**C**H_3)$_3$], 33.26 (NH_2CH_2**C**H_2CH_2NH), 38.39 (**C**H_2NH), 39.61 (NH_2**C**H_2), 79.09 [O**C**(CH_3)$_3$], 156.15 (NH**C**O_2C); LC-MS (ESI^+): m/z (%) = 175.2 (100) $[M+H]^+$; HR-MS ($C_8H_{18}N_2O_2$): calc: 174.1363; found: 174.1361. Spectral data are consistent with the literature.[I]

***tert*-Butyl *N*-(4-aminobutyl)carbamate (6)**

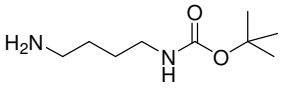

Yield: 0.61 g (65%); yellow oil

IR (neat): ν (cm^{-1}) = 3363, 2975, 2929, 1526, 1171; ^{1}H NMR (500 MHz, $CDCl_3$): δ [ppm] = 1.43 [s, 9H, (C**H**$_3$)$_3$], 1.45 – 1.53 [m, 4H, NH_2CH_2(C**H**$_2$)$_2$$CH_2NH$], 1.80 (s, 2H, N**H**$_2$), 2.71 (t, *J* = 6.7 Hz, 2H, NH_2C**H**$_2$), 3.10 – 3.12 (m, 2H, C**H**$_2$NH), 4.69 (br s, 1H, N**H**); ^{13}C NMR (125 MHz, $CDCl_3$): δ [ppm] = 27.43 (**C**H_2CH_2NH), 28.40 [(**C**H_3)$_3$], 30.56 (NH_2CH_2 **C**H_2), 40.38 (**C**H_2NH), 41.65 (NH_2**C**H_2), 79.06 [O**C**(CH_3)$_3$], 156.01 (NH**C**O_2C); LC-MS (ESI^+): m/z (%) = 189.2 (100) $[M+H]^+$; 211.2 (6) $[M+Na]^+$; HR-MS ($C_9H_{20}N_2O_2$): calc: 188.1519; found: 188.1520. Spectral data are consistent with the literature.[I]

***tert*-Butyl *N*-(5-aminopentyl)carbamate (9)**

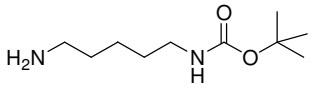

Yield: 0.60 g (59%); yellow oil

IR (neat): ν (cm^{-1}) = 3331, 2974, 2931, 1521, 1170; ^{1}H NMR (500 MHz, $CDCl_3$): δ [ppm] = 1.33 – 1.38 [m, 2H, $NH_2(CH_2)_2C\mathbf{H}_2(CH_2)_2NH$], 1.43 [s, 9H, $(C\mathbf{H}_3)_3$], 1.46 – 1.52 (m, 4H, $NH_2CH_2C\mathbf{H}_2CH_2C\mathbf{H}_2CH_2NH$), 1.91 (br s, 2H, $N\mathbf{H}_2$), 2.70 (t, *J* = 7.0 Hz, 2H, $NH_2C\mathbf{H}_2$), 3.09 – 3.13 (m, 2H, $C\mathbf{H}_2NH$), 4.56 (br s, 1H, N**H**); ^{13}C NMR (125 MHz, $CDCl_3$): δ [ppm] = 24.01 $[NH_2(CH_2)_2\mathbf{C}H_2(CH_2)_2NH]$, 28.40 $[(\mathbf{C}H_3)_3]$, 29.86 ($\mathbf{C}H_2CH_2NH$), 32.95 ($NH_2CH_2\mathbf{C}H_2$), 40.46 ($\mathbf{C}H_2NH$), 41.88 ($NH_2\mathbf{C}H_2$), 79.04 $[O\mathbf{C}(CH_3)_3]$, 155.98 ($NH\mathbf{C}O_2C$); LC-MS (ESI^+): m/z (%) = 203.2 (100) $[M+H]^+$; HR-MS ($C_{10}H_{22}N_2O_2$): calc: 202.1676; found: 202.1670. Spectral data are consistent with the literature.[I]

***tert*-Butyl *N*-(6-aminohexyl)carbamate (2)**

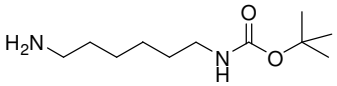

Yield: 0.66 g (61%); yellow oil

IR (neat): ν (cm^{-1}) = 3367, 1683, 1519; ^{1}H NMR (400 MHz, $CDCl_3$): δ [ppm] = 1.31 – 1.34 [m, 4H, $NH_2(CH_2)_2(C\mathbf{H}_2)_2(CH_2)_2NH$], 1.43 – 1.50 [m, 13H, $NH_2CH_2C\mathbf{H}_2(CH_2)_2C\mathbf{H}_2CH_2NH$, $C(C\mathbf{H}_3)_3$], 1.89 (s, 2H, $N\mathbf{H}_2$), 2.68 (t, *J* = 7.0 Hz, 2H, $NH_2C\mathbf{H}_2$), 3.08 – 3.10 (m, 2H, $C\mathbf{H}_2NH$), 4.54 (br s, 1H, N**H**); ^{13}C NMR (100 MHz, $CDCl_3$): δ [ppm] = 26.47 $[NH_2(CH_2)_2\mathbf{C}H_2CH_2(CH_2)_2NH]$, 26.57 $[NH_2(CH_2)_2CH_2\mathbf{C}H_2(CH_2)_2NH]$, 28.40 $[(\mathbf{C}H_3)_3]$, 30.01 ($\mathbf{C}H_2CH_2NH$), 33.35 ($NH_2CH_2\mathbf{C}H_2$), 40.47 ($\mathbf{C}H_2NH$), 41.95 ($NH_2\mathbf{C}H_2$), 79.01 $[O\mathbf{C}(CH_3)_3]$, 155.98 ($NH\mathbf{C}O_2C$); LC-MS (ESI^+): m/z (%) = 217.2 (100) $[M+H]^+$; HR-MS ($C_{11}H_{24}N_2O_2$): calc: 216.1832; found: 216.1835. Spectral data are consistent with the literature.[I]

***tert*-Butyl *N*-{2-[2-(2-aminoethoxy)ethoxy]ethyl}carbamate (10)**

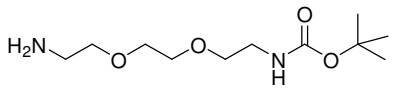

Yield: 0.81 g (65%); yellow oil

IR (neat): ν (cm^{-1}) = 3367, 1685; ^{1}H NMR (400 MHz, $CDCl_3$): δ [ppm] = 1.44 [s, 9H, C(C**H**$_3$)$_3$]; 1.73 (s, 2H, N**H**$_2$), 2.88 (t, *J* = 5.2 Hz, 2H, C**H**$_2$NH$_2$), 3.31 – 3.32 (m, 2H, C**H**$_2$NH), 3.51 – 3.55 [m, 4H, CH$_2$O(C**H**$_2$)$_2$OCH$_2$], 3.61 [br s, 4H, NHCH$_2$C**H**$_2$O(CH$_2$)$_2$OC**H**$_2$CH$_2$NH$_2$] 5.18 (br s, 1H, N**H**); ^{13}C NMR (100 MHz, $CDCl_3$): δ [ppm] = 28.40 [(**C**H$_3$)$_3$], 40.33 (C**H**$_2$NH), 41.65 (NH$_2$C**H**$_2$), 70.18 [NH$_2$(CH$_2$)$_2$O(C**H**$_2$)$_2$O], 70.21 (OC**H**$_2$CH$_2$NH), 73.25 (NH$_2$CH$_2$C**H**$_2$), 79.18 [O**C**(CH$_3$)$_3$], 156.02 (NH**C**O$_2$C); LC-MS (ESI$^+$): m/z (%) = 249.2 (100) [M+H]$^+$; 271.2 (14) [M+Na]$^+$; HR-MS ($C_{11}H_{24}N_2O_4$): calc: 248.1731; found: 248.1729. Spectral data are consistent with the literature.[II]

***tert*-Butyl *N*-(3-{2-[2-(3-aminopropoxy)ethoxy]ethoxy}propyl)carbamate (11)**

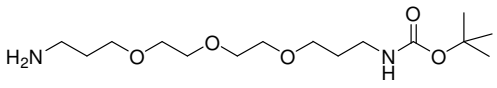

Yield: 1.07 g (67%); yellow oil

IR (neat): ν (cm^{-1}) = 3348, 2866, 1692, 1521, 1109; ^{1}H NMR (500 MHz, $CDCl_3$): δ [ppm] = 1.42 [s, 9H, (C**H**$_3$)$_3$], 1.75 [quin., *J* = 6.4 Hz, 4H, NH$_2$CH$_2$C**H**$_2$(CH$_2$OCH$_2$)$_3$C**H**$_2$], 2.08 (s, 2H, N**H**$_2$), 2.83 (t, *J* = 6.6 Hz, 2H, NH$_2$C**H**$_2$), 3.20 – 3.22 (m, 2H, C**H**$_2$NH), 3.53 [t, *J* = 6.0 Hz, 2H, NH$_2$(CH$_2$)$_2$C**H**$_2$O], 3.55 – 3.60 [m, 6H, NH$_2$(CH$_2$)$_3$O(C**H**$_2$)$_2$O(CH$_2$)$_2$OC**H**$_2$], 3.62 – 3.64 [m, 4H, NH$_2$(CH$_2$)$_3$O(CH$_2$)$_2$O(C**H**$_2$)$_2$O], 5.1 (br s, 1H, N**H**); ^{13}C NMR (125 MHz, $CDCl_3$): δ [ppm] = 28.43 [(**C**H$_3$)$_3$], 29.63 (**C**H$_2$CH$_2$NH), 32.57 (NH$_2$CH$_2$**C**H$_2$), 38.41 (NH$_2$**C**H$_2$), 39.61 (CH$_2$**C**H$_2$NH), 69.44 [NH$_2$(CH$_2$)$_2$**C**H$_2$O], 69.55 [O**C**H$_2$(CH$_2$)$_2$NH], 70.12 [NH$_2$(CH$_2$)$_3$O**C**H$_2$], 70.16 [NH$_2$(CH$_2$)$_3$OCH$_2$**C**H$_2$], 70.49 [NH$_2$(CH$_2$)$_3$O(CH$_2$)$_2$O**C**H$_2$], 70.53 [NH$_2$(CH$_2$)$_3$O(CH$_2$)$_2$OCH$_2$**C**H$_2$], 78.91 [O**C**(CH$_3$)$_3$], 156.13 (NH**C**O$_2$C); LC-MS (ESI$^+$): m/z (%) = 321.2 (100) [M+H]$^+$; 343.2 (5) [M+Na]$^+$; HR-MS ($C_{15}H_{32}N_2O_5$): calc: 320.2306; found: 320.2307. Spectral data are consistent with the literature.[III]

***tert*-Butyl *N*-{2-[(2-aminoethyl)amino]ethyl}carbamate (12)**

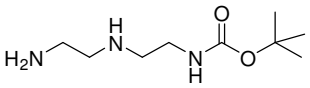

Yield: 0.56 g (55%); yellow oil

IR (neat): ν (cm^{-1}) = 3296, 2974, 2931, 1686, 1517, 1166; ^{1}H NMR (500 MHz, $CDCl_3$): δ [ppm] = 1.43 [s, 9H, ($C\mathbf{H}_3$)$_3$], 2.07 (s, 2H, $N\mathbf{H}_2$), 2.67 (t, *J* = 5.8 Hz, 2H, $NH_2C\mathbf{H}_2$), 2.72 (t, *J* = 5.8 Hz, 2H, $NH_2CH_2C\mathbf{H}_2$), 2.80 (t, *J* = 5.8 Hz, 2H, $NHC\mathbf{H}_2CH_2NH$), 3.21 – 3.22 (m, 2H, $CH_2C\mathbf{H}_2NH$), 5.06 (br s, 1H, $N\mathbf{H}CO_2C$); ^{13}C NMR (125 MHz, $CDCl_3$): δ [ppm] = 28.38 [($\mathbf{C}H_3$)$_3$], 40.24 ($NH_2\mathbf{C}H_2$), 41.46 ($\mathbf{C}H_2NHCO$), 48.94 ($NH\mathbf{C}H_2CH_2NH$), 51.63 ($NH_2CH_2\mathbf{C}H_2NH$), 79.15 [$O\mathbf{C}(CH_3)_3$], 156.15 ($NH\mathbf{C}O_2C$); LC-MS (ESI^+): m/z (%) = 204.1 (38) $[M+H]^+$. Spectral data are consistent with the literature.[IV]

***tert*-Butyl *N*-{3-[(3-aminopropyl)amino]propyl}carbamate (13)**

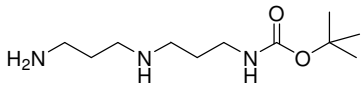

Yield: 0.46 g (40%); yellow oil

IR (neat): ν (cm^{-1}) = 3353, 2982, 2865, 1682, 1519; ^{1}H NMR (500 MHz, $CDCl_3$): δ [ppm] = 1.43 [s, 9H, ($C\mathbf{H}_3$)$_3$], 1.65 (sex, *J* = 6.6 Hz, 4H, $NH_2CH_2C\mathbf{H}_2CH_2NHCH_2C\mathbf{H}_2$), 1.84 (s, 2H, $N\mathbf{H}_2$), 2.68 (t, *J* = 6.4 Hz, 4H, $C\mathbf{H}_2NHC\mathbf{H}_2$), 2.79 (t, *J* = 6.7 Hz, 2H, $NH_2C\mathbf{H}_2$), 3.19 – 3.20 (m, 2H, $C\mathbf{H}_2NH$), 5.19 (br s, 1H, $N\mathbf{H}CO_2C$); ^{13}C NMR (125 MHz, $CDCl_3$): δ [ppm] = 28.41 [($\mathbf{C}H_3$)$_3$], 29.66 ($NHCH_2\mathbf{C}H_2CH_2NH$), 33.07 ($NH_2CH_2\mathbf{C}H_2CH_2$), 39.07 ($\mathbf{C}H_2NHCO$), 40.45 ($NH_2\mathbf{C}H_2$), 47.63 [$NH\mathbf{C}H_2(CH_2)_2NH$], 47.84 [$NH_2(CH_2)_2\mathbf{C}H_2NH$], 79.00 [$O\mathbf{C}(CH_3)_3$], 156.14 ($NH\mathbf{C}O_2C$); LC-MS ($ESI^+$): m/z (%) = 232.3 (100) $[M+H]^+$; 254.2 (8) $[M+Na]^+$. Spectral data are consistent with the literature.[IV]

5.3.2 Flow Mediated Mono-Fmoc Carbamation

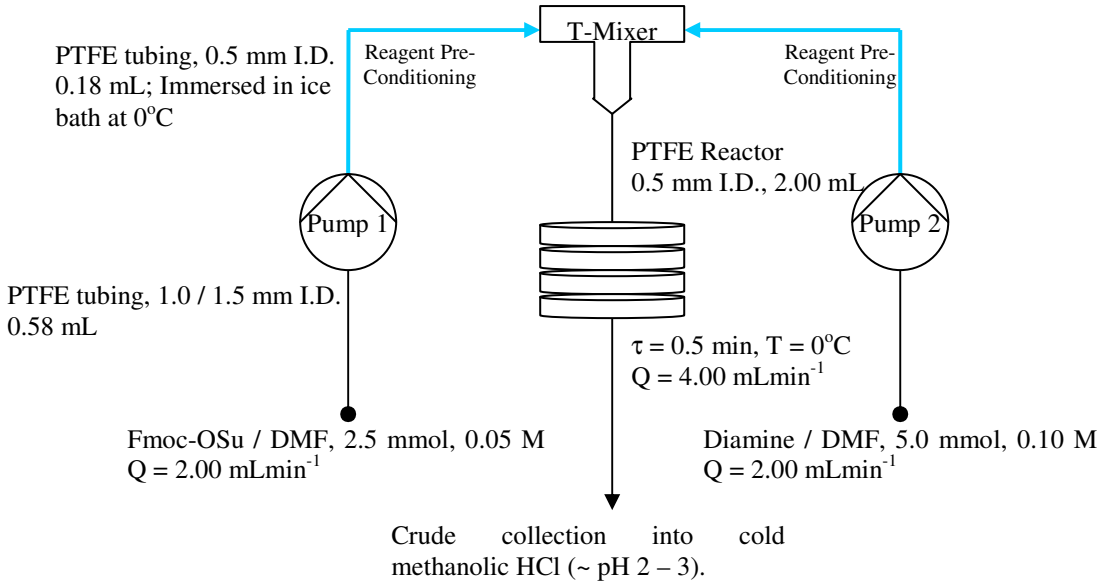

Figure 5.3 Mono-Fmoc carbamation via continuous flow synthesis.

General Scale-Out Procedure:

Diamines **1a** – **1g** (0.05 M, 50 mL) and Fmoc-OSu (0.10 M, 50 mL) in DMF were fed continuously into a PTFE reactor (0.50 mm I.D., 2.00 mL total volume) immersed in an ice bath (0°C). The reactants were introduced via two separate pre-conditioning segments (temperature set at 0°C) of PTFE tubing (0.5 mm I.D., 0.18 mL volume). The reactants converged in the T-mixer and the total flow rate of reaction stream was fixed at 4.00 $mLmin^{-1}$ to give a residence time of 0.5 min. The reaction stream (100 mL) was collected at steady state after 1.5 reactor volume, into a flask filled with cold methanolic HCl (50 mL, –20°C, pH 2 – 3) under rigorous stirring. The solution was concentrated *in vacuo* and distilled water (50 mL) was added into the crude mixture to precipitate the insoluble side product. The white solid was filtered off and the aqueous solution was washed with EtOAc (2 x 50 mL). Subsequently, the aqueous layer was adjusted to pH 8 by adding saturated $NaHCO_3$ solution (30 mL) and extracted with DCM (2 x 100 mL). The organic layer was washed with brine (2 x 100 mL) and dried over $NaSO_4$. The drying agent was filtered off and the filtrate was acidified to pH 3 using methanolic HCl (1.25 M, 10 mL). The filtrate was concentrated *in vacuo* to give:

9H-Fluoren-9-ylmethyl *N*-(2-aminoethyl)carbamate hydrochloride (14)

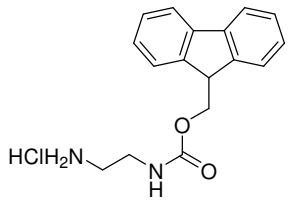

Yield: 0.44 g (63%); off-white solid

M.p. 115 – 117°C; IR (neat): ν (cm^{-1}) = 3287, 2948, 2837, 1647, 1407, 1015; ^{1}H NMR (500 MHz, MeOD): δ [ppm] = 3.04 – 3.05 (m, 2H, HCl.$NH_2C\mathbf{H}_2$), 3.39 (t, *J* = 5.4 Hz, 2H, $C\mathbf{H}_2NHCO$), 4.23 (t, *J* = 6.5 Hz, 1H, C**H**-9), 4.42 (d, *J* = 6.6 Hz, 2H, $CO_2C\mathbf{H}_2CH$-9), 7.32 (t, *J* = 7.4 Hz, 2H, C**H**-2 and -7), 7.40 (t, *J* = 7.4 Hz, 2H, C**H**-3 and -6), 7.66 (d, *J* = 7.4 Hz, 2H, C**H**-1 and -8), 7.81 (d, *J* = 7.5 Hz, 2H, C**H**-4 and -5); ^{13}C NMR (125 MHz, MeOD): δ [ppm] = 39.50 (HCl.$NH_2\mathbf{C}H_2$), 41.20 ($\mathbf{C}H_2NHCO$), 68.05 ($CO_2\mathbf{C}H_2CH$-9), 121.01 (**C**H-3 and -6), 126.44 (**C**H-2 and -7), 128.19 (**C**H-4 and -5), 128.87 (**C**H-1 and -8), 142.70 (**C**H-4a and -4b), 145.30 (**C**H-8a and -9a), 159.42 ($NH\mathbf{C}O_2$); LC-MS (ESI^+): m/z (%) = 283.2 (90) $[M+H]^+$; 305.2 (10) $[M+Na]^+$; HR-MS ($C_{17}H_{18}N_2O_2$): calc: 282.1363; found: 282.1359. Spectral data are consistent with the literature.[V]

9H-Fluoren-9-ylmethyl *N*-(3-aminopropyl)carbamate hydrochloride (15)

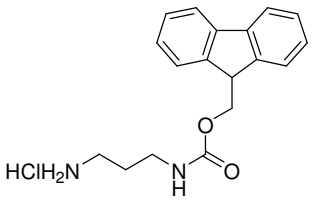

Yield: 0.44 g (59%); off-white solid

M.p. 127 – 129°C; IR (neat): ν (cm^{-1}) = 3331, 2945, 2833, 1645, 1448, 1320, 1110; ^{1}H NMR (500 MHz, MeOD): δ [ppm] = 1.77 – 1.85 (m, 2H, HCl.$NH_2CH_2C\mathbf{H}_2CH_2NH$), 2.91 (t, *J* = 7.3 Hz, 2H, HCl.$NH_2C\mathbf{H}_2$), 3.21 (t, *J* = 6.5 Hz, 2H, $C\mathbf{H}_2NHCO$), 4.21 (t, *J* = 6.5 Hz, 1H, C**H**-9), 4.42 (d, *J* = 6.6 Hz, 2H, $CO_2C\mathbf{H}_2CH$-9), 7.32 (t, *J* = 7.4 Hz, 2H, C**H**-2 and -7), 7.40 (t, *J* = 7.4 Hz, 2H, C**H**-3 and -6), 7.64 (d, *J* = 7.5 Hz, 2H, C**H**-1 and -8), 7.80 (d, *J* = 7.5 Hz, 2H, C**H**-4 and -5);

^{13}C NMR (125 MHz, MeOD): δ [ppm] = 29.26 (HCl.NH_2CH_2**C**H_2CH_2NH), 38.32 (HCl.NH_2**C**H_2), 43.64 (**C**H_2NHCO), 54.85 (**C**H-9), 67.73 (CO_2**C**H_2CH-9), 121.06 (**C**H-3 and -6), 126.11 (**C**H-2 and -7), 128.18 (**C**H-4 and -5), 128.86 (**C**H-1 and -8), 142.72 (**C**H-4a and -4b), 145.31 (**C**H-8a and -9a), 159.43 (NH**C**O_2); LC-MS (ESI$^+$): m/z (%) = 297.2 (87) $[M+H]^+$; HR-MS ($C_{18}H_{20}N_2O_2$): calc: 296.1519; found: 296.1519. Spectral data are consistent with the literature.[VI]

9H-Fluoren-9-ylmethyl *N*-(4-aminobutyl)carbamate hydrochloride (16)

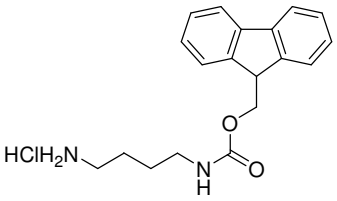

Yield: 0.40 g (51%); off-white solid

M.p. 110 – 112°C; IR (neat): ν (cm^{-1}) = 3304, 2943, 2831, 1449, 1024; ^{1}H NMR (500 MHz, MeOD): δ [ppm] = 1.55 – 1.60 (m, 2H, HCl.NH_2CH_2C**H**$_2$), 1.64 – 1.70 (m, 2H, C**H**$_2CH_2NHCO$), 2.94 (t, *J* = 7.3 Hz, 2H, C**H**$_2$NHCO), 3.15 (t, *J* = 6.6 Hz, 2H, HCl.NH_2C**H**$_2$), 4.20 (t, *J* = 6.7 Hz, 1H, C**H**-9), 4.37 (d, *J* = 6.7 Hz, 2H, CO_2C**H**$_2$CH-9), 7.31 (t, *J* = 7.4 Hz, 2H, C**H**-2 and -7), 7.40 (t, *J* = 7.4 Hz, 2H, C**H**-3 and -6), 7.65 (d, *J* = 7.4 Hz, 2H, C**H**-1 and -8), 7.80 (d, *J* = 7.5 Hz, 2H, C**H**-4 and -5); ^{13}C NMR (125 MHz, MeOD): δ [ppm] = 25.79 (HCl.NH_2CH_2**C**H2), 27.90 [HCl.$NH_2(CH_2)_2$**C**H_2], 40.45 (HCl.NH_2**C**H_2), 40.92 (**C**H_2NHCO), 67.69 (CO_2**C**H_2CH-9), 120.99 (**C**H-3 and -6), 126.14 (**C**H-2 and -7), 128.17 (**C**H-4 and -5), 128.83 (**C**H-1 and -8), 142.68 (**C**H-4a and -4b), 145.36 (**C**H-8a and -9a), 159.08 (NH**C**O_2); LC-MS (ESI$^+$): m/z (%) = 311.2 (100) $[M+H]^+$; 333.2 (7) $[M+Na]^+$; HR-MS ($C_{19}H_{22}N_2O_2$): calc: 310.1676; found: 310.1675. Spectral data are consistent with the literature.[VII]

9H-Fluoren-9-ylmethyl *N*-(5-aminopentyl)carbamate hydrochloride (17)

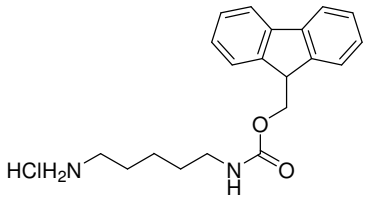

Yield: 0.50 g (62%); off-white solid

M.p. 94 – 96°C; IR (neat): ν (cm^{-1}) = 3333, 2943, 2831, 1566, 1450, 1106; ^{1}H NMR (500 MHz, MeOD): δ [ppm] = 1.35 – 1.43 (m, 2H, $HCl.NH_2(CH_2)_2C\mathbf{H}2$), 1.51 – 1.57 (m, 2H, $C\mathbf{H}_2CH_2NHCO$), 1.64 – 1.70 (m, 2H, $HCl.NH_2CH_2C\mathbf{H}_2$), 2.91 (t, *J* = 7.6 Hz, 2H, $C\mathbf{H}_2NHCO$), 3.12 (t, *J* = 6.9 Hz, 2H, $HCl.NH_2C\mathbf{H}_2$), 4.20 (t, *J* = 6.7 Hz, 1H, C**H**-9), 4.37 (d, *J* = 6.7 Hz, 2H, $CO_2C\mathbf{H}_2CH$-9), 7.31 (t, *J* = 7.5 Hz, 2H, C**H**-2 and -7), 7.40 (t, *J* = 7.4 Hz, 2H, C**H**-3 and -6), 7.64 (d, *J* = 7.5 Hz, 2H, C**H**-1 and -8), 7.80 (d, *J* = 7.5 Hz, 2H, C**H**-4 and -5); ^{13}C NMR (125 MHz, MeOD): δ [ppm] = 24.55 [$HCl.NH_2(CH_2)_2\mathbf{C}H_2$], 28.20 ($HCl.NH_2CH_2\mathbf{C}H_2$), 30.41 ($\mathbf{C}H_2CH_2NHCO$), 40.70 ($HCl.NH_2\mathbf{C}H_2$), 41.28 ($\mathbf{C}H_2NHCO$), 43.56 (**C**H-9), 67.59 ($CO_2\mathbf{C}H_2CH$-9), 120.99 (**C**H-3 and -6), 126.14 (**C**H-2 and -7), 128.16 (**C**H-4 and -5), 128.82 (**C**H-1 and -8), 142.68 (**C**H-4a and -4b), 145.38 (**C**H-8a and -9a), 159.05 ($NH\mathbf{C}O_2$); LC-MS (ESI^+): m/z (%) = 325.2 (74) $[M+H]^+$; HR-MS ($C_{20}H_{24}N_2O_2$): calc: 324.1832; found: 324.1827. Spectral data are consistent with the literature.[VII]

9H-Fluoren-9-ylmethyl *N*-(6-aminohexyl)carbamate hydrochloride (18)

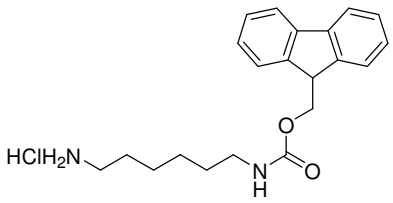

Yield: 0.38 g (45%); off-white solid

M.p. 99 – 101°C; IR (neat): ν (cm^{-1}) = 2955, 2867, 1637, 1569, 1466, 1321, 1097; ^{1}H NMR (500 MHz, MeOD): δ [ppm] = 1.37 – 1.44 [m, 4H, $HCl.NH_2(CH_2)_2(C\mathbf{H}_2)_2$], 1.52 (quin., *J* = 6.9 Hz, 2H, $C\mathbf{H}_2CH_2NHCO$), 1.66 (quin., *J* = 7.4 Hz, 2H, $HCl.NH_2CH_2C\mathbf{H}_2$), 2.91 (t, *J* = 7.5 Hz, 2H, $C\mathbf{H}_2NHCO$), 3.11 (t, *J* = 6.9 Hz, 2H,

HCl.$NH_2C\mathbf{H}_2$), 4.20 (t, *J* = 6.8 Hz, 1H, C**H**-9), 4.36 (d, *J* = 6.8 Hz, 2H, $CO_2C\mathbf{H}_2$CH-9), 7.31 (t, *J* = 7.4 Hz, 2H, C**H**-2 and -7), 7.40 (t, *J* = 7.5 Hz, 2H, C**H**-3 and -6), 7.65 (d, *J* = 7.5 Hz, 2H, C**H**-1 and -8), 7.81 (d, *J* = 7.6 Hz, 2H, C**H**-4 and -5); ^{13}C NMR (125 MHz, MeOD): δ [ppm] = 27.20 [HCl.$NH_2(CH_2)_3\mathbf{C}H_2$], 28.54 [HCl.$NH_2(CH_2)_2\mathbf{C}H_2$], 30.70 (HCl.$NH_2CH_2\mathbf{C}H_2$), 35.43 ($\mathbf{C}H_2CH_2NHCO$), 40.72 (HCl.$NH_2\mathbf{C}H_2$), 41.46 ($\mathbf{C}H_2NHCO$), 67.61 ($CO_2\mathbf{C}H_2$CH-9), 120.99 (**C**H-3 and -6), 126.17 (**C**H-2 and -7), 128.17 (**C**H-4 and -5), 128.82 (**C**H-1 and -8), 142.68 (**C**H-4a and -4b), 145.40 (**C**H-8a and -9a), 159.03 ($NH\mathbf{C}O_2$); LC-MS (ESI$^+$): m/z (%) = 339.2 (87) $[M+H]^+$; 361.2 (8) $[M+Na]^+$; HR-MS ($C_{21}H_{26}N_2O_2$): calc: 338.1989; found: 338.1983. Spectral data are consistent with the literature.[VII]

9H-Fluoren-9-ylmethyl *N*-{2-[2-(2-aminoethoxy)ethoxy]ethyl}carbamate hydrochloride (19)

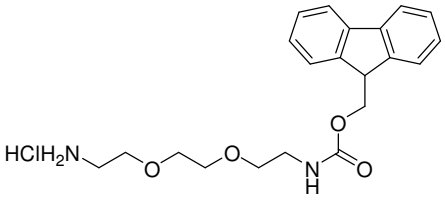

Yield: 0.56 g (61%); off-white solid

M.p. 113 – 115°C; IR (neat): ν (cm^{-1}) = 3313, 2942, 2830, 1449, 1114; ^{1}H NMR (500 MHz, MeOD): δ [ppm] = 3.06 (t, *J* = 5.0 Hz, 2H, C$\mathbf{H}_2$NHCO), 3.28 – 3.29 (m, 2H, HCl.$NH_2C\mathbf{H}_2$), 3.53 [t, *J* = 5.6 Hz, 2H, OC$\mathbf{H}_2CH_2$NH), 3.60 – 3.67 [m, 6H, HCl.$NH_2CH_2C\mathbf{H}_2O(C\mathbf{H}_2)_2O$], 4.20 (t, *J* = 6.7 Hz, 1H, C**H**-9), 4.35 (d, *J* = 6.7 Hz, 2H, $CO_2C\mathbf{H}_2$CH-9), 7.30 (t, *J* = 7.4 Hz, 2H, C**H**-2 and -7), 7.38 (t, *J* = 7.4 Hz, 2H, C**H**-3 and -6), 7.63 (d, *J* = 7.5 Hz, 2H, C**H**-1 and -8), 7.79 (d, *J* = 7.6 Hz, 2H, C**H**-4 and -5); ^{13}C NMR (125 MHz, MeOD): δ [ppm] = ^{13}C NMR (125 MHz, MeOD): δ [ppm] = 40.71 ($\mathbf{C}H_2NHCO$), 41.60 (HCl.$NH_2\mathbf{C}H_2$), 67.75 ($CO_2\mathbf{C}H_2$CH-9), 67.90 (O$\mathbf{C}H_2\mathbf{C}H_2O$), 71.12 (O$\mathbf{C}H_2CH_2NH$), 71.39 (HCl.$NH_2CH_2\mathbf{C}H_2$), 121.02 (**C**H-3 and -6), 126.17 (**C**H-2 and -7), 128.19 (**C**H-4 and -5), 128.86 (**C**H-1 and -8), 142.68 (**C**H-4a and -4b), 145.36 (**C**H-8a and -9a), 159.06 ($NH\mathbf{C}O_2$); LC-MS (ESI$^+$): m/z (%) = 371.2 (100) $[M+H]^+$; 393.2 (20) $[M+Na]^+$; HR-MS ($C_{21}H_{26}N_2O_4$): calc: 370.1887; found: 370.1881. Compound has not been reported in the literature.

9H-Fluoren-9-ylmethyl *N*-(3-{2-[2-(3-aminopropoxy)ethoxy]ethoxy}propyl) carbamate hydrochloride (20)

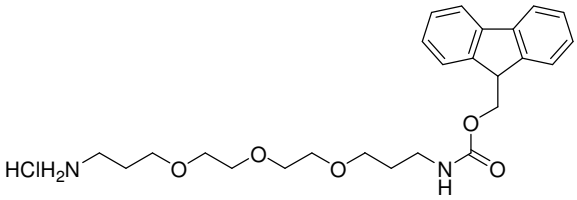

Yield: 0.56 g (51%); off-white solid

M.p. 71 – 73°C; IR (neat): ν (cm^{-1}) = 3312, 2942, 2830, 1567, 1449, 1115; ^{1}H NMR (500 MHz, MeOD): δ [ppm] = 1.73 (quin., *J* = 6.4 Hz, 2H, $CH_2C\mathbf{H}_2CH_2NHCO$), 1.88 (quin., *J* = 6.0 Hz, 2H, $HCl.NH_2CH_2C\mathbf{H}_2CH_2O$), 3.05 (t, *J* = 6.4 Hz, 2H, $HCl.NH_2C\mathbf{H}_2$), 3.16 – 3.20 (m, 2H, $C\mathbf{H}_2NHCO$), 3.48 [t, *J* = 6.0 Hz, 2H, $HCl.NH_2(CH_2)_2C\mathbf{H}_2O$], 3.55 – 3.63 [m, 10H, $HCl.NH_2(CH_2)_3\{O(C\mathbf{H}_2)_2\}_2OC\mathbf{H}_2$], 4.20 (t, *J* = 6.7 Hz, 1H, C**H**-9), 4.36 (d, *J* = 6.8 Hz, 2H, $CO_2C\mathbf{H}_2$CH-9), 7.30 (t, *J* = 7.4 Hz, 2H, C**H**-2 and -7), 7.38 (t, *J* = 7.4 Hz, 2H, C**H**-3 and -6), 7.63 (d, *J* = 7.5 Hz, 2H, C**H**-1 and -8), 7.79 (d, *J* = 7.5 Hz, 2H, C**H**-4 and -5); ^{13}C NMR (125 MHz, $CDCl_3$): δ [ppm] = 28.06 ($\mathbf{C}H_2CH_2NH$), 30.93 ($HCl.NH_2CH_2\mathbf{C}H_2$), 35.42 ($HCl.NH_2\mathbf{C}H_2$), 39.02 ($CH_2\mathbf{C}H_2NH$), 67.62 [$HCl.NH_2(CH_2)_2\mathbf{C}H_2O$], 69.59 [$O\mathbf{C}H_2(CH_2)_2NH$], 70.43 [$HCl.NH_2(CH_2)_3O\mathbf{C}H_2$], 71.03 [$HCl.NH_2(CH_2)_3OCH_2\mathbf{C}H_2$], 71.09 [$HCl.NH_2(CH_2)_3O(CH_2)_2O\mathbf{C}H_2$], 71.41 [$HCl.NH_2(CH_2)_3O(CH_2)_2OCH_2\mathbf{C}H_2$], 121.02 (**C**H-3 and -6), 126.17 (**C**H-2 and -7), 128.19 (**C**H-4 and -5), 128.85 (**C**H-1 and -8), 142.69 (**C**H-4a and -4b), 145.38 (**C**H-8a and -9a), 159.02 ($NH\mathbf{C}O_2$); LC-MS (ESI^+): m/z (%) = 443.3 (100) $[M+H]^+$; 465.2 (11) $[M+Na]^+$; HR-MS ($C_{25}H_{34}N_2O_5$): calc: 442.2462; found: 442.2461. Compound has not been reported in the literature.

5.3.3 Batch Synthesis of Dd*iv* Group Precursor

Dimedone (5.02 g, 36 mmol), isovaleric acid (4.31 mL, 39 mmol), DMAP (4.77 g, 39 mmol) and EDCI.HCl (7.48 g, 39 mmol) were dissolved in DMF (70 mL), and left to stir at room temperature overnight. The solution was then concentrated *in vacuo*, re-dissolved in DCM and washed with HCl (1 M, 2 x 50 mL) and saturated $NaHCO_3$ solution (2 x 50 mL). The organic layer was dried over $MgSO_4$, filtered and concentrated *in vacuo*. The crude mixture was purified via flash column chromatography (60:40 petroleum ether / EtOAc) to give a yellow oil (5.33 g, 66% yield). Procedure was modified from the literature.[VIII]

2-(1-Hydroxy-3-methylbutylidene)-5,5-dimethylcyclohexane-1,3-dione

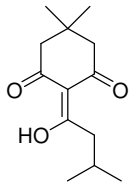

IR (neat): ν (cm^{-1}) = 2957, 2871, 1665, 1551, 1448, 1387, 1369, 1316, 1148, 1095, 1040, 918; ^{1}H NMR (500 MHz, $CDCl_3$): δ [ppm] = 0.96 [d, *J* = 6.7 Hz, 6H, $CH(C\mathbf{H}_3)_2$], 1.07 [s, 6H, Dd*iv*$C(C\mathbf{H}_3)_2$], 2.13 [sep., *J* = 6.7 Hz, 1H, $C\mathbf{H}(CH_3)_3$], 2.35 and 2.52 (br s, 4H, 2 x $COC\mathbf{H}_2$), 2.91 (d, *J* = 6.6 Hz, 2H, $(CH_3)_2CHC\mathbf{H}_2$); ^{13}C NMR (125 MHz, $CDCl_3$): δ [ppm] = 22.75 [$\mathbf{C}H(CH_3)_2$], 28.18 and 28.95 [$CH(\mathbf{C}H_3)_2$], 29.73 and 29.97 [Dd*iv*$C(\mathbf{C}H_3)_2$], 37.55 [Dd*iv*$\mathbf{C}(CH_3)_2$], 40.96 [$(CH_3)_2C\mathbf{H}CH_2$], 53.42 (2 x $CO\mathbf{C}H_2$), 107.23 (NHC=**C**), 176.60 (NH**C**=C), 192.95 (2 x **C**O); LC-MS (ESI^+): m/z (%) = 225.2 (92) $[M+H]^+$; 247.2 ((11) $[M+Na]^+$

5.3.4 Flow Mediated Mono Enamination with the Dd*iv* Group

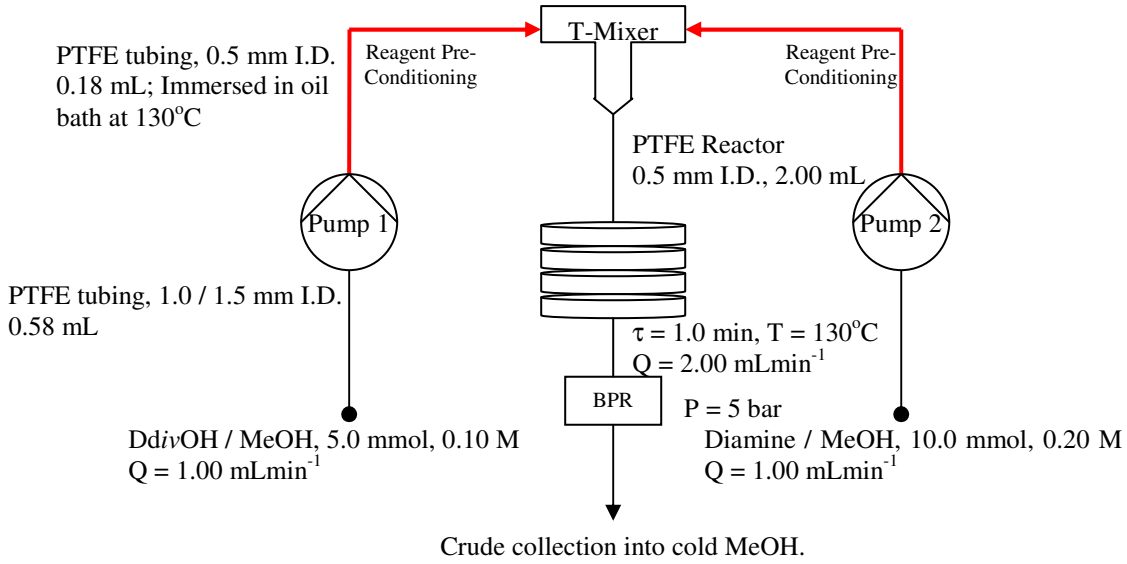

Figure 5.4 Mono-Dd*iv* enamination via continuous flow synthesis.

Flow Screening Procedure:

Diamine **1a** (0.10 M, 2 mL) and Dd*iv*OH (0.10 M, 2 mL) in MeOH were fed continuously into a PTFE reactor (0.50 mm I.D., 2.00 mL total volume) immersed in an oil bath set to the desired working temperature (120 or 130°C) and pressurised to 5 bar. The reactants were introduced via two separate pre-conditioning segments of PTFE tubing (0.5 mm I.D., 0.18 mL volume) immersed in a temperature adjusted bath. The reactants converged in the T-mixer and the stoichiometry as well as residence time of the reaction were determined by adjusting the individual flow rates of the HPLC pumps. The reaction stream (4 mL) was collected at steady state after 1.5 reactor volume, into a flask filled with cold MeOH (10 mL, –20°C). An aliquot of the solution (5 µL) was sampled and added to an internal standard solution (methyl benzoate, 2 mM, 200 µL) and analysed via HPLC. The individual components (product, side product and internal standard) in the solution were monitored with UV detection at 254 nm and the integrated areas of their respective peaks were obtained. The product yield and product to side product ratio were established based on Equation 3:

$$\text{Conc.}_{Product/By\text{-}Product} = \frac{\text{Area}_{Product/By\text{-}Product}}{\text{Area}_{IS}} \times \frac{\text{Conc.}_{IS}}{\text{DRF}_{Product/By\text{-}Product}} \qquad (\mathbf{3})$$

where $DRF_{Product}$ (Detector Response Factor of the *N*-Dd*iv* compound) = 10.66

$DRF_{Side\ Product}$ (Detector Response Factor of the *N,N*-Dd*iv* compound) = 27.82

General Scale-Out Procedure:

Diamines **1a** – **1g** (0.10 M, 50 mL) and Dd*iv*OH (0.20 M, 50 mL) in MeOH were fed continuously into a PTFE reactor (0.50 mm I.D., 2.00 mL total volume) immersed in an oil bath set at the desired working conditions (130°C, 5 bar). The reactants were introduced via two separate pre-conditioning segments (130°C) of PTFE tubing (0.5 mm I.D., 0.18 mL volume). The reactants converged in the T-mixer and the total flow rate of reaction stream was fixed at 2.00 $mLmin^{-1}$ to give a residence time of 1.0 min. The reaction stream (100 mL) was collected at steady state after 1.5 reactor volume, into a flask filled with cold methanol (200 mL, –20°C) under rigorous stirring. The solution was concentrated *in vacuo* and the crude mixture was purified via flash column chromatography (silica gel, 90:10 DCM / MeOH with 0.1% TEA) to give:

2-{1-[(2-Aminoethyl)amino]-3-methylbutylidene}-5,5-dimethylcyclohexane-1,3-dione (23)

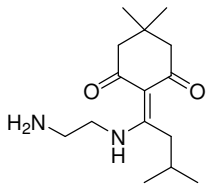

Yield: 1.21 g (91%); yellow oil

IR (neat): ν (cm^{-1}) = 3355, 2956, 1632, 1565, 1028; ^{1}H NMR (500 MHz, $CDCl_3$): δ [ppm] = 0.99 [d, *J* = 6.7 Hz, 6H, $CH(C\mathbf{H}_3)_2$], 1.03 [s, 6H, Dimedone($C\mathbf{H}_3)_2$], 1.51 (br s, 2H, $N\mathbf{H}_2$), 1.98 [sep., *J* = 6.8 Hz, 1H, $C\mathbf{H}(CH_3)_2$], 2.34 – 2.40 (m, 4H, 2 x $COC\mathbf{H}_2$), 3.00 – 3.02 [m, 3H, $(CH_3)_2CHC\mathbf{H}_2$, $NH_2C\mathbf{H}_2$], 3.44 – 3.52 [m, 3H, $NH_2(C\mathbf{H}_2)_2NH$]; ^{13}C NMR (125 MHz, $CDCl_3$): δ [ppm] = 22.60 [$\mathbf{C}(CH_3)_2$], 28.22 and 28.98 [$C(\mathbf{C}H_3)_2$], 29.69 and 29.93 [Dd*iv*$C(\mathbf{C}H_3)_2$], 37.55 [Dd*iv*$\mathbf{C}(CH_3)_2$], 41.06 [$(CH_3)_2CH\mathbf{C}H_2$, $NH_2\mathbf{C}H_2$], 46.53 ($NH_2CH_2\mathbf{C}H_2NH$), 53.41 (2 x $CO\mathbf{C}H_2$), 107.23 (NHC=**C**), 176.60 (NH**C**=C), 192.95 (2 x **C**O); LC-MS (ESI^+): m/z (%) = 267.1

(100) $[M+H]^+$; 289.0 (8) $[M+Na]^+$; HR-MS ($C_{15}H_{27}N_2O_2$): calc: 267.2067; found: 267.2060. Compound has been reported in the literature as an intermediate in a sequence of reaction. Isolation was not performed.[IX]

2-{1-[(3-Aminopropyl)amino]-3-methylbutylidene}-5,5-dimethylcyclohexane-1,3-dione (24)

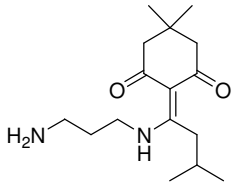

Yield: 1.12 g (80%); yellow oil

IR (neat): ν (cm^{-1}) = 2957, 1638, 1567, 1466, 1318; ^{1}H NMR (500 MHz, $CDCl_3$): δ [ppm] = 0.98 [d, *J* = 6.7 Hz, 6H, $CH(C\mathbf{H}_3)_2$], 1.02 [s, 6H, Dimedone($C\mathbf{H}_3)_2$], 1.52 (br s, 2H, $N\mathbf{H}_2$), 1.82 (quin., *J* = 6.8 Hz, 2H, $NH_2CH_2C\mathbf{H}_2CH_2NH$), 1.97 [sep., *J* = 6.8 Hz, 1H, $C\mathbf{H}(CH_3)_2$], 2.36 (s, 4H, 2 x $COC\mathbf{H}_2$), 3.01 [br s, 2H, $(CH_3)_2CHC\mathbf{H}_2$], 2.86 (t, *J* = 6.8 Hz, 2H, $NH_2C\mathbf{H}_2$), 3.52 – 3.56 (m, 2H, $C\mathbf{H}_2NHC{=}C$); ^{13}C NMR (125 MHz, $CDCl_3$): δ [ppm] = 22.58 [$\mathbf{C}(CH_3)_2$], 28.20 [$C(\mathbf{C}H_3)_2$], 28.95 and 29.92 [Dd*iv*$C(\mathbf{C}H_3)_2$], 32.62 ($NH_2CH_2\mathbf{C}H_2CH_2NH$), 37.34 [Dd*iv*$\mathbf{C}(CH_3)_2$], 39.15 [$(CH_3)_2C\mathbf{C}H_2$, $NH_2\mathbf{C}H_2$], 40.41 [$NH_2(CH_2)_2\mathbf{C}H_2NH$], 41.21 (2 x $CO\mathbf{C}H_2$), 107.07 (NHC=**C**), 176.56 (N**C**=C), 201.72 (2 x **C**O); LC-MS (ESI^+): m/z (%) = 281.1 (100) $[M+H]^+$; 303.0 (8) $[M+Na]^+$; HR-MS ($C_{15}H_{27}N_2O_2$): calc: 281.2224; found: 281.2218. Compound has not been reported in the literature.

2-{1-[(4-Aminobutyl)amino]-3-methylbutylidene}-5,5-dimethylcyclohexane-1,3-dione (25)

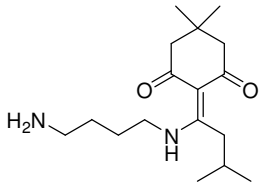

Yield: 1.06 g (72%); yellow oil

IR (neat): ν (cm^{-1}) = 3328, 2955, 1635, 1563, 1465, 1322, 1029; ^{1}H NMR (500 MHz, $CDCl_3$): δ [ppm] = 0.98 [d, *J* = 6.7 Hz, 6H, $CH(C\mathbf{H}_3)_2$], 1.02 [s, 6H, Dimedone$(C\mathbf{H}_3)_2$], 1.60 (quin., *J* = 7.4 Hz, 2H, $NH_2CH_2C\mathbf{H}_2$), 1.74 (quin., *J* = 7.4 Hz, 2H, $NH_2(CH_2)_2C\mathbf{H}_2$), 1.88 (br s, 2H, $N\mathbf{H}_2$), 1.96 [sep., *J* = 6.8 Hz, 1H, $C\mathbf{H}(CH_3)_2$], 2.35 (s, 4H, 2 x $COC\mathbf{H}_2$), 2.77 (t, *J* = 6.9 Hz, 2H, $NH_2C\mathbf{H}_2$), 2.98 [br s, 2H, $(CH_3)_2CHC\mathbf{H}_2$], 3.46 (q, *J* = 6.1 Hz, 2H, $C\mathbf{H}_2NHC{=}C$); ^{13}C NMR (125 MHz, $CDCl_3$): δ [ppm] = 22.59 [$\mathbf{C}(CH_3)_2$], 26.73 [$C(\mathbf{C}H_3)_2$], 28.19 and 28.95 [Dd*iv*$C(\mathbf{C}H_3)_2$], 29.92 [$NH_2(CH_2)_2\mathbf{C}H_2$], 30.48 [$NH_2CH_2\mathbf{C}H_2$], 37.39 [Dd*iv*$\mathbf{C}(CH_3)_2$], 41.50 [$(CH_3)_2C\mathbf{H}CH_2$, $NH_2\mathbf{C}H_2$], 43.53 ($\mathbf{C}H_2NHC{=}C$), 53.12 (2 x $CO\mathbf{C}H_2$), 107.02 (NHC=**C**), 176.44 (NH**C**=C), 201.72 (2 x **C**O); LC-MS (ESI^+): m/z (%) = 295.0 (100) $[M+H]^+$; 317.0 (8) $[M+Na]^+$; HR-MS ($C_{17}H_{31}N_2O_2$): calc: 295.2380; found: 295.2382. Compound has not been reported in the literature.

2-{1-[(5-Aminopentyl)amino]-3-methylbutylidene}-5,5-dimethylcyclohexane-1,3-dione (26)

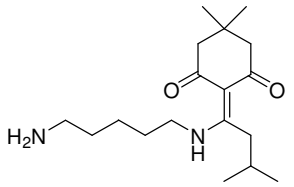

Yield: 1.11 g (72%); yellow oil

IR (neat): ν (cm^{-1}) = 3333, 2943, 2831, 1626, 1566, 1450, 1106; ^{1}H NMR (500 MHz, $CDCl_3$): δ [ppm] = 0.98 [d, *J* = 6.7 Hz, 6H, $CH(C\mathbf{H}_3)_2$], 1.02 [s, 6H, Dimedone$(C\mathbf{H}_3)_2$], 1.44 – 1.55 (m, 4H, $NH_2CH_2C\mathbf{H}_2CH_2C\mathbf{H}_2$), 1.70 (quin, *J* = 7.2 Hz, 2H, $[NH_2(CH_2)_2C\mathbf{H}_2]$, 1.88 (br s, 2H, $N\mathbf{H}_2$), 1.96 [sep., *J* = 6.8 Hz, 1H, $C\mathbf{H}(CH_3)_2$], 2.36 (s, 4H, 2 x $COC\mathbf{H}_2$), 2.74 (t, *J* = 6.8 Hz, 2H, $NH_2C\mathbf{H}_2$), 2.98 [br s, 2H, $(CH_3)_2CHC\mathbf{H}_2$], 3.44 (q, *J* = 6.4 Hz, 2H, $C\mathbf{H}_2NHC{=}C$); ^{13}C NMR (125 MHz, $CDCl_3$): δ [ppm] = 22.60 [$\mathbf{C}(CH_3)_2$], 24.17 [$NH_2(CH_2)_2\mathbf{C}H_2$], 28.20 [$C(\mathbf{C}H_3)_2$], 28.95 and 29.13 [Dd*iv*$C(\mathbf{C}H_3)_2$], 29.92 ($\mathbf{C}H_2CH_2NH$), 32.74 ($NH_2CH_2\mathbf{C}H_2$), 37.39 [Dd*iv*$\mathbf{C}(CH_3)_2$], 41.66 [$(CH_3)_2C\mathbf{H}CH_2$, $NH_2\mathbf{C}H_2$], 43.62 ($\mathbf{C}H_2NHC{=}C$), 53.12 (2 x $CO\mathbf{C}H_2$), 107.00 (NHC=**C**), 176.41 (NH**C**=C), 205.95 (2 x **C**O); LC-MS (ESI^+): m/z (%) = 309.1 (100) $[M+H]^+$; 331.1 (10) $[M+Na]^+$; HR-MS ($C_{18}H_{33}N_2O_2$): calc: 309.2537; found: 309.2537. Compound has not been reported in the literature.

2-{1-[(6-Aminohexyl)amino]-3-methylbutylidene}-5,5-dimethylcyclohexane-1,3-dione (21)

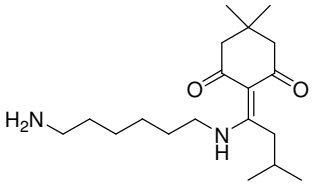

Yield: 0.94 g (58%); yellow oil

IR (neat): ν (cm^{-1}) = 2955, 2867, 1637, 1569, 1466, 1321; ^{1}H NMR (500 MHz, $CDCl_3$): δ [ppm] = 0.98 [d, *J* = 6.7 Hz, 6H, CH(C**H**$_3$)$_2$], 1.02 [s, 6H, Dimedone(C**H**$_3$)$_2$], 1.36 – 1.53 [m, 6H, NH_2CH_2(C**H**$_2$)$_3CH_2$], 1.68 (quin., *J* = 7.0 Hz, 2H, C**H**$_2CH_2NH$), 1.95 [sep, *J* = 6.8 Hz, 1H, C**H**(CH$_3$)$_2$], 2.35 (br s, 4H, 2 x COC**H**$_2$), 2.72 (t, *J* = 7.0 Hz, 2H, NH_2C**H**$_2$), 2.98 [br s, 2H, $(CH_3)_2$CHC**H**$_2$], 3.42 (q, *J* = 6.4 Hz, 2H, C**H**$_2$NHC=C); ^{13}C NMR (125 MHz, $CDCl_3$): δ [ppm] = 22.59 [**C**(CH$_3$)$_2$], 26.42 and 26.68 [C(**C**H$_3$)$_2$], 26.76 [$NH_2(CH_2)_2$**C**H$_2$], 27.14 [$NH_2(CH_2)_3$**C**H$_2$], 28.19 [Dd*iv*C(**C**H$_3$)$_2$], 28.94 [Dd*iv***C**(CH$_3$)$_2$], 29.22 (**C**H$_2CH_2NH$), 29.28 (NH_2CH_2**C**H$_2$), 32.88 [$(CH_3)_2$CH**C**H$_2$], 37.39 (NH_2**C**H$_2$), 41.79 (**C**H$_2$NHC=C), 43.64 (CO**C**H$_2$), 51.20 (CO**C**H$_2$), 106.98 (NHC=**C**), 176.39 (NH**C**=C), 206.96 (2 x **C**O); LC-MS (ESI^+): m/z (%) = 323.1 (100) $[M+H]^+$; 345.1 (7) $[M+Na]^+$; HR-MS ($C_{19}H_{35}N_2O_2$): calc: 323.26930; found: 323.26919. Compound has not been reported in the literature.

2-[1-({2-[2-(2-Aminoethoxy)ethoxy]ethyl}amino)-3-methylbutylidene]-5,5-dimethylcyclohexane-1,3-dione (27)

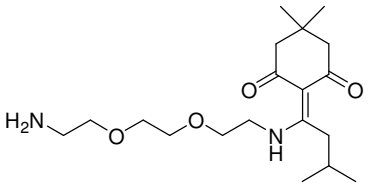

Yield: 1.12 g (63%); yellow oil

IR (neat): ν (cm^{-1}) = 3313, 2942, 2830, 1449, 1114; ^{1}H NMR (500 MHz, $CDCl_3$): δ [ppm] = 0.98 [d, *J* = 6.7 Hz, 6H, CH(C**H**$_3$)$_2$], 1.02 [s, 6H, Dimedone(C**H**$_3$)$_2$], 1.77 [br s, 2H, N**H**$_2$], 1.96 [sep., *J* = 6.8 Hz, 1H, C**H**(CH$_3$)$_2$], 2.36 (br s, 4H, 2 x COC**H**$_2$), 2.88 (t, *J* = 5.2 Hz, 2H, NH_2C**H**$_2$), 3.01 [br s, 2H, $(CH_3)_2$CHC**H**$_2$], 3.53 [t, *J* = 5.2 Hz, 2H,

OC**H**$_2$CH$_2$NH), 3.62 – 3.63 (m, 2H, OCH$_2$C**H**$_2$NH), 3.66 – 3.72 [m, 6H, NH$_2$CH$_2$C**H**$_2$O(C**H**$_2$)$_2$O]; ^{13}C NMR (125 MHz, CDCl$_3$): δ [ppm] = 22.59 [**C**(CH$_3$)$_2$], 28.19 and 28.95 [C(**C**H$_3$)$_2$], 29.68 and 29.90 [Dd*iv*C(**C**H$_3$)$_2$], 30.91 [Dd*iv***C**(CH$_3$)$_2$], 37.43 (**C**H$_2$NHC=C), 41.71 (NH$_2$**C**H$_2$), 43.64 (CH$_2$**C**H$_2$NH), 51.20 (2 x CO**C**H$_2$), 69.00 (O**C**H$_2$CH$_2$O), 70.26 (OCH$_2$**C**H$_2$O), 70.90 (O**C**H$_2$CH$_2$NH), 73.23 (NH$_2$**C**H$_2$), 107.19 (NHC=**C**), 176.50 (NH**C**=C), 206.96 (2 x **C**O); LC-MS (ESI$^+$): m/z (%) = 355.1 (100) [M+H]$^+$; 377.1 (15) [M+Na]$^+$; HR-MS (C$_{19}$H$_{35}$N$_2$O$_4$): calc: 355.25913; found: 355.25914. Compound has not been reported in the literature.

2-(1-Amino-17-methyl-4,7,10-trioxa-14-azaoctadecan-15-ylidene)-5,5-dimethyl cyclohexane-1,3-dione (28)

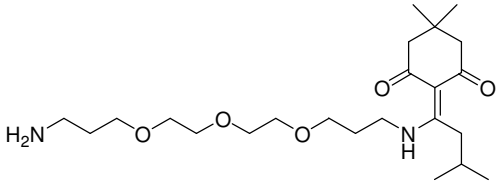

Yield: 1.51 g (71%); yellow oil

IR (neat): ν (cm^{-1}) = 3312, 2942, 2830, 1567, 1449, 1115; ^{1}H NMR (500 MHz, CDCl$_3$): δ [ppm] = 0.98 [d, *J* = 6.7 Hz, 6H, CH(C**H**$_3$)$_2$], 1.02 [s, 6H, Dimedone(C**H**$_3$)$_2$], 1.75 [br s, 2H, N**H**$_2$], 1.91 – 1.98 [m, 3H, C**H**(CH$_3$)$_2$, NH$_2$CH$_2$C**H**$_2$], 2.36 (br s, 4H, 2 x COC**H**$_2$), 2.81 (t, *J* = 6.7 Hz, 2H, NH$_2$C**H**$_2$), 3.01 [br s, 2H, (CH$_3$)$_2$CHC**H**$_2$], 3.54 – 3.65 (m, 16H, ether bridge); ^{13}C NMR (125 MHz, CDCl$_3$): δ [ppm] = 22.56 [**C**(CH$_3$)$_2$], 28.20 and 28.94 [C(**C**H$_3$)$_2$], 29.46 and 29.92 [Dd*iv*C(**C**H$_3$)$_2$], 32.93 [**C**H$_2$ CH$_2$NH, Dd*iv***C**(CH$_3$)$_2$], 37.14 [NH$_2$CH$_2$**C**H$_2$, (CH$_3$)$_2$CH**C**H$_2$], 39.60 (NH$_2$**C**H$_2$), 40.59 (**C**H$_2$NHC=C), 58.42 (2 x CO**C**H$_2$), 67.59 [NH$_2$(CH$_2$)$_2$**C**H$_2$], 69.53 [O**C**H$_2$(CH$_2$)$_2$NH], 70.14, 70.39, 70.51 and 70.56 (ether bridge), 107.06 (NHC=**C**), 176.64 (NH**C**=C), 206.96 (2 x **C**O); LC-MS (ESI$^+$): m/z (%) = 427.1 (100) [M+H]$^+$; 449.1 (12) [M+Na]$^+$; HR-MS (C$_{23}$H$_{43}$N$_2$O$_5$): calc: 427.31665; found: 427.31672. Compound has not been reported in the literature.

5.3.5 Stability Study of Mono-Dd*iv* Protected Compounds

The *N*-Dd*iv* compounds (**21, 23** – **28**) were dissolved in MeOH to give a series of solutions. In general, an aliquot of the *N*-Dd*iv* solution (100 μL) was added to an internal standard solution (methyl benzoate, 2 mM, 400 μL) and analysed via HPLC. The mono-protected compound and internal standard were monitored with UV detection at 254 nm and the integrated areas of their respective peaks were obtained. The initial concentration of the *N*-Dd*iv* solution was established based on Equation 3:

$$\text{Conc.}_{N\text{Dd}iv} = \frac{\text{Area}_{N\text{Dd}iv}}{\text{Area}_{\text{IS}}} \times \frac{\text{Conc.}_{\text{IS}}}{\text{DRF}_{N\text{Dd}iv}} \qquad (\mathbf{3})$$

where $\text{DRF}_{N\text{Dd}iv}$ (Detector Response Factor of the *N*-Dd*iv* compound) = 10.66

Subsequently, the sample was heated to 80°C for 16.5 h and re-analysed accordingly. Using Equation 3, the final concentration of the mono-protected compound was computed and in all cases, the calculated concentrations were adjusted for the dilution factor of sample preparation. A calibration curve of compound concentration against time was plotted and the half life of the *N*-Dd*iv* compound was then determined from the calibration curve.

Table 5.2 Determination of half lives of *N*-Dd*iv*-diamines at 80°C.

Entry	Product[i]	$[\text{Conc.}]_{\text{initial}}$ (mM)	$[\text{Conc.}]_{\text{final}}$ (mM)	Calibration curve
a	**26** 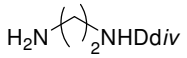	1.58	0.04	y = -0.0933x + 1.58
b	**27** 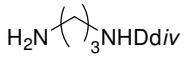	2.20	0.05	y = -0.1303x + 2.2
c	**28** 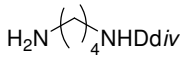	1.63	0.49	y = -0.0691x + 1.63
d	**29** 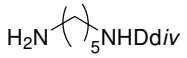	1.49	0.68	y = -0.0491x + 1.49
e	**30** 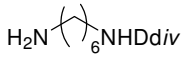	1.41	0.95	y = -0.0279x + 1.41
f	**31** 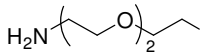	1.79	0.16	y = -0.0988x + 1.79
g	**32** 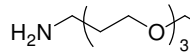	1.10	0.35	y = -0.0455x + 1.1

[i]Compounds were dissolved in MeOH.

5.4 Experimental for Chapter 3

5.4.1 Selective Mono-Alkylation of Mono-Boc Protected Diamines

Batch Procedure:

Benzyl 2-bromoacetate (5.55 mL, 35 mmol) in MeCN (600 mL) was added dropwise into a stirred solution of **2** (7.53 g, 35 mmol) and DIPEA (12.0 mL, 87.5 mmol) in MeCN (600 mL) at room temperature. The reaction was left to stir for 21 h and concentrated *in vacuo*. The crude mixture was dissolved in EtOAc and washed with brine solution (3 x 50 mL). The organic layer was concentrated *in vacuo* and purified via flash column chromatography (silica gel, 60:40 hexane / EtOAc) to give **29a** (7.51 g, 59% yield; yellow oil).

Flow Screening Procedure:

Mono-Boc diamine **2** (40 mM) and base (3.0 equiv) in MeCN (0.5 mL), along with benzyl 2-bromoacetate (40 mM) in MeCN (0.5 mL) were fed continuously into a PTFE reactor (0.50 mm I.D., 2.00 mL total volume) immersed in an oil bath set to the desired working temperature (80 – 130^{o}C) and pressurised to 2 bar. The reactants were introduced via two separate pre-conditioning segments of PTFE tubing (0.5 mm I.D., 0.18 mL volume) immersed in a temperature adjusted bath. The reactants converged in the T-mixer and the residence time of the reaction (3 or 5 min) was determined by adjusting the total flow rate of the HPLC pump-driven reaction stream. The reaction stream (1 mL) was collected at steady state after 1.5 reactor volume, into a vial filled with cold MeCN (4 mL, -20^{o}C) containing an excess of trisamine scavenger (13 mg, 20 μmol) under stirring and subsequently, filtered off. An aliquot of the diluted solution (100 μL) was sampled and added to an internal standard solution (methyl benzoate, 1 mM, 100 μL) and analysed via HPLC. The individual components (product, side product and internal standard) in the solution were monitored with UV detection at 254 nm and the integrated areas of their respective peaks were obtained. The product yield and product to side product ratio were established based on Equation 3:

$$\text{Conc.}_{\textit{Product/Side Product}} = \frac{\text{Area}_{\textit{Product/Side Product}}}{\text{Area}_{\text{IS}}} \times \frac{\text{Conc.}_{\text{IS}}}{\text{DRF}_{\textit{Product/Side Product}}} \qquad (\mathbf{3})$$

where $\text{DRF}_{\textit{Product}}$ (Detector Response Factor of **29a**) = 0.173

$\text{DRF}_{\textit{Side Product}}$ (Detector Response Factor of **29b**) = 0.540

General Scale-Out Procedure:

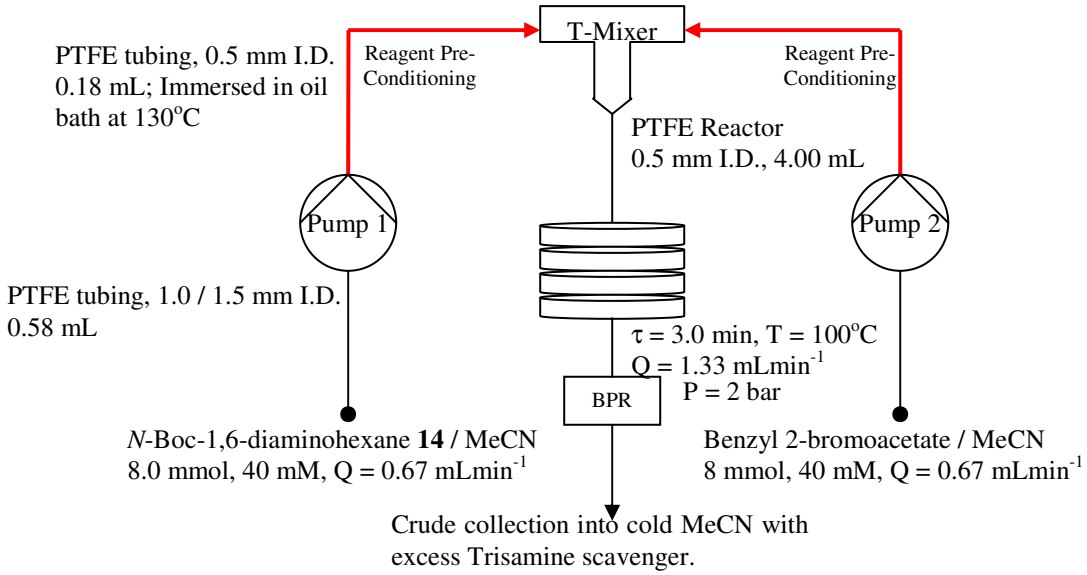

Figure 5.5 Selective mono-alkylation via continuous flow synthesis.

Mono-Boc diamine **2** or **10** (40 mM, 8 mmol) and DIPEA (4.2 mL, 24 mmol) in MeCN (200 mL), along with benzyl 2-bromoacetate (40 mM, 1.3 mL, 8 mmol) in MeCN (200 mL) were fed continuously into a PTFE reactor (0.50 mm I.D., 4.00 mL total volume) immersed in an oil bath set at 130°C and pressurised to 2 bar. The reactants were introduced via two separate pre-conditioning segments (temperature set at 130°C) of PTFE tubing (0.5 mm I.D., 0.18 mL volume). The reactants converged in the T-mixer and the total flow rate of reaction stream was fixed at 1.33 mLmin^{-1} to give a residence time of 3.0 min. The reaction stream (400 mL) was collected at steady state after 1.5 reactor volume, into a flask filled with cold MeCN (400 mL, -20°C) containing an excess of trisamine scavenger (3.04 g, 4.8mol; assuming 70% alkylation efficiency) under rigorous stirring. The solution was filtered off and concentrated *in vacuo*. The crude mixture was purified via flash column chromatography (silica gel, 60:40 hexane / EtOAc) to give:

Benzyl 2-[(6-{[(*tert*-butoxy)carbonyl]amino}hexyl)amino]acetate (29a)

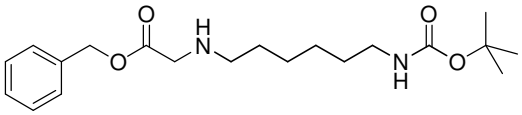

Yield: 1.95 g (67%); yellow oil

IR (neat): ν (cm^{-1}) = 3361, 2929, 2857, 1687, 1518, 1389, 1167; ^{1}H NMR (500 MHz, $CDCl_3$): δ [ppm] = 1.29 – 1.32 [m, 4H, BocNH$(CH_2)_2$(C**H**$_2)_2$], 1.43 [s, 9H, C(C**H**$_3)_3$], 1.46 – 1.49 [m, 4H, BocNHCH$_2$C**H**$_2$(CH$_2)_2$C**H**$_2$], 2.58 (t, *J* = 7.2 Hz, 2H, C**H**$_2$NHCH$_2$CO), 3.09 – 3.10 (m, 2H, C**H**$_2$NHCO), 3.44 (s, 2H, NHC**H**$_2$CO), 5.16 (s, 2H, CO$_2$C**H**$_2$Ph), 7.30 – 7.38 (m, 5H, C$_6$**H**$_5$); ^{13}C NMR (125 MHz, $CDCl_3$): δ [ppm] = 26.58 [BocNH$(CH_2)_2$**C**H$_2$], 26.81 [BocNH$(CH_2)_3$**C**H$_2$], 28.40 [C(**C**H$_3)_3$], 29.88 (BocNHCH$_2$**C**H$_2$), 29.94 (**C**H$_2$CH$_2$NHCH$_2$), 40.47 (**C**H$_2$NHCO), 49.43 (**C**H$_2$NHCH$_2$CO), 50.92 (NH**C**H$_2$CO), 66.52 (CO$_2$**C**H$_2$Ph), 79.02 [**C**(CH$_3)_3$], 128.34, 128.37, 128.58 and 135.59 (**C**$_6$H$_5$), 155.97 [**C**O$_2$C(CH$_3)_3$], 172.45 (**C**O$_2$Bn); LC-MS (ESI$^+$): m/z (%) = 365.3 (99) [M+H]$^+$; 387.3 (5) [M+Na]$^+$; HR-MS ($C_{20}H_{32}N_2O_4$): calc: 364.2357; found: 364.2359. Spectral data are consistent with the literature.[X]

Benzyl 2-({2-[2-(2-{[(*tert*-butoxy)carbonyl]amino}ethoxy)ethoxy]ethyl}amino) acetate (32)

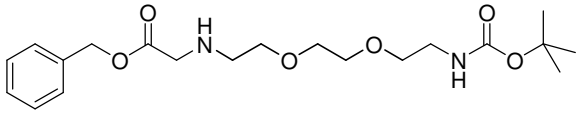

Yield: 1.90 g (60%); yellow oil

IR (neat): ν (cm^{-1}) = 3335, 2867, 1705, 1517, 1365, 1249, 1172; ^{1}H NMR (500 MHz, $CDCl_3$): δ [ppm] = 1.43 [s, 9H, C(C**H**$_3)_3$], 2.82 (t, *J* = 5.2 Hz, 2H, C**H**$_2$NHCH$_2$CO), 3.30 – 3.31 (m, 2H, C**H**$_2$NHBoc), 3.50 (s, 2H, NHC**H**$_2$CO), 3.52 (t, *J* = 5.1 Hz, 2H, C**H**$_2$CH$_2$NHCH$_2$CO), 3.58 – 3.60 [m, 6H, C**H**$_2$O(C**H**$_2)_2$O(CH$_2)_2$NHBoc], 5.16 (s, 2H, CO$_2$C**H**$_2$Ph), 7.31 – 7.38 (m, 5H, C$_6$**H**$_5$); ^{13}C NMR (125 MHz, $CDCl_3$): δ [ppm] = 28.40 [C(**C**H$_3)_3$], 40.35 (**C**H$_2$NHBoc), 48.69 (**C**H$_2$NHCH$_2$CO), 50.89 (NH**C**H$_2$CO), 66.49 (CO$_2$**C**H$_2$Ph), 70.13, 70.23 and 70.69 (ether bridge), 79.09 [**C**(CH$_3)_3$], 128.34, 128.57 and 135.61 (**C**$_6$H$_5$), 156.02 [**C**O$_2$(CH$_3)_3$], 172.23 (**C**O$_2$Bn); LC-MS (ESI$^+$):

m/z (%) = 397.2 (99) $[M+H]^+$; 419.2 (26) $[M+Na]^+$; HR-MS ($C_{20}H_{32}N_2O_6$): calc: 396.2255; found: 396.2266. Compound has not been reported in the literature.

5.4.2 In-Line Scavenging of Excess Alkylating Agent

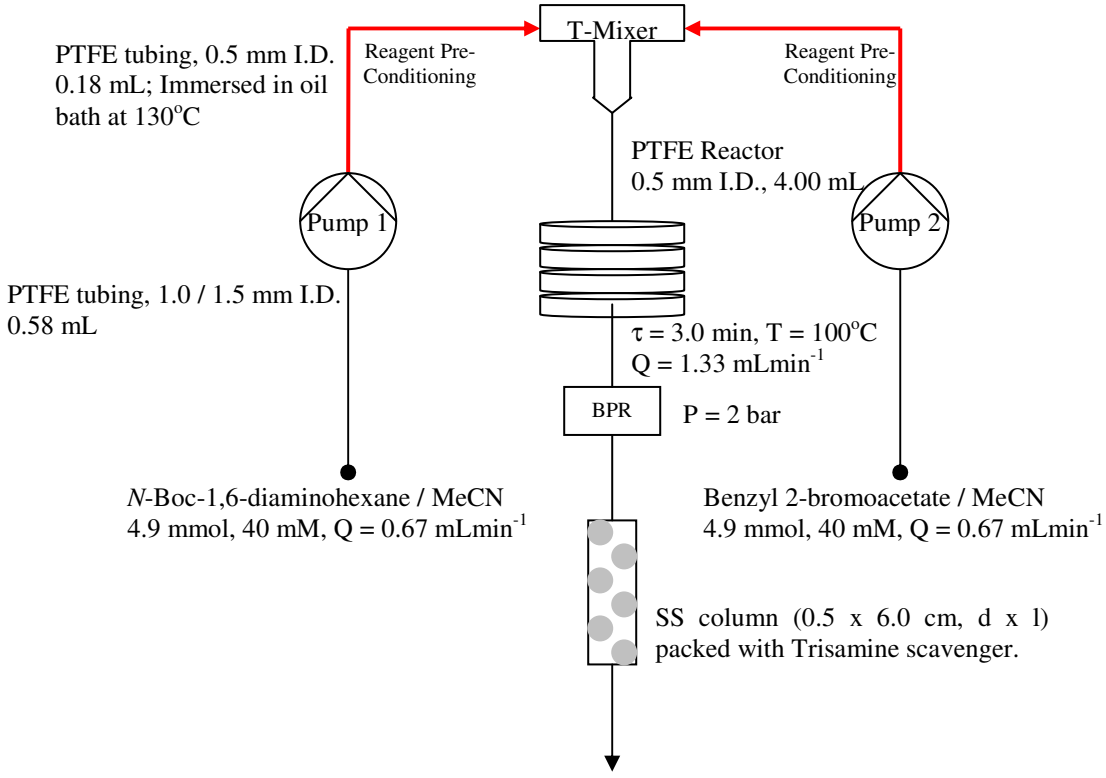

Figure 5.6 Selective mono-alkylation via continuous flow synthesis with in-line scavenging.

Mono-Boc diamine **2** or **10** (40 mM, 4.9 mmol) and DIPEA (2.6 mL, 14.7 mmol) in MeCN (123 mL), along with benzyl 2-bromoacetate (40 mM, 0.8 mL, 4.9 mmol) in MeCN (123 mL) were fed continuously into a PTFE reactor (0.50 mm I.D., 4.00 mL total volume) immersed in an oil bath set at 130°C and pressurised to 2 bar. The reactants were introduced via two separate pre-conditioning segments (temperature set at 130°C) of PTFE tubing (0.5 mm I.D., 0.18 mL volume). The reactants converged in the T-mixer and the total flow rate of reaction stream was fixed at 1.33 $mLmin^{-1}$ to give a residence time of 3.0 min. Post back pressure regulator, the reaction stream was connected to a stainless steel scavenger column (0.5 x 6.0 cm, d x l) packed with trisamine scavenger (0.62 g, 0.98 mmol). The solution (246 mL) was collected at steady state after 1.5 reactor volume, into a flask filled with cold MeCN (150 mL) and subsequently, concentrated *in vacuo*. The crude mixture was purified

via flash column chromatography (silica gel, 60:40 hexane / EtOAc) to give **29a** (1.20 g, 67% yield) or **32** (1.17 g, 60%).

5.4.3 Fmoc Carbamation of N^{α}-Alkyl-N^{ω}-Boc-Diamines

Batch Procedure:

Fmoc-OSu (6.95 g, 21 mmol) was added into a stirred solution of **29a** (7.51 g, 21 mmol) in MeCN (200 mL). The reaction was left to stir overnight at room temperature. Subsequently, silica-based trisamine scavenger (6.00 g, 9.48 mmol) was added into the solution and the reaction was left to stir for 21 h. The scavenger resins were filtered off and the solution was concentrated *in vacuo*. The crude mixture was dissolved in EtOAc (50 mL) and washed with brine solution (3 x 50 mL). The organic layer was concentrated *in vacuo* to give **30** (12.09 g, 98% yield; yellow oil).

General Scale-Out Procedure:

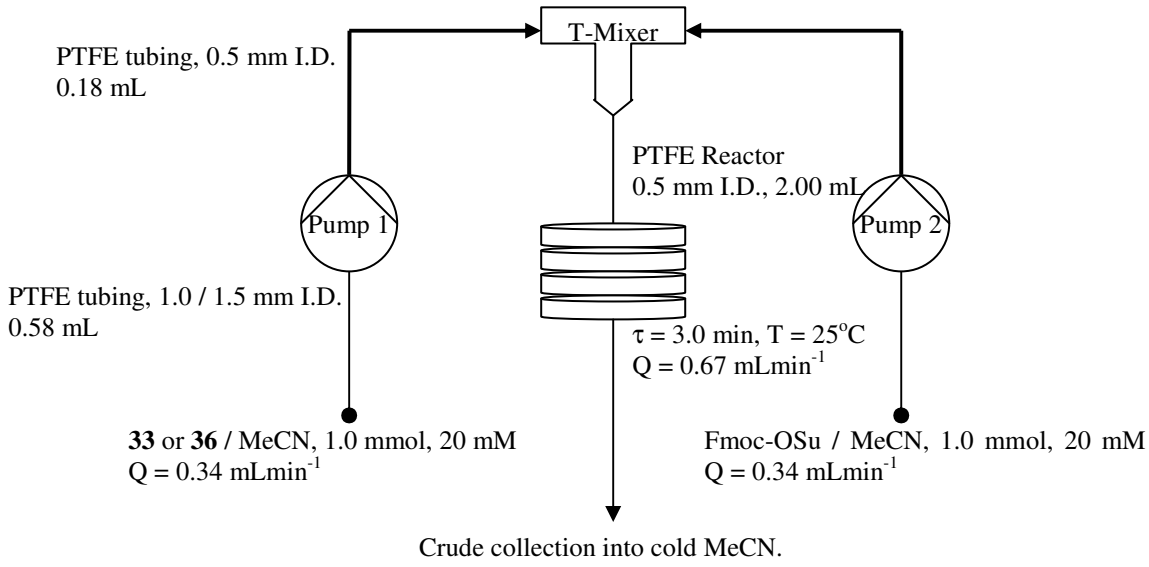

Figure 5.7 Fmoc carbamation via continuous flow synthesis.

N^{α}-alkyl-N^{ω}-Boc-diamines **29a** or **32** (20 mM, 1.0 mmol) in MeCN (50 mL) and Fmoc-OSu (20 mM, 0.34 g, 1.0 mmol) in MeCN (50 mL) were fed continuously into a PTFE reactor (0.50 mm I.D., 2.00 mL total volume) immersed in water bath set at 25°C. The reactants were introduced via two separate segments of PTFE tubing (0.5 mm I.D., 0.18 mL volume). The reactants converged in the T-mixer and the total flow rate of reaction stream was fixed at 0.67 $mLmin^{-1}$ to give a residence time of 3.0 min.

The reaction stream (100 mL) was collected at steady state after 1.5 reactor volume, into a flask filled with cold MeCN (100 mL, -20°C) under stirring and concentrated *in vacuo*. The crude mixture was dissolved in EtOAc (25 mL) and washed with brine solution (3 x 25 mL). The organic layer was concentrated *in vacuo* to give:

Benzyl 2-[(6-{[(*tert*-butoxy)carbonyl]amino}hexyl)[(9H-fluoren-9-yl methoxy) carbonyl]amino]acetate (30)

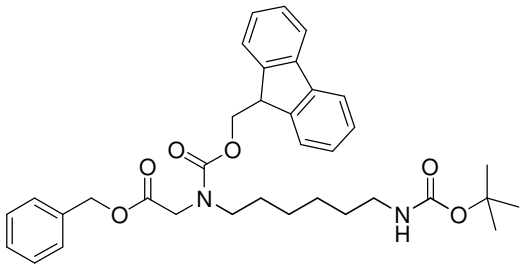

Yield: 0.57 g (98%); yellow oil

IR (neat): ν (cm^{-1}) = 3371, 2932, 2854, 1739, 1705, 1682, 1524, 1446, 1195, 1168; ^{1}H NMR (500 MHz, $CDCl_3$) two rotamers: δ [ppm] = 1.24 – 1.27 [m, 4H, (C**H**$_2$)$_2$(CH$_2$)$_2$NHBoc], 1.44 – 1.45 [m, 9H, C(C**H**$_3$)$_3$], 1.60 [s, 4H, C**H**$_2$(CH$_2$)$_2$C**H**$_2$CH$_2$NHBoc], 3.08 – 3.09 (m, 2H, C**H**$_2$NHBoc), 3.14 and 3.32 (t, *J* = 7.6 Hz, 2H, C**H**$_2$NR'R"), 3.94 and 4.01 (s, 2H, NR'C**H**$_2$CO$_2$Bn), 4.25 (t, *J* = 6.1 Hz, 1H, C**H**-9), 4.38 and 4.51 (d, *J* = 6.4 Hz, 2H, NCO$_2$C**H**$_2$CH-9), 5.11 and 5.16 (s, 2H, CO$_2$C**H**$_2$Ph), 7.27 – 7.41 (m, 9H, C$_6$**H**$_5$ and C**H**-2/7 and C**H**-3/6), 7.52 – 7.58 (d, *J* = 7.5 Hz, 2H, C**H**-1/8), 7.73 – 7.79 (m, 2H, C**H**-4/5); ^{13}C NMR (125 MHz, $CDCl_3$): two rotamers δ [ppm] = 26.23 [**C**H$_2$(CH$_2$)$_2$NHBoc], 26.38 and 26.49 [**C**H$_2$(CH$_2$)$_3$NHBoc], 27.79 (**C**H$_2$CH$_2$NR'R"), 28.22 and 28.42 [C(**C**H$_3$)$_3$], 29.88 and 29.98 (**C**H$_2$CH$_2$NHBoc), 40.44 (**C**H$_2$NHBoc), 47.24 and 47.25 (**C**H-9), 48.75 and 48.81 (**C**H$_2$NR'R"), 50.35 (NR'**C**H$_2$CO$_2$Bn), 66.91 (CO$_2$**C**H$_2$CH-9), 67.29 and 67.55 (CO$_2$**C**H$_2$Ph), 126.97 (**C**H-3/6), 127.01 and 127.07; 127.58 and 127.63 (**C**$_6$H$_5$), 128.30 (**C**H-2/7), 128.37 (**C**H-4/5), 128.45 (**C**H-1/8), 128.55 and 128.58 (**C**$_6$H$_5$), 141.26 and 141.37 (**C**H-4a/4b), 141.51 (**C**$_6$H$_5$), 143.93 and 143.97 (**C**H-8a/9a), 155.86 and 155.96 (NR'**C**O$_2$CH$_2$CH-9), 156.45 [NH**C**O$_2$(CH$_3$)$_3$], 169.49 and 169.58 (NHR'CH$_2$**C**O$_2$Bn); LC-MS (ESI$^+$): m/z (%) = 587.4 (51) [M+H]$^+$; 609.4 (97) [M+Na]$^+$; HR-MS ($C_{35}H_{42}N_2O_6$): calc: 586.3037; found: 586.3043. Spectral data are consistent with the literature.[X]

Benzyl 2-(12-{[(*tert*-butoxy)carbonyl]amino}-1-(9H-fluoren-9-yl)-3-oxo-2,7,10-trioxa-4-azadodecan-4-yl)acetate (33)

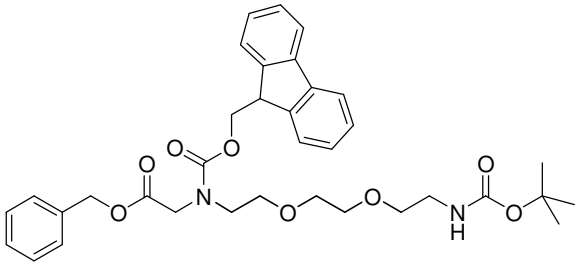

Yield: 0.61 g (98%); yellow oil

IR (neat): ν (cm^{-1}) = 3352, 2867, 1747, 1702, 1501, 1451, 1364, 1244, 1173, 1139, 1001; ^{1}H NMR (500 MHz, $CDCl_3$): two rotamers δ [ppm] = 1.43 [s, 9H, C(C**H**$_3$)$_3$], 3.27 – 3.28 (m, 2H, C**H**$_2$NHBoc), 3.34 – 3.41 and 3.46 – 3.50 (m, 8H, ether bridge), 3.56 – 3.58 and 3.61 – 3.63 (m, 2H, C**H**$_2$NR'R"), 3.94 and 4.01 (s, 2H, NR'C**H**$_2$CO$_2$Bn), 4.25 (t, *J* = 6.1 Hz, 1H, C**H**-9), 4.37 and 4.51 (d, *J* = 6.5 Hz, 2H, NCO$_2$C**H**$_2$CH-9), 5.11 and 5.15 (s, 2H, CO$_2$C**H**$_2$Ph), 7.25 – 7.34 (m, 9H, C$_6$**H**$_5$ and C**H**-2/7 and C**H**-3/6), 7.36 – 7.41 (m, 2H, C**H**-1/8), 7.51 and 7.57 (d, *J* = 7.4 Hz, 2H, C**H**-4/5); ^{13}C NMR (125 MHz, $CDCl_3$): two rotamers δ [ppm] = 28.40 [C(**C**H$_3$)$_3$], 40.28 (**C**H$_2$NHBoc), 47.17 and 47.22 (**C**H-9), 48.46 (**C**H$_2$NR'R"), 50.13 and 50.26 (NR'**C**H$_2$CO$_2$Bn), 66.82 (CO$_2$**C**H$_2$CH-9), 67.46 and 67.71 (CO$_2$**C**H$_2$Ph), 70.06 and 70.11 (**C**H$_2$CH$_2$NR'R"), 70.21 [**C**H$_2$CH$_2$O(CH$_2$)$_2$NHBoc], 70.23 and 70.25 [**C**H$_2$O(CH$_2$)$_2$NHBoc], 70.33 and 70.35 (**C**H$_2$CH$_2$NHBoc), 124.82 and 124.91 (**C**H-3/6), 127.02 and 127.09; 127.64 and 127.67 (**C**$_6$H$_5$), 128.27 (**C**H-2/7), 128.35 (**C**H-4/5), 128.41 (**C**H-1/8), 128.58 (**C**$_6$H$_5$), 141.26 and 141.35 (**C**H-4a/4b), 143.88 and 143.93 (**C**H-8a/9a), 155.95 (NR'**C**O$_2$CH$_2$CH-9), 156.17 [NH**C**O$_2$(CH$_3$)$_3$], 169.64 and 169.70 (NHR'CH$_2$**C**O$_2$Bn); LC-MS (ESI$^+$): m/z (%) = 619.3 (25) [M+H]$^+$; 641.4 (100) [M+Na]$^+$; HR-MS ($C_{35}H_{42}N_2O_8$): calc: 618.2936; found: 618.2933. Compound has not been reported in the literature.

5.4.4 Tandem Alkylation and Fmoc Carbamation in Flow

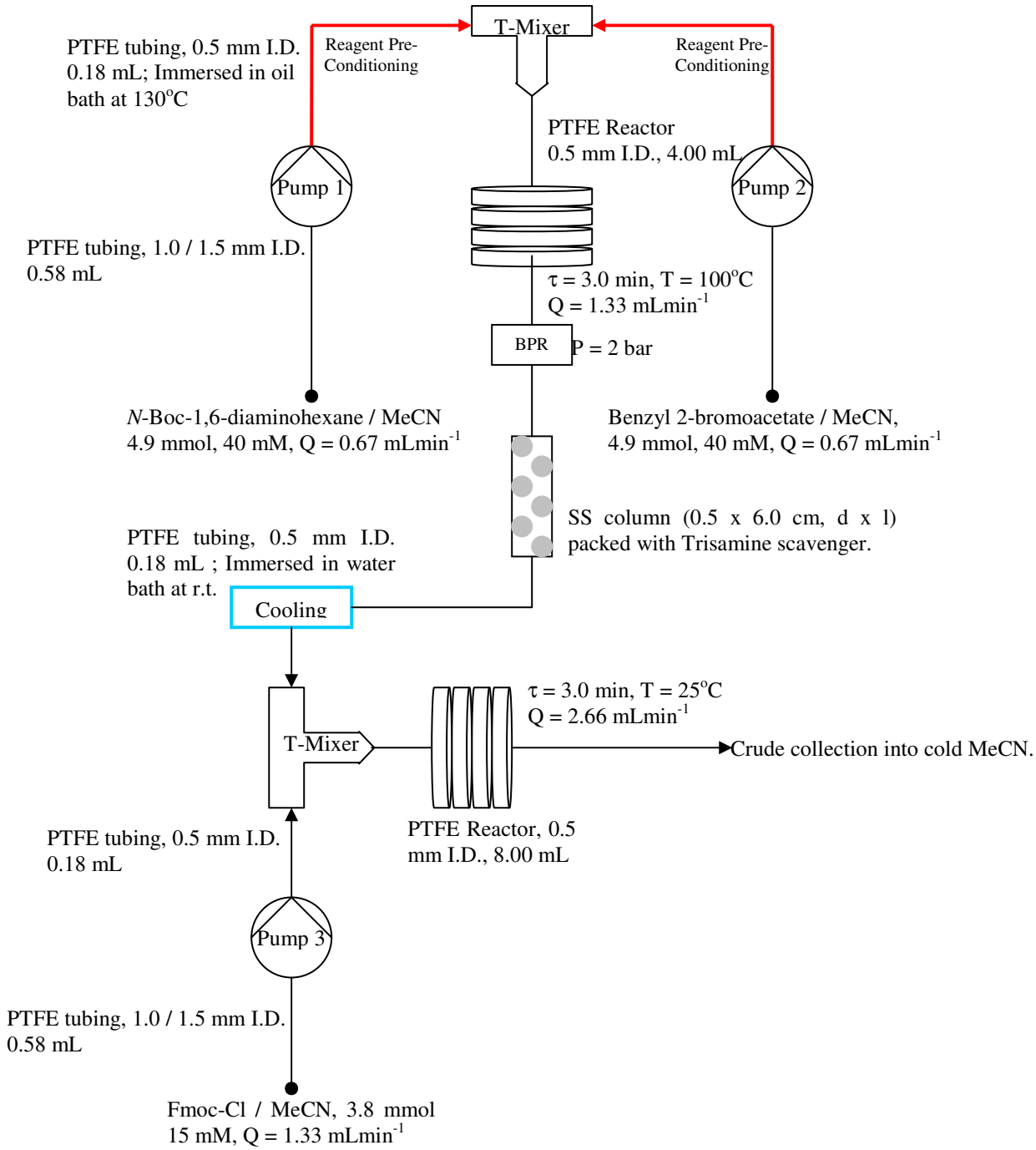

Figure 5.8 Tandem alkylation and Fmoc carbamation via continuous flow synthesis.

Mono-Boc diamine **2** or **10** (40 mM, 4.9 mmol) and DIPEA (2.6 mL, 14.7 mmol) in MeCN (123 mL), along with benzyl 2-bromoacetate (40 mM, 0.8 mL, 4.9 mmol) in MeCN (123 mL) were fed continuously into a PTFE reactor (0.50 mm I.D., 4.00 mL total volume) immersed in an oil bath set at 130°C and pressurised to 2 bar. The

reactants were introduced via two separate pre-conditioning segments (temperature set at 130°C) of PTFE tubing (0.5 mm I.D., 0.18 mL volume). The reactants converged in the T-mixer and the total flow rate of reaction stream was fixed at 1.33 $mLmin^{-1}$ to give a residence time of 3.0 min. Post back pressure regulator, the reaction stream was connected to a stainless steel scavenger column (0.5 x 6.0 cm, d x l) packed with trisamine scavenger (0.62 g, 0.98 mmol). The exiting reaction stream (cooled via a segment of PTFE tubing immersed in water bath) and Fmoc-Cl (0.97 g, 3.8 mmol) in MeCN (15 mM, 250 mL) was immediately fed into another PTFE reactor (0.50 mm I.D., 8.00 mL total volume) immersed in water bath set at 25°C. The reactants converged in the second T-mixer and the total flow rate of reaction stream was fixed at 2.66 $mLmin^{-1}$ to give a residence time of 3.0 min. The reaction stream (492 mL) was collected at steady state after 1.5 reactor volume, into a flask filled with cold MeCN (200 mL, -20°C) under stirring and concentrated *in vacuo*. The crude mixture was purified via flash column chromatography (silica gel, 60:40 hexane / EtOAc) to give **30** (1.39 g, 69% yield; yellow oil) or **33** (1.87 g, 62% yield; yellow oil).

5.4.5 Catalytic Transfer Hydrogenolysis of the Benzyl Group

Batch Procedure:

Ammonium formate (3.25 g, 51 mmol) was added into a stirred solution of benzyl 2-[(6-{[(*tert*-butoxy)carbonyl]amino}hexyl)[(9H-fluoren-9-ylmethoxy)carbonyl]amino] acetate **30** (12.09 g, 21 mmol) and 10% Pd/C (1.79 g, 1.68 mmol) in EtOH (525 mL). The solution was stirred vigorously and the progress of reaction was monitored by HPLC. After 19 min, the reaction was immediately quenched by filtering the solution through celite and the filtrate was concentrated *in vacuo*. The crude mixture was dissolved in EtOAc (50 mL) and washed with brine solution (3 x 50 mL). The organic layer was concentrated *in vacuo* and and purified via flash column chromatography (silica gel, 90:10 DCM / MeOH with 0.1% AcOH) to give a viscous yellow oil. The compound was subsequently recrystallised using hexane / EtOAc to give **31a** (5.59 g, 54% yield; white solid).

Batch-Mode Microwave Procedure:

Fmoc protected N^{α}-alkyl-N^{ω}-Boc-diamine **30** (0.48 or 1.20 mmol) and 10% Pd/C (4.5 mol%) in EtOH (0.25 M) were microwave irradiated in the presence of H_2 gas in a microwave module fitted with a gas addition unit. The reaction conditions (time, temperature and gas pressure) were adjusted accordingly via the control panel of the microwave module. The reaction was quenched by filtering the solution through celite. An aliquot of the diluted solution (100 μL) was sampled and added to an internal standard solution (aniline, 1 mM, 100 μL) and analysed via HPLC. The individual components (starting material, product and internal standard) in the solution were monitored with UV detection at 254 nm and the integrated areas of their respective peaks were obtained. The product yield and product to side product ratio were established based on Equation 3:

$$\text{Conc.}_{Product} = \frac{\text{Area}_{Product}}{\text{Area}_{\text{IS}}} \times \frac{\text{Conc.}_{\text{IS}}}{\text{DRF}_{Product}} \qquad (\mathbf{3})$$

where $\text{DRF}_{Product}$ (Detector Response Factor of **31a**) = 48.417

Flow Screening Procedure:

Fmoc protected N^{α}-alkyl-N^{ω}-Boc-diamine **30** (7.5 μmol) and 1,4-cyclohexadiene (2.5 equiv) in EtOH were prepared at different concentrations (15, 30 or 50 mM) and fed continuously into a modified H-Cube (generation of H_2 gas was deactivated). The catalyst compartment was fitted with the catalyst of choice (CatCart's 10% Pd/C or 20% $Pd(OH)_2$/C) and the desired working temperature was adjusted accordingly (25 or 40^{o}C). The contact time between the substrate and the catalyst was approximately 23 sec based on the reaction stream flow rate of 1.00 mLmin-1. The reaction stream (1 mL) was collected at steady state after 1.5 CatCart volume, into a vial filled with cold EtOH (4 mL, -20^{o}C) under stirring. An aliquot of the diluted solution (100 μL) was sampled and added to an internal standard solution (aniline, 1 mM, 100 μL) and analysed via HPLC. The individual components (starting material, product and internal standard) in the solution were monitored with UV detection at 254 nm and the integrated areas of their respective peaks were obtained. The product yield and product to side product ratio were established based on Equation 3:

$$\text{Conc.}_{Product} = \frac{\text{Area}_{Product}}{\text{Area}_{IS}} \times \frac{\text{Conc.}_{IS}}{\text{DRF}_{Product}} \qquad (\mathbf{3})$$

where $DRF_{Product}$ (Detector Response Factor of **31a**) = 48.417

General Scale-Out Procedure:

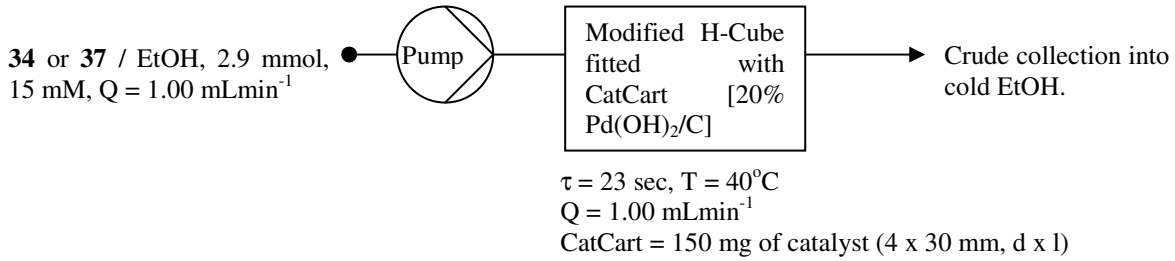

Figure 5.9 Catalytic transfer flow hydrogenolysis.

Fmoc protected N^{α}-alkyl-N^{ω}-Boc-diamine **30** or **33** (15 mM, 2.9 mmol) and 1,4-cyclohexadiene (0.7 mL, 7.3 mmol) in EtOH (192 mL) were fed continuously into a modified H-Cube (generation of H_2 gas was deactivated). The catalyst compartment was fitted with CatCart's 20% $Pd(OH)_2/C$ and the desired working temperature was set at 40°C. The contact time between the substrate and the catalyst was approximately 23 sec based on the reaction stream flow rate of 1.00 mLmin-1. The reaction stream (192 mL) was collected at steady state after 1.5 CatCart volume, into a flask filled with cold EtOH (100 mL, -20°C) under stirring and concentrated *in vacuo*. The crude mixture was dissolved in EtOAc (50 mL) and washed with brine solution (3 x 50 mL). The organic layer was concentrated *in vacuo* and and purified via flash column chromatography (silica gel, 90:10 DCM / MeOH with 0.1% AcOH) to give a viscous yellow oil. The compound was subsequently recrystallised using hexane / EtOAc to give:

2-[(6-{[(*tert*-Butoxy)carbonyl]amino}hexyl)[(9H-fluoren-9-ylmethoxy)carbonyl] amino]acetic acid (31a)

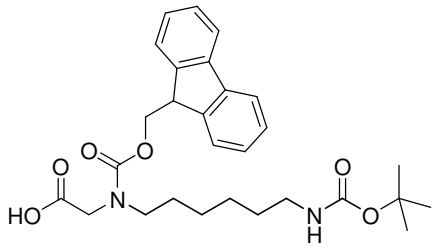

Yield: 1.00 g (70%); white solid

M.p. 80 – 82°C; IR (neat): ν (cm^{-1}) = 3359, 2978, 2930, 2851, 1728, 1680, 1519, 1416, 1367, 1168, 960, 918; ^{1}H NMR (500 MHz, $CDCl_3$): two rotamers δ [ppm] = 1.21 – 1.34 [m, 8H, R'R"$NCH_2(C\mathbf{H}_2)_4CH_2NHBoc$], 1.44 [s, 9H, $C(C\mathbf{H}_3)_3$], 3.08 – 3.09 (m, 2H, $C\mathbf{H}_2NHBoc$), 3.13 and 3.33 (t, *J* = 7.2 Hz, 2H, $C\mathbf{H}_2NR'R"$), 3.90 and 3.98 (s, 2H, $NR'C\mathbf{H}_2CO_2H$), 4.20 – 4.25 (m, 1H, C**H**-9), 4.43 and 4.54 (d, *J* = 5.3 Hz, 2H, $NCO_2C\mathbf{H}_2CH$-9), 7.27 – 7.32 (m, 2H, C**H**-2/7), 7.36 – 7.41 (m, 2H, C**H**-3/6), 7.57 (t, *J* = 8.7 Hz, 2H, C**H**-1/8), 7.75 (t, *J* = 8.1 Hz, 2H, C**H**-4/5); ^{13}C NMR (125 MHz, $CDCl_3$): two rotamers δ [ppm] = 25.96 and 26.15 [$\mathbf{C}H_2(CH_2)_2NHBoc$], 26.21 and 26.31 [$\mathbf{C}H_2(CH_2)_3NHBoc$], 27.76 and 28.09 ($\mathbf{C}H_2CH_2NR'R"$), 28.41 [$C(\mathbf{C}H_3)_3$], 29.69 ($\mathbf{C}H_2CH_2NHBoc$), 40.40 ($\mathbf{C}H_2NHBoc$), 47.26(**C**H-9), 48.53 and 48.78 ($\mathbf{C}H_2NR'R"$), 50.35 ($NR'\mathbf{C}H_2CO_2H$), 67.39 and 67.70 ($CO_2\mathbf{C}H_2CH$-9), 79.33 [$\mathbf{C}(CH_3)_3$], 124.77 and 124.93 (**C**H-3/6), 127.05 (**C**H-2/7), 127.61 (**C**H-4/5), 127.67 (**C**H-1/8), 141.30 and 141.38 (**C**H-4a/4b), 143.87 and 143.93 (**C**H-8a/9a), 155.96 ($NR'\mathbf{C}O_2CH_2CH$-9), 156.78 [$NH\mathbf{C}O_2(CH_3)_3$], 172.63 ($NHR'CH_2\mathbf{C}O_2H$); LC-MS (ESI^+): m/z (%) = 519.3 (38) $[M+Na]^+$; HR-MS ($C_{28}H_{36}N_2O_6$): calc: 496.2568; found: 496.2560. Spectral data are consistent with the literature.[X]

2-(12-{[(*tert*-Butoxy)carbonyl]amino}-1-(9H-fluoren-9-yl)-3-oxo-2,7,10-trioxa-4-azadodecan-4-yl)acetic acid (34)

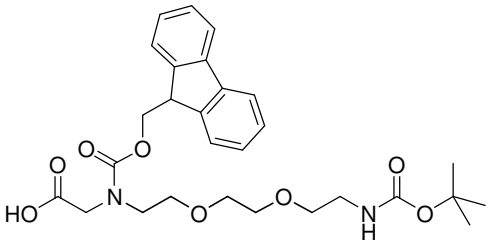

Yield: 1.04 g (68%); yellow oil

IR (neat): ν (cm^{-1}) = 2870, 2248, 1692, 1511, 1476, 1451, 1409, 1365, 1244, 1139, 998, 909; ^{1}H NMR (500 MHz, $CDCl_3$): two rotamers δ [ppm] = 1.44 [s, 9H, C(**C**H_3)$_3$], 3.30 – 3.67 (m, 12H, ether bridge), 4.1 (s, 2H, NR'C**H**$_2$$CO_2H$), 4.21 – 4.26 (m, 1H, C**H**-9), 4.38 and 4.52 (br s, 2H, NCO_2C**H**$_2$CH-9), 7.29 – 7.32 (m, 2H, C**H**-2/7), 7.36 – 7.41 (m, 2H, C**H**-3/6), 7.57 (d, *J* = 7.4 Hz, C**H**-1/8), 7.75 (t, *J* = 6.8 Hz, 2H, C**H**-4/5); ^{13}C NMR (125 MHz, $CDCl_3$): two rotamers δ [ppm] = 28.40 [C(**C**H_3)$_3$], 40.26 (**C**H_2NHBoc), 47.16 and 47.21 (**C**H-9), 48.40 (**C**H_2NR'R"), 50.59 (NR'**C**$H_2$$CO_2H$), 67.44 ($CO_2$**C**$H_2$CH-9), 67.99 (**C**$H_2$$CH_2$NR'R"), 69.98 [**C**$H_2$$CH_2O(CH_2)_2$NHBoc], 70.07 [**C**$H_2O(CH_2)_2$NHBoc], 70.25 (**C**$H_2$$CH_2$NHBoc), 124.81 (**C**H-3/6), 125.07 (**C**H-2/7), 127.07 (**C**H-4/5), 127.62 (**C**H-1/8), 141.23 and 141.34 (**C**H-4a/4b), 143.90 (**C**H-8a/9a), 156.02 (NR'**C**$O_2$$CH_2$CH-9), 156.19 [NH**C**$O_2$$(CH_3)_3$], 172.27 and 172.44 (NHR'CH_2**C**O_2H); LC-MS (ESI^+): m/z (%) = 529.3 (32) $[M+H]^+$; 551.3 (99) $[M+Na]^+$; HR-MS ($C_{28}H_{36}N_2O_8$): calc: 528.2466; found: 528.2464. Compound has not been reported in the literature.

5.5 Experimental for Chapter 4

5.5.1 Rink Amide Functionalisation of Aminomethyl Polystyrene Resins

Fmoc-linker (0.60 g, 1.11 mmol, 3 equiv) and Oxyma (0.16 g, 1.11 mmol, 3 equiv) were dissolved in DMF (0.37 M, 3 mL) and left to mix via shaking for 5 – 10 min. DIC (0.17 mL, 1.11 mmol, 3 equiv) was subsequently added to the mixture and shaken for another 2 min. The final mixture was added to the aminomethyl PS resins (0.30 g, 0.37 mmol) and left to react on the rotary wheel for 1.5 h. The reaction solution was drained and the resins washed with DMF, DCM and MeOH (3x each). The progress of reaction was monitored with ninhydrin test and a yellow ninhydrin solution was indicative of a complete coupling reaction.

5.5.2 Solid Phase Synthesis of Standard Peptoids

20% piperidine in DMF (1.00 mL) was added to the Rink amide-functionalised aminomethyl PS resins (60 mg, 44.37 μmol) and left to react for 15 min. The Fmoc deprotection step was performed twice at room temperature. The resins were washed with DMF and DCM (3x each) after the cleavage cocktail was drained off. Monomer **31a** (44 mg, 88.74 μmol, 2 equiv) and Oxyma (13 mg, 88.74 μmol, 2 equiv) were dissolved in DMF (0.15 M, 0.60 mL) and left to mix via shaking for 5 – 10 min. DIC (0.17 mL, 1.11 mmol, 2 equiv) was subsequently added to the mixture and shaken for another 2 min. The final mixture was added to the Fmoc-deprotected resins (60 mg, 44.37 μmol) and left to react on the rotary wheel for 30 min at room temperature. The reaction solution was drained and the resins washed with DMF, DCM and MeOH (3x each).

For oligomers > 5 residues, the coupling reaction was heated to 60^{o}C for 15 min, followed by an extended 15 min of mechanical agitation at room temperature. The coupling and deprotection protocol was reiterated until the desired oligomer back bone length was achieved. *N*-Fmoc-6-aminohexanoic acid (31 mg, 88.74 μmol, 2 equiv) was added to the final residue, followed by 5(6)-carboxyfluorescein (33 mg, 88.74 μmol, 2 equiv). The coupling and Fmoc deprotection conditions were as previously stated. The progress of reaction was monitored with chloranil test and blue beads were indicative of a complete coupling reaction. The target compound was

cleaved from the solid support with the addition of 95% TFA : 2.5% TIS : 2.5% H_2O (1.00 mL). The reaction was left on the rotary wheel for 3 h at room temperature.

The reaction solution was drained from the solid phase cartridge and collected into an Eppendorf tube. The beads were rinsed twice with the cleavage cocktail and the TFA solution concentrated with N_2 gas to a minimal volume. Cold diethyl ether was added into the Eppendorf tube to precipitate the oligomer. The precipitate was centrifuged at 4°C and 10^4 RPM for 10 min. The ether solution was decanted and the solid precipitate was sonicated upon the addition of fresh diethyl ether. The rinsing cycle was repeated thrice, and the precipitate was blown dry with N_2 gas and left in the desiccator overnight. The oligomer was dissolved in H_2O and analysed via HPLC and MALDI.

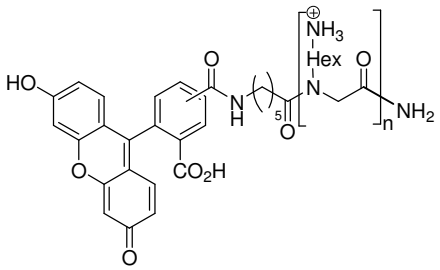

n = 5 **S5**
= 7 **S7**
= 9 **S9**

Standard Peptoids

Standard Pentamer S5

Yield: 40 mg (71%); yellow solid

UV/Vis HPLC (495 nm): t_R = 2.46 and 2.64 min; MALDI ($C_{67}H_{104}N_{12}O_{12}$): calc: 1269.6159; found: 1269.8614. Melting point was not measured.

Standard Heptamer S7

Yield: 42 mg (60%); yellow solid

UV/Vis HPLC (495 nm): t_R = 2.30 and 2.39 min; MALDI ($C_{83}H_{136}N_{16}O_{14}$): calc: 1582.0667; found: 1582.7013. Melting point was not measured.

Standard Nonamer S9

Yield: 46 mg (55%); yellow solid

UV/Vis HPLC (495 nm): t_R = 2.13 and 2.32 min; MALDI ($C_{99}H_{168}N_{20}O_{16}$): calc: 1894.5176; found: 1895.3915. Melting point was not measured.

5.5.3 Microwave-Assisted Solid Phase Synthesis of TEG Peptoids

20% piperidine in DMF (1.00 mL) was added to the Rink amide-functionalised aminomethyl PS resins (60 mg, 44.37 μmol) and left to react for 15 min. The Fmoc deprotection step was performed twice at room temperature. The resins were washed with DMF and DCM (3x each) after the cleavage cocktail was drained off. Monomer **34** (47 mg, 88.74 μmol, 2 equiv) and Oxyma (13 mg, 88.74 μmol, 2 equiv) were dissolved in 3 : 1 of DMF : DCM (0.14 M, 0.63 mL) and left to mix via shaking for 5 – 10 min. DIC (0.17 mL, 1.11 mmol, 2 equiv) was subsequently added to the mixture and shaken for another 2 min. The final mixture was added to the Fmoc-deprotected resins (60 mg, 44.37 μmol) and microwave irradiated for 25 min at 70°C. The reaction solution was drained and the resins washed with DMF, DCM and MeOH (3x each).

Once the first residue was successfully coupled, the subsequent Fmoc deprotection procedure was performed twice via microwave irradiation at 60°C for 10 min. The coupling and deprotection protocol was reiterated until the desired oligomer back bone length was achieved. *N*-Fmoc-6-aminohexanoic acid (31 mg, 88.74 μmol, 2 equiv) was added to the final residue, followed by 5(6)-carboxyfluorescein (33 mg, 88.74 μmol, 2 equiv). The coupling and Fmoc deprotection conditions were as previously stated. The progress of reaction was monitored with chloranil test and blue beads were indicative of a complete coupling reaction. The target compound was cleaved from the solid support with the addition of 95% TFA : 2.5% TIS : 2.5% H_2O (1.00 mL). The reaction was left on the rotary wheel for 3 h at room temperature.

The reaction solution was drained from the solid phase cartridge and collected into an Eppendorf tube. The beads were rinsed twice with the cleavage cocktail and the TFA solution concentrated with N_2 gas to a minimal volume. Cold petroleum ether was added into the Eppendorf tube and the mixture was centrifuged at 4°C and 10^4 RPM for 10 min. The petroleum ether solution was decanted and the immiscible

oil was sonicated upon the addition of fresh petroleum ether. The rinsing cycle was repeated thrice, and the viscous oil was blown dry with N_2 gas and left in the desiccator overnight. The oligomer was dissolved in H_2O and analysed via HPLC and MALDI.

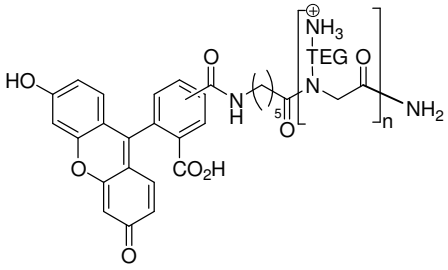

n = 5 **T5**
= 7 **T7**
= 9 **T9**

TEG Peptoids
(TEG = Triethylene glycol)

TEG Pentamer T5

Yield: 29 mg (45%); orange-red oil

UV/Vis HPLC (495 nm): t_R = 2.42 and 2.52 min; MALDI ($C_{67}H_{104}N_{12}O_{22}$): calc: 1429.6099; found: 1429.7113

TEG Heptamer T7

Yield: 34 mg (42%); orange-red oil

UV/Vis HPLC (495 nm): t_R = 2.22 and 2.33 min; MALDI ($C_{83}H_{136}N_{16}O_{28}$): calc: 1806.0583; found: 1806.2077

TEG Nonamer T9

Yield: 37 mg (38%); orange-red oil

UV/Vis HPLC (495 nm): t_R = 2.10 and 2.19 min; MALDI ($C_{99}H_{168}N_{20}O_{34}$): calc: 2182.5068; found: 2183.4156

5.5.4 Microwave-Assisted Solid Phase Synthesis of Hybrid Peptoids

20% piperidine in DMF (1.00 mL) was added to the Rink amide-functionalised aminomethyl PS resins (60 mg, 44.37 μmol) and left to react for 15 min. The Fmoc deprotection step was performed twice at room temperature. The resins were washed with DMF and DCM (3x each) after the cleavage cocktail was drained off. Monomer **31a** or **34** (88.74 μmol, 2 equiv) and Oxyma (13 mg, 88.74 μmol, 2 equiv) were dissolved in 3 : 1 of DMF : DCM (0.14 M, 0.63 mL) and left to mix via shaking for 5 – 10 min. DIC (0.17 mL, 1.11 mmol, 2 equiv) was subsequently added to the mixture and shaken for another 2 min. The final mixture was added to the Fmoc-deprotected resins (60 mg, 44.37 μmol) and microwave irradiated for 25 min at 70°C. The reaction solution was drained and the resins washed with DMF, DCM and MeOH (3x each).

Once the first residue was successfully coupled, the subsequent Fmoc deprotection procedure was performed twice via microwave irradiation at 60°C for 10 min (up to 7 residues). The Fmoc deprotection cocktail was changed to 4% DBU : 4% piperidine in DMF for octamer and beyond. The coupling (performed using **31a** and **34** in successive manner) and deprotection protocol was reiterated until the desired oligomer back bone length was achieved. *N*-Fmoc-6-aminohexanoic acid (31 mg, 88.74 μmol, 2 equiv) was added to the final residue, followed by 5(6)-carboxyfluorescein (33 mg, 88.74 μmol, 2 equiv). The coupling and Fmoc deprotection conditions were as previously stated. The progress of reaction was monitored with chloranil test and blue beads were indicative of a complete coupling reaction.

The target compound was cleaved from the solid support with the addition of 95% TFA : 2.5% TIS : 2.5% H_2O (1.00 mL). The reaction was left on the rotary wheel for 3 h at room temperature. The reaction solution was drained from the solid phase cartridge and collected into an Eppendorf tube. The beads were rinsed twice with the cleavage cocktail and the TFA solution concentrated with N_2 gas to a minimal volume. Cold petroleum ether was added into the Eppendorf tube and the mixture was centrifuged at 4°C and 10^4 RPM for 10 min. The petroleum ether solution was decanted and the immiscible oil was sonicated upon the addition of fresh petroleum ether. The rinsing cycle was repeated thrice, and the viscous oil was blown dry with N_2 gas and left in the desiccator overnight. The oligomer was dissolved in H_2O and analysed via HPLC and MALDI.

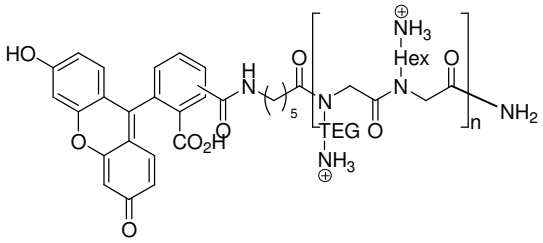

n = 2 **H5**
= 3 **H7**
= 4 **H9**

Hybrid Peptoids

Hybrid Pentamer H5

Yield: 7 mg (12%); orange-red oil

UV/Vis HPLC (495 nm): t_R = 2.49 and 2.60 min; MALDI ($C_{67}H_{104}N_{12}O_{16}$): calc: 1333.6135; found: 1333.8332

Hybrid Heptamer H7

Yield: 6 mg (8%); orange-red oil

UV/Vis HPLC (495 nm): t_R = 2.31 and 2.42 min; MALDI ($C_{83}H_{136}N_{12}O_{20}$): calc: 1678.0631; found: 1679.0334

Hybrid Nonamer H9

Yield: 4 mg (5%); orange-red oil

UV/Vis HPLC (495 nm): t_R = 2.19 min; MALDI ($C_{99}H_{168}N_{20}O_{24}$): calc: 2022.5128; found: 2023.5198

5.5.5 Biological Evaluation of Peptoids

Cells were grown in DMEM or Ham's F12 medium supplemented with glutamine (4 mM), 10% FCS and 100 UmL^{-1} of penicillin / streptomycin in T75 cell culture flasks until 70% confluence. The cells were maintained in a humid chamber at 37°C in an atmosphere of 5% CO_2.

5.5.5.1 Cell Viability Assays

For cell viability assays, 1 x 10^4 cells per well were seeded in 96-well plates and incubated overnight. Twenty four hours after the addition of the peptoids (10 μM), cell death was measured using an MTT cell proliferation assay. Absorbance was spectrophotometrically measured at 570 nm. For the propidium iodide (PI) cell death assay, 3 x 10^4 cells per well were seeded in 48-well plates and incubated overnight. The following day, the test compounds were mixed with the corresponding medium to give a final concentration of 10 μM. The old media were removed from the wells and the cells were washed twice with warm phosphate buffer saline (PBS) solution. The peptoid / media mixture was added (250 μL or 1.6 mL to each 48- or 6-well plate, respectively). Each experiment was performed in triplicate. After incubating the cells for a specific duration (at 37ºC and 5% CO_2), they were washed twice with PBS and incubated with the fluorochrome solution (0.1% wt/v sodium citrate, 0.1% v/v Triton X-100 and 50 mgL^{-1} PI in distilled water) for 1 h at 4°C. The cells were washed again with PBS and detached with trypsin / EDTA. They were harvested with 2% fetal bovine serum (FBS) in PBS, centrifuged and resuspended with 2% FBS in PBS (supplemented with Trypan Blue [0.04%]), and analysed using a BD FACSAria® flow cytometer.

5.5.5.2 Cellular Uptake Assays

Cells were suspended using 0.25% trypsin / EDTA and counted. For the flow cytometry assay, 3 x 10^4 cells per well were seeded in 48-well plates and incubated overnight. For the confocal assays, 4 x 10^5 cells were seeded onto glass cover slip within a 6-well plate. The following day, the test compounds were mixed with the corresponding medium to give a range of concentrations (1.0, 2.5 or 10.0 μM). The old media were removed from the wells and the cells were washed with warm

phosphate buffer saline (PBS) solution. The peptoid / media mixture was added (250 µL or 1.6 mL to each 48- or 6-well plate, respectively). Each experiment was performed in triplicate. After incubating the cells for a specific duration (at 37ºC and 5% CO_2), they were washed twice with PBS and detached with trypsin / EDTA. They were harvested with 2% fetal bovine serum (FBS) in PBS, centrifuged and resuspended with 2% FBS in PBS (supplemented with Trypan Blue [0.04%]), and analysed using a BD FACSAria® flow cytometer.

5.5.5.3 Confocal Microscopy Analysis

The cells used for confocal microscopy imaging were fixed with paraformaldehyde (4% w/v in PBS) and the nuclei were stained with Hoechst-33342 (1% w/v in PBS). Cellular fluorescence of fixed cells was analyzed by confocal microscopy using a Leica SP5 Confocal Microscope under laser excitation at 488 nm and 407 nm, respectively.

5.6 Spectral Data References

(I) Pittelkow, M.; Lewinsky, R.; Christensen, J. B. *Synthesis* **2002**, *15*, 2195-2202.

(II) Friscourt, F.; Ledin, P. A.; Mbua, N. E.; Flanagan-Steet, H. R.; Wolfert, M. A.; Steet, R.; Boons, G.-J. *Journal of the American Chemical Society* **2012**, *134*, 5381-5389.

(III) Dhar, S.; Liu, Z.; Thomale, J.; Dai, H.; Lippard, S. J. *Journal of the American Chemical Society* **2008**, *130*, 11467-11476.

(IV) Sølvhøj, A. B.; Tortzen, C.; Christensen, J. B. *Organic Preparations and Procedures International* **2012**, *44*, 397-400.

(V) Boeijen, A.; van Ameijde, J.; Liskamp, R. M. J. *The Journal of Organic Chemistry* **2001**, *66*, 8454-8462.

(VI) Etsuko, K.; Yusuku, O.; Kazuo, K. In *Espacenet* Office, E. P., Ed. Japan, 2007; Vol. WO2007029364 (A1).

(VII) Adamczyk, M.; Grote, J. *Organic Preparations and Procedures International* **1995**, *27*, 239-242.

(VIII) Kellam, B.; Chan, W. C.; Chhabra, S. R.; Bycroft, B. W. *Tetrahedron Letters* **1997**, *38*, 5391-5394.

(IX) Zhang, Z.; Fan, E. *The Journal of Organic Chemistry* **2005**, *70*, 8801-8810.

(X) Unciti-Broceta, A.; Diezmann, F.; Ou-Yang, C.; Fara, M.; Bradley, M. *Bioorganic & Medicinal Chemistry* **2009**, *17*, 959-966.

REFERENCES

(1) Leone, G.; Rahn, R. D. *Fundamentals of Flow Manufacturing*; First ed.; Flow Publishing Inc.: Boulder, 2002.

(2) Lapkin, A. A.; Plucinski, P. K. In *Chemical Reactions and Processes under Flow Conditions*; The Royal Society of Chemistry: 2009, p 1-43.

(3) Watts, P.; Wiles, C. *Journal of Chemical Research* **2012**, *36*, 181-193.

(4) Malet-Sanz, L.; Susanne, F. *Journal of Medicinal Chemistry* **2012**, *55*, 4062-4098.

(5) Anderson, N. G. *Organic Process Research & Development* **2001**, *5*, 613-621.

(6) Roberge, D. M.; Ducry, L.; Bieler, N.; Cretton, P.; Zimmermann, B. *Chemical Engineering & Technology* **2005**, *28*, 318-323.

(7) Roberge, D. M.; Zimmermann, B.; Rainone, F.; Gottsponer, M.; Eyholzer, M.; Kockmann, N. *Organic Process Research & Development* **2008**, *12*, 905-910.

(8) Greenway, G. M.; Haswell, S. J.; Morgan, D. O.; Skelton, V.; Styring, P. *Sensors and Actuators B: Chemical* **2000**, *63*, 153-158.

(9) Haswell, S. J.; Middleton, R. J.; O'Sullivan, B.; Skelton, V.; Watts, P.; Styring, P. *Chemical Communications* **2001**, 391-398.

(10) Barrow, D. In *Microreactors in Organic Synthesis and Catalysis*; Wirth, T., Ed.; Wiley-VCH Verlag GmbH & Co. KGaA: 2008, p 43-57.

(11) Pennemann, H.; Watts, P.; Haswell, S. J.; Hessel, V.; Löwe, H. *Organic Process Research & Development* **2004**, *8*, 422-439.

(12) Jähnisch, K.; Hessel, V.; Löwe, H.; Baerns, M. *Angewandte Chemie International Edition* **2004**, *43*, 406-446.

(13) Fukuyama, T.; Rahman, M. T.; Ryu, I.; Baxendale, I. R.; Hayward, J. J.; Lanners, S.; Ley, S. V.; Smith, C. D.; Ahmed-Omer, B.; Wirth, T.; Hessel, V.; Löb, P.; Löwe, H.; Koch, K.; Rutjes, F. P. J. T.; van Hest, J. C. M. In *Microreactors in Organic Synthesis and Catalysis*; Wirth, T., Ed.; Wiley-VCH Verlag GmbH & Co. KGaA: 2008, p 59-209.

(14) Browne, D. L.; Deadman, B. J.; Ashe, R.; Baxendale, I. R.; Ley, S. V. *Organic Process Research & Development* **2011**, *15*, 693-697.

(15) Leduc, A. B.; Jamison, T. F. *Organic Process Research & Development* **2012**, *16*, 1082-1089.

(16) Shu, W.; Pellegatti, L.; Oberli, M. A.; Buchwald, S. L. *Angewandte Chemie* **2011**, *123*, 10853-10857.

(17) Baxendale, I. R.; Ley, S. V.; Mansfield, A. C.; Smith, C. D. *Angewandte Chemie International Edition* **2009**, *48*, 4017-4021.

(18) Razzaq, T.; Glasnov, T. N.; Kappe, C. O. *European Journal of Organic Chemistry* **2009**, *2009*, 1321-1325.

(19) Nagaki, A.; Togai, M.; Suga, S.; Aoki, N.; Mae, K.; Yoshida, J.-i. *Journal of the American Chemical Society* **2005**, *127*, 11666 - 11675.

(20) Razzaq, T.; Kappe, C. O. *Chemistry – An Asian Journal* **2010**, *5*, 1274-1289.

(21) Yoshida, J.-i.; Nagaki, A.; Yamada, D. *Drug Discovery Today: Technologies* **2013**, *10*, e53-e59.

(22) Kockmann, N.; Gottsponer, M.; Zimmermann, B.; Roberge, D. M. *Chemistry – A European Journal* **2008**, *14*, 7470-7477.

(23) Wheeler, R. C.; Benali, O.; Deal, M.; Farrant, E.; MacDonald, S. J. F.; Warrington, B. H. *Organic Process Research & Development* **2007**, *11*, 704-710.

(24) Karolin, G.; Jeroen, D. C. C.; Peter, H. S. *Chemistry - A European Journal* **2006**, *12*, 8434 - 8442.

(25) Li, C.-J.; Trost, B. M. *Proceedings of the National Academy of Sciences* **2008**, *105*, 13197 - 13202.

(26) Mason, B. P.; Price, K. E.; Steinbacher, J. L.; Bogdan, A. R.; McQuade, D. T. *Chemical Reviews* **2007**, *107*, 2300-2318.

(27) Panke, G.; Schwalbe, T.; Stirner, W.; Taghavi-Moghadam, S.; Wille, G. *Synthesis* **2003**, *18*, 2827 - 2830.

(28) McQuade, D. T.; Seeberger, P. H. *The Journal of Organic Chemistry* **2013**.

(29) Carter, C. F.; Baxendale, I. R.; O'Brien, M.; Pavey, J. B. J.; Ley, S. V. *Organic & Biomolecular Chemistry* **2009**, *7*, 4594-4597.

(30) O'Brien, A. G.; Horváth, Z.; Lévesque, F.; Lee, J. W.; Seidel-Morgenstern, A.; Seeberger, P. H. *Angewandte Chemie International Edition* **2012**, *51*, 7028-7030.

(31) Hamlin, T. A.; Leadbeater, N. E. *Beilstein Journal of Organic Chemistry* **2013**, *9*, 1843-1852.

(32) Wegner, J.; Ceylan, S.; Kirschning, A. *Chemical Communications* **2011**, *47*, 4583-4592.

(33) Wiles, C.; Watts, P. *Green Chemistry* **2014**, *16*, 55-62.

(34) Styring, P.; Parracho, A. I. R. *Beilstein Journal of Organic Chemistry* **2009**, *5*, 29.

(35) Jas, G.; Kirschning, A. *Chemistry – A European Journal* **2003**, *9*, 5708-5723.

(36) Hornung, C. H.; Mackley, M. R.; Baxendale, I. R.; Ley, S. V. *Organic Process Research & Development* **2007**, *11*, 399 - 405.

(37) Aldrich Chemical Co., Inc.: Milwaukee, 2009; Vol. 9, p 1-20.

(38) Baxendale, I. R.; Ley, S. V.; Smith, C. D.; Tranmer, G. K. *Chemical Communications* **2006**, 4835-4837.

(39) Seeberger, P. H. *Nature Chemistry* **2009**, *1*, 258 - 260.

(40) Webb, D.; Jamison, T. F. *Chemical Science* **2010**, *1*, 675-680.

(41) Smith, C. D.; Baxendale, I. R.; Tranmer, G. K.; Baumann, M.; Smith, S. C.; Lewthwaite, R. A.; Ley, S. V. *Organic & Biomolecular Chemistry* **2007**, *5*, 1562-1568.

(42) Smith, C. D.; Baxendale, I. R.; Lanners, S.; Hayward, J. J.; Smith, S. C.; Ley, S. V. *Organic & Biomolecular Chemistry* **2007**, *5*, 1559-1561.

(43) Nikbin, N.; Ladlow, M.; Ley, S. V. *Organic Process Research & Development* **2007**, *11*, 458-462.

(44) Bogdan, A. R.; Poe, S. L.; Kubis, D. C.; Broadwater, S. J.; McQuade, D. T. *Angewandte Chemie International Edition* **2009**, *48*, 8547-8550.

(45) Fuse, S.; Tanabe, N.; Yoshida, M.; Yoshida, H.; Doi, T.; Takahashi, T. *Chemical Communications* **2010**, *46*, 8722-8724.

(46) Baxendale, I. R.; Deeley, J.; Griffiths-Jones, C. M.; Ley, S. V.; Saaby, S.; Tranmer, G. K. *Chemical Communications* **2006**, 2566-2568.

(47) Glasnov, T. N.; Kappe, C. O. *Advanced Synthesis & Catalysis* **2010**, *352*, 3089-3097.

(48) Lévesque, F.; Seeberger, P. H. *Angewandte Chemie International Edition* **2012**, *51*, 1706-1709.

(49) Dalla-Vechia, L.; Reichart, B.; Glasnov, T.; Miranda, L. S. M.; Kappe, C. O.; de Souza, R. O. M. A. *Organic & Biomolecular Chemistry* **2013**, *11*, 6806-6813.

(50) Kupracz, L.; Kirschning, A. *Advanced Synthesis & Catalysis* **2013**, *355*, 3375-3380.

(51) Hartwig, J.; Ceylan, S.; Kupracz, L.; Coutable, L.; Kirschning, A. *Angewandte Chemie International Edition* **2013**, *52*, 9813-9817.

(52) Nie, Z.; Xu, S.; Seo, M.; Lewis, P. C.; Kumacheva, E. *Journal of the American Chemical Society* **2005**, *127*, 8058-8063.

(53) Marre, S.; Jensen, K. F. *Chemical Society Reviews* **2010**, *39*, 1183-1202.

(54) Glasnov, T. N.; Kappe, C. O. *Chemistry – A European Journal* **2011**, *17*, 11956-11968.

(55) Jarowicki, K.; Kocienski, P. *Journal of the Chemical Society, Perkin Transactions 1* **1998**, 4005-4037.

(56) Young, I. S.; Baran, P. S. *Nature Chemistry* **2009**, *1*, 193 - 205.

(57) Bycroft, B. W.; Chan, W. C.; Hone, N. D.; Millington, S.; Nash, I. A. *Journal of the American Chemical Society* **1994**, *116*, 7415-7416.

(58) Dixon, M. J.; Maurer, R. I.; Biggi, C.; Oyarzabal, J.; Essex, J. W.; Bradley, M. *Bioorganic & Medicinal Chemistry* **2005**, *13*, 4513-4526.

(59) Schröder, T.; Schmitz, K.; Niemeier, N.; Balaban, T.; Krug, H.; Schepers, U.; Bräse, S. *Bioconjugate Chemistry* **2007**, *18*, 342-354.

(60) Jacobson, A. R.; Makris, A. N.; Sayre, L. M. *The Journal of Organic Chemistry* **1987**, *52*, 2592-2594.

(61) Bendavid, A.; Burns, C. J.; Field, L. D.; Hashimoto, K.; Ridley, D. D.; Samankumara Sandanayake, K. R. A.; Wieczorek, L. *The Journal of Organic Chemistry* **2001**, *66*, 3709-3716.

(62) Bender, J. A.; Meanwell, N. A.; Wang, T. *Tetrahedron* **2002**, *58*, 3111-3128.

(63) Pittelkow, M.; Lewinsky, R.; Christensen, J. B. *Synthesis* **2002**, *15*, 2195-2202.

(64) Pringle, W. *Tetrahedron Letters* **2008**, *49*, 5047-5049.

(65) Das, B.; Venkateswarlu, K.; Krishnaiah, M.; Holla, H. *Tetrahedron Letters* **2006**, *47*, 7551-7556.

(66) Oliver, M.; Jorgensen, M. R.; Miller, A. D. *Synlett* **2003**, *3*, 0453-0456.

(67) Wender, P. A.; Verma, V. A.; Paxton, T. J.; Pillow, T. H. *Accounts of Chemical Research* **2007**, *41*, 40-49.

(68) Ham, J.-Y.; Kang, H.-S. *Bulletin of the Korean Chemical Society* **1994**, *15*.

(69) Zhang, Z.; Yin, Z.; Meanwell, N. A.; Kadow, J. F.; Wang, T. *Organic Letters* **2003**, *5*, 3399-3402.

(70) Chankeshwara, S. V.; Chakraborti, A. K. *Tetrahedron Letters* **2006**, *47*, 1087-1091.

(71) Lee, D. W.; Ha, H.-J.; Lee, W. K. *Synthetic Communications* **2007**, *37*, 737-742.

(72) Krapcho, A. P.; Kuell, C. S. *Synthetic Communications* **1990**, *20*, 2559 - 2564.

(73) Trost, B. M. *Science* **1991**, *254*, 1471-1477.

(74) Wuts, P. G. M.; Greene, T. W. *Greene's Protective Groups in Organic Synthesis*; 4 ed.; John Wiley & Sons, Inc.: Hoboken, 2007.

(75) Chhabra, S. R.; Hothi, B.; Evans, D. J.; White, P. D.; Bycroft, B. W.; Chan, W. C. *Tetrahedron Letters* **1998**, *39*, 1603-1606.

(76) Maurya, R. A.; Hoang, P. H.; Kim, D.-P. *Lab on a Chip* **2012**, *12*, 65-68.

(77) Fick, A. *Journal of Membrane Science* **1995**, *100*, 33-38.

(78) Mandal, P. K.; Ren, Z.; Chen, X.; Xiong, C.; McMurray, J. S. *Journal of Medicinal Chemistry* **2009**, *52*, 6126-6141.

(79) Bycroft, B. W.; Chan, W. C.; Chhabra, S. R.; Teesdale-Spittle, P. H.; Hardy, P. M. *Journal of the Chemical Society, Chemical Communications* **1993**, 776-777.

(80) Díaz-Mochón, J. J.; Bialy, L.; Bradley, M. *Organic Letters* **2004**, *6*, 1127-1129.

(81) Augustyns, K.; Kraas, W.; Jung, G. *Journal of Peptide Research* **1998**, *51*, 127 - 133.

(82) Zhang, X.-X.; Eden, H. S.; Chen, X. *Journal of Controlled Release* **2012**, *159*, 2-13.

(83) Diao, L.; Meibohm, B. *Clinical Pharmacokinetics* **2013**, *52*, 855-868.

(84) Giannis, A.; Kolter, T. *Angewandte Chemie International Edition in English* **1993**, *32*, 1244-1267.

(85) Farmer, P. S.; Ariëns, E. J. *Trends in Pharmacological Sciences* **1982**, *3*, 362-365.

(86) Simon, R.; Kania, R.; Zuckermann, R.; Huebner, V.; Jewell, D.; Banville, S.; Ng, S.; Wang, L.; Rosenberg, S.; Marlowe, C. *Proceedings of the National Academy of Sciences of the United States of America* **1992**, *89*, 9367-9371.

(87) Fowler, S.; Blackwell, H. *Organic & Biomolecular Chemistry* **2009**, *7*, 1508-1524.

(88) Murphy, J.; Uno, T.; Hamer, J.; Cohen, F.; Dwarki, V.; Zuckermann, R. *Proceedings of the National Academy of Sciences of the United States of America* **1998**, *95*, 1517-1522.

(89) Xu, Z. P.; Zeng, Q. H.; Lu, G. Q.; Yu, A. B. *Chemical Engineering Science* **2006**, *61*, 1027-1040.

(90) Trabulo, S.; Cardoso, A. L.; Mano, M.; De Lima, M. C. P. *Pharmaceuticals* **2010**, *3*, 961-993.

(91) Safari, J.; Zarnegar, Z. *Journal of Saudi Chemical Society* **2013**.

(92) Frankel, A.; Pabo, C. *Cell* **1988**, *55*, 1189-1193.

(93) Debaisieux, S.; Rayne, F.; Yezid, H.; Beaumelle, B. *Traffic (Copenhagen, Denmark)* **2012**, *13*, 355-363.

(94) Lindgren, M.; Hällbrink, M.; Prochiantz, A.; Langel, U. *Trends in Pharmacological Sciences* **2000**, *21*, 99-103.

(95) Tan, N. C.; Yu, P.; Kwon, Y.-U.; Kodadek, T. *Bioorganic & Medicinal Chemistry* **2008**, *16*, 5853 - 5861.

(96) Stewart, K.; Horton, K.; Kelley, S. *Organic & Biomolecular Chemistry* **2008**, *6*, 2242-2255.

(97) Jiao, C.-Y.; Delaroche, D.; Burlina, F.; Alves, I. D.; Chassaing, G.; Sagan, S. *Journal of Biological Chemistry* **2009**, *284*, 33957-33965.

(98) Wender, P.; Mitchell, D.; Pattabiraman, K.; Pelkey, E.; Steinman, L.; Rothbard, J. *Proceedings of the National Academy of Sciences of the United States of America* **2000**, *97*, 13003-13008.

(99) Futaki, S.; Suzuki, T.; Ohashi, W.; Yagami, T.; Tanaka, S.; Ueda, K.; Sugiura, Y. *Journal of Biological Chemistry* **2001**, *276*, 5836-5840.

(100) Huang, W.; Seo, J.; Lin, J.; Barron, A. *Molecular bioSystems* **2012**, *8*, 2626-2628.

(101) Schröder, T.; Niemeier, N.; Afonin, S.; Ulrich, A.; Krug, H.; Bräse, S. *Journal of Medicinal Chemistry* **2008**, *51*, 376-379.

(102) Mitchell, D. J.; Steinman, L.; Kim, D. T.; Fathman, C. G.; Rothbard, J. B. *The Journal of Peptide Research* **2000**, *56*, 318-325.

(103) Vollrath, S. B. L.; Furniss, D.; Schepers, U.; Brase, S. *Organic & Biomolecular Chemistry* **2013**, *11*, 8197-8201.

(104) Gajbhiye, V.; Kumar, P. V.; Tekade, R. K.; Jain, N. K. *Current Pharmaceutical Design* **2007**, *13*, 415-429.

(105) Fant, K.; Esbjörner, E.; Jenkins, A.; Grossel, M.; Lincoln, P.; Nordén, B. *Molecular Pharmaceutics* **2010**, *7*, 1734-1746.

(106) Fox, M.; Guillaudeu, S.; Fréchet, J.; Jerger, K.; Macaraeg, N.; Szoka, F. *Molecular Pharmaceutics* **2009**, *6*, 1562-1572.

(107) Guo, L.; Zhang, D. *Journal of the American Chemical Society* **2009**, *131*, 18072-18074.

(108) Sun, J.; Zuckermann, R. *ACS Nano* **2013**, *7*, 4715-4732.

(109) Yu, P.; Liu, B.; Kodadek, T. *Nature Biotechnology* **2005**, *23*, 746-751.

(110) Juan, J. D.-M.; Mario, A. F.; Rosario, M. S.-M.; Mark, B. *Tetrahedron Letters* **2008**, *49*, 923 - 926.

(111) Martin, E.; Blaney, J.; Siani, M.; Spellmeyer, D.; Wong, A.; Moos, W. *Journal of Medicinal Chemistry* **1995**, *38*, 1431-1436.

(112) Unciti-Broceta, A.; Diezmann, F.; Ou-Yang, C.; Fara, M.; Bradley, M. *Bioorganic & Medicinal Chemistry* **2009**, *17*, 959-966.

(113) Ronald, N. Z.; Janice, M. K.; Stephen, B. H. K.; Walter, H. M. *Journal of the American Chemical Society* **1992**, *114*, 10646 - 10647.

(114) Zuckermann, R. *Biopolymers* **2010**, *96*, 545-555.

(115) Peretto, I.; Sanchez-Martin, R. M.; Wang, X.-h.; Ellard, J.; Mittoo, S.; Bradley, M. *Chemical Communications* **2003**, 2312-2313.

(116) Gottfried, B.; Terry, J. N. *Chemical Reviews* **1974**, *74*, 567 - 580.

(117) Atherton, E.; Ceri, B.; Sheppard, R. C.; Williams, B. J. *Tetrahedron Letters* **1979**, *20*.

(118) Martinez, J.; Tolle, J. C.; Bodanszky, M. *The Journal of Organic Chemistry* **1979**, *44*, 3596-3598.

(119) Taylor, J.; Bull, S.; Williams, J. *Chemical Society Reviews* **2012**, *41*, 2109-2121.

(120) Kappe, C. O.; Pieber, B.; Dallinger, D. *Angewandte Chemie International Edition* **2012**, *52*, 1088-1094.

(121) Ley, S. V.; Baxendale, I. R.; Bream, R. N.; Jackson, P. S.; Leach, A. G.; Longbottom, D. A.; Nesi, M.; Scott, J. S.; Storer, R. I.; Taylor, S. J. *Journal of the Chemical Society, Perkin Transactions 1* **2000**, 3815-4195.

(122) Sinfelt, J. H. *Catalysis Letters* **1991**, *9*, 159-171.

(123) Blaser, H.-U.; Indolese, A.; Schnyder, A.; Steiner, H.; Studer, M. *Journal of Molecular Catalysis A: Chemical* **2001**, *173*, 3-18.

(124) Tsuji, J. In *Palladium Reagents and Catalysts*; John Wiley & Sons, Ltd: 2005, p 1-26.

(125) Dale, L. B.; Mark, W. L.; Masaharu, K. *Journal of the American Chemical Society* **1999**, *121*, 1098 - 1099.

(126) Smith, G. V.; Notheisz, F. *Heterogeneous Catalysis in Organic Chemistry*; Elsevier, 2000.

(127) Grossman, R. B. *The Art of Writing Reasonable Organic Reaction Mechanisms*; 2 ed.; Springer-Verlag: New York, 2003.

(128) Bensel, N.; Klär, D.; Catala, C.; Schneckenburger, P.; Hoonakker, F.; Goncalves, S.; Wagner, A. *European Journal of Organic Chemistry* **2010**, 2261-2264.

(129) Bryan, M.; Wernick, D.; Hein, C.; Petersen, J.; Eschelbach, J.; Doherty, E. *Beilstein Journal of Organic Chemistry* **2011**, *7*, 1141-1149.

(130) Ram, S.; Ehrenkaufer, R. E. *Synthesis* **1988**, 91-95.

(131) Arthur, M. F.; Edgar, P. H.; Theodore, J. L.; Chryssa, T.; Johannes, M. *The Journal of Organic Chemistry* **1978**, *43*, 4194 - 4196.

(132) Dobrovolná, R.; Červeny, L. *Research on Chemical Intermediates* **2000**, *26*, 489 - 497.

(133) Fields, G. In *Methods in Molecular Biology* Pennington, M. W., Dunn, B. M., Eds.; Humana Press Inc.: Tolowa, 1994; Vol. 35, p 17-27.

(134) Linstead, R. P.; Braude, F. A.; Mitchell, P. W. D.; Wooldridge, K. R. H.; Jackman, L. M. *Nature* **1952**, *169*, 100 - 103.

(135) Pearlman, W. M. *Tetrahedron Letters* **1967**, *8*, 1663-1664.

(136) Toebes, M. L.; van Dillen, J. A.; de Jong, K. P. *Journal of Molecular Catalysis A: Chemical* **2001**, *173*, 75-98.

(137) Galema, S. A. *Chemical Society Reviews* **1997**, *26*, 233-238.

(138) Perreux, L.; Loupy, A. *Tetrahedron* **2001**, *57*, 9199 - 9223

(139) Kappe, C. O. *Angewandte Chemie* **2004**, *43*, 6250 - 6284.

(140) Subirós-Funosas, R.; Prohens, R.; Barbas, R.; El-Faham, A.; Albericio, F. *Chemistry (Weinheim an der Bergstrasse, Germany)* **2009**, *15*, 9394-9403.

(141) Bacsa, B.; Horváti, K.; Bõsze, S.; Andreae, F.; Kappe, C. O. *The Journal of Organic Chemistry* **2008**, *73*, 7532-7542.

(142) Pedersen, S. L.; Tofteng, A. P.; Malik, L.; Jensen, K. J. *Chemical Society Reviews* **2011**, *41*, 1826-1844.

(143) Luke, D. L.; Ronald, T. R. *ACS Chemical Biology* **2008**, *3*.

(144) http://www.markergene.com/ProductDetails.php/M0122#; Marker Gene Technologies: 1993 - 2014.

(145) Mosmann, T. *Journal of Immunological Methods* **1983**, *65*, 55-63.

(146) Suzuki, T.; Fujikura, K.; Higashiyama, T.; Takata, K. *Journal of Histochemistry & Cytochemistry* **1997**, *45*, 49-53.

(147) BD Biosciences: 2000; Vol. 11-11032-01.

(148) Laerum, O. D.; Farsund, T. *Cytometry* **1981**, *2*, 1-13.

(149) Rudat, B.; Birtalan, E.; Vollrath, S.; Fritz, D.; Kölmel, D.; Nieger, M.; Schepers, U.; Müllen, K.; Eisler, H.-J.; Lemmer, U.; Bräse, S. *European Journal of Medicinal Chemistry* **2011**, *46*, 4457-4465.

(150) Strober, W. In *Current Protocols in Immunology*; John Wiley & Sons, Inc.: 2001.

(151) Goodson, B.; Ehrhardt, A.; Ng, S.; Nuss, J.; Johnson, K.; Giedlin, M.; Yamamoto, R.; Moos, W.; Krebber, A.; Ladner, M.; Giacona, M.; Vitt, C.; Winter, J. *Antimicrobial Agents and Chemotherapy* **1999**, *43*, 1429-1434.

(152) Sternberg, U.; Birtalan, E.; Jakovkin, I.; Luy, B.; Schepers, U.; Bräse, S.; Muhle-Goll, C. *Organic & Biomolecular Chemistry* **2013**, *11*, 640-647.

(153) Bahnsen, J.; Franzyk, H.; Sandberg-Schaal, A.; Nielsen, H. *Biochimica et Biophysica Acta* **2013**, *1828*, 223-232.